Particle Detectors

Lecture at the African School for Fundamental Physics and Applications, 28/11-09/12 2022
Nelson Mandela University, South Africa

Lecture IV

Advanced detectors and some new developments

First Workshop NextGAPES -2019
Lomonosov Moscow State University, Physics Department, Skobeltsyn Institute of Nuclear Physics.
Moscow - June, 21-22, 2019

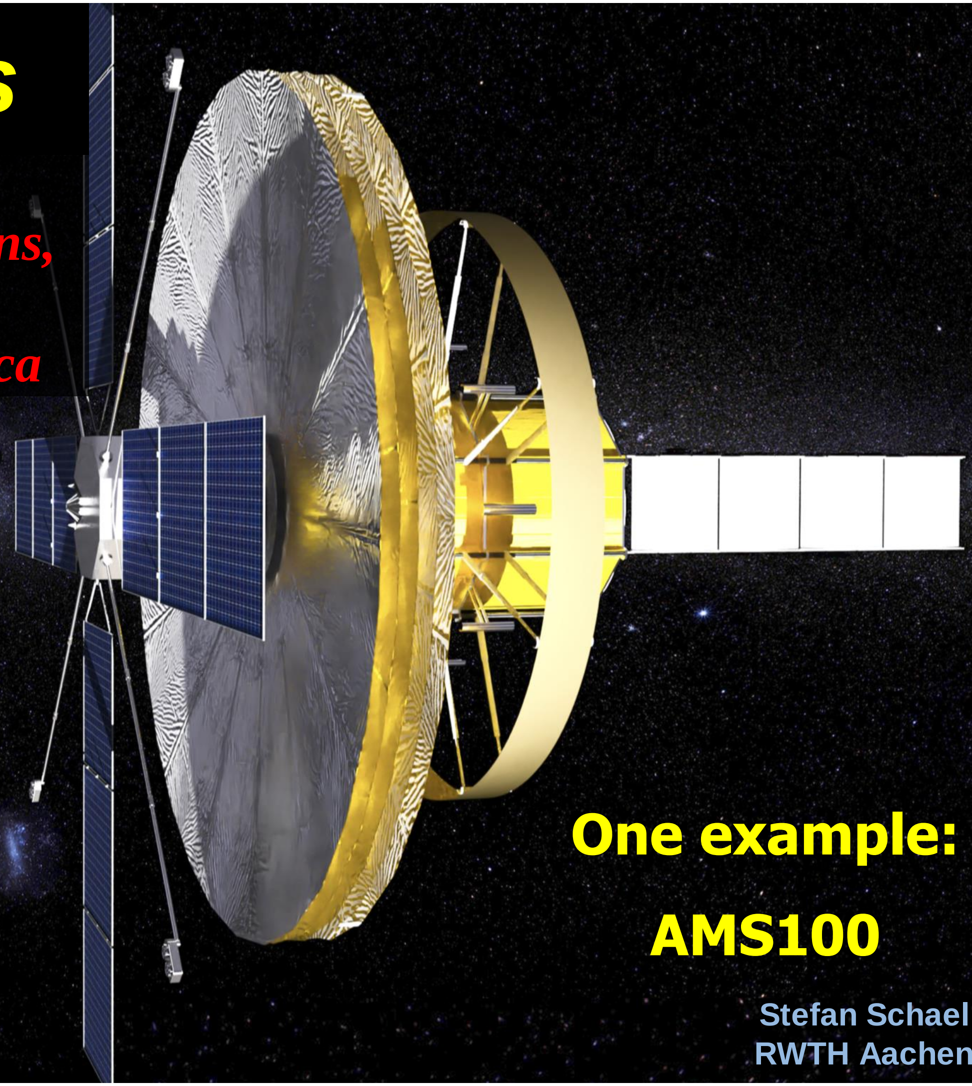

CERN seminar 4-11-2022

Université de Strasbourg

Particle Detectors

Lecture at the African School for Fundamental Physics and Applications,
28/11-09/12 2022
Nelson Mandela University, South Africa

Goal this lecture:

to discuss some examples

Looking at recent technological developments

infinite number of ideas for new detectors

Lecture IV

- **High purity segmented Ge-detectors for Nuclear physics**
- **LHC detectors**
- **Recent developments of CMOS pixel detectors**
- **Fast detectors for time of flight measurements**
- **High granularity calorimeters**
- **AMS100 in space**

Exercises!!!!!

iPHC Institut Pluridisciplinaire Hubert CURIEN STRASBOURG

Ulrich.Goerlach@iphc.cnrs.fr, ASP Particle detectors

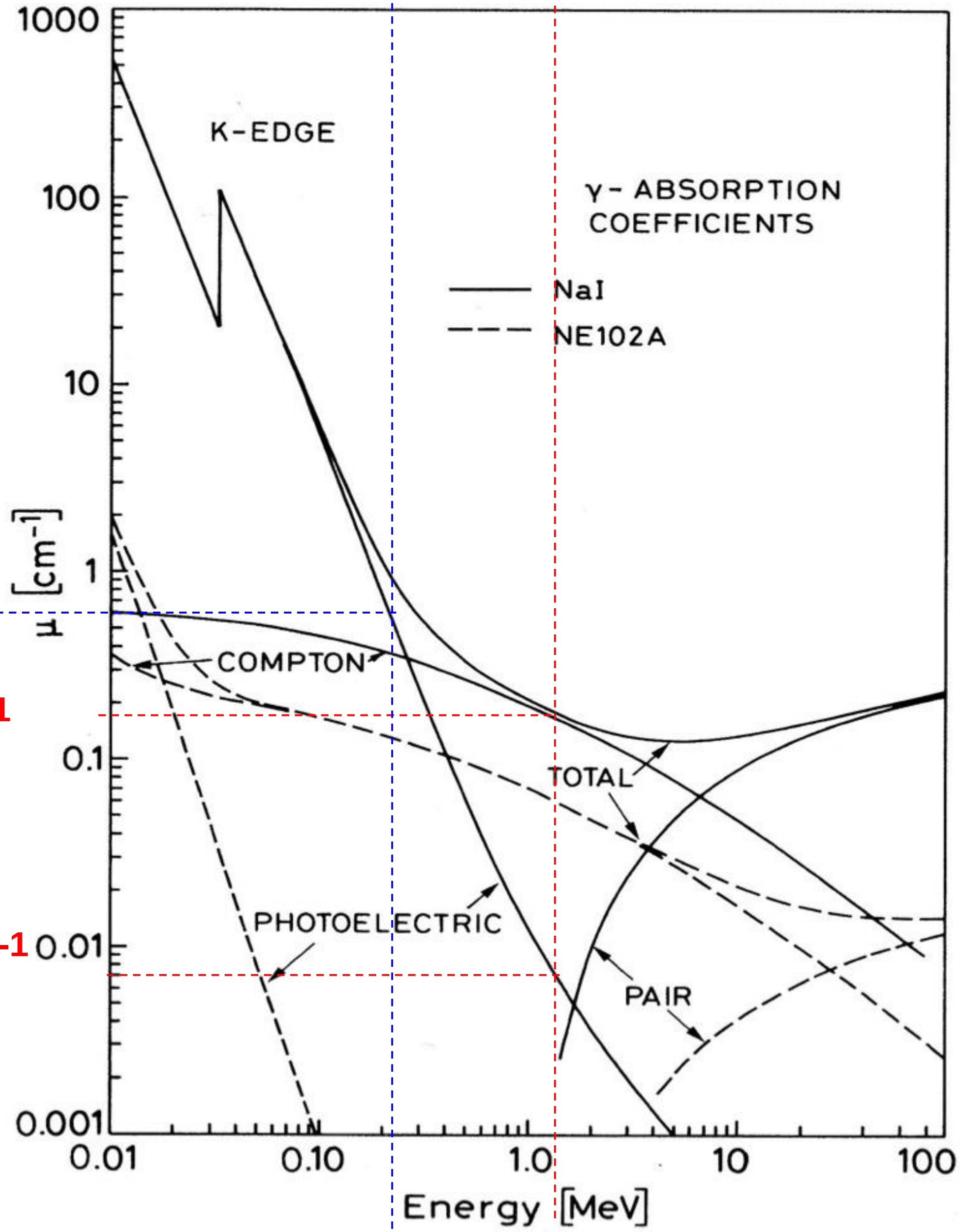

μ = 0.6 cm^{-1}

μ = 0.18 cm^{-1}

μ = 0.007 cm^{-1}

Photo-electric effect

Absorption of γ

Compton scattering

scattering γ –> γ'

Creation of (e^+e^-) pairs

Absorption of γ

Respone of NaI

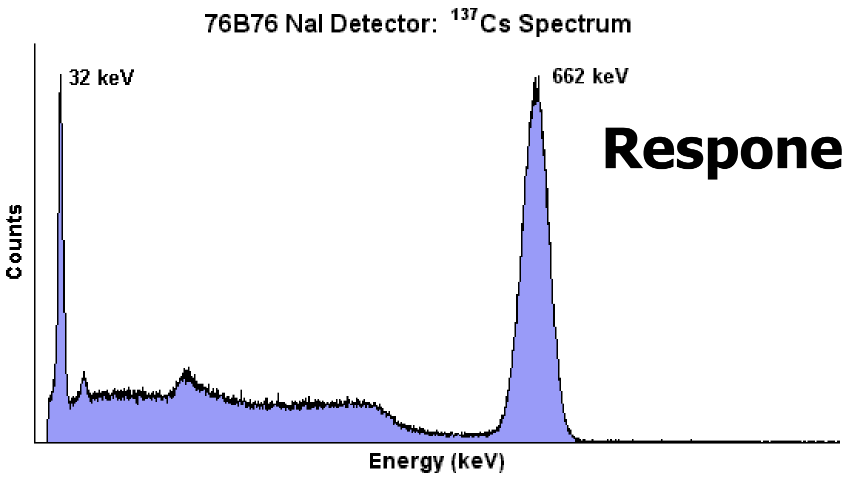

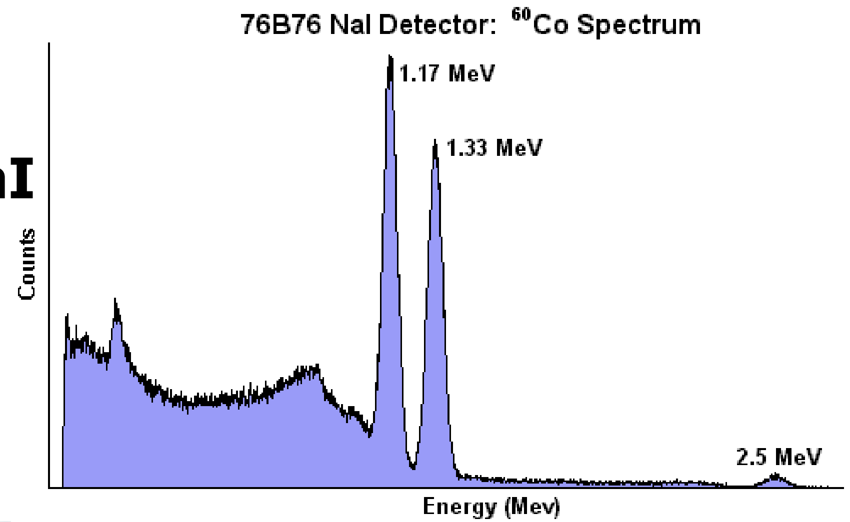

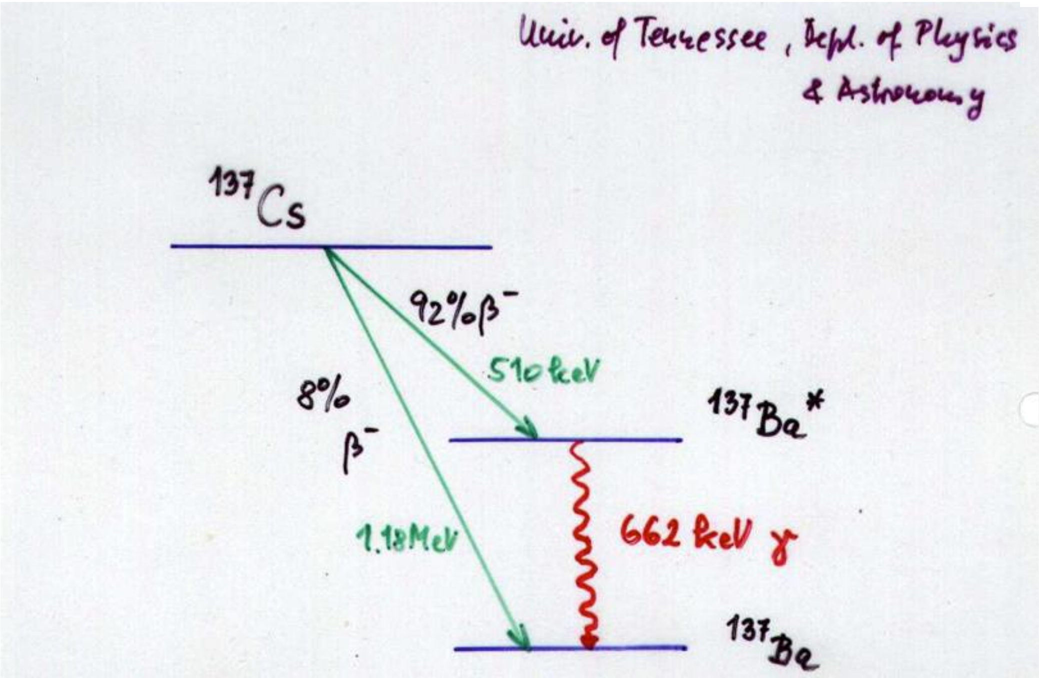

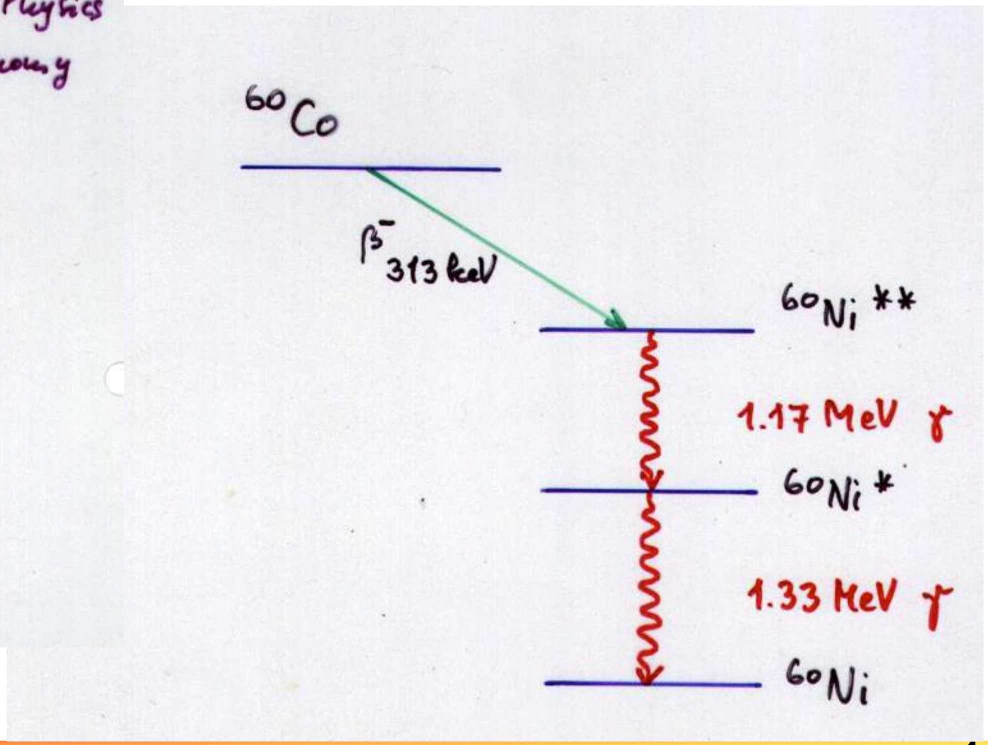

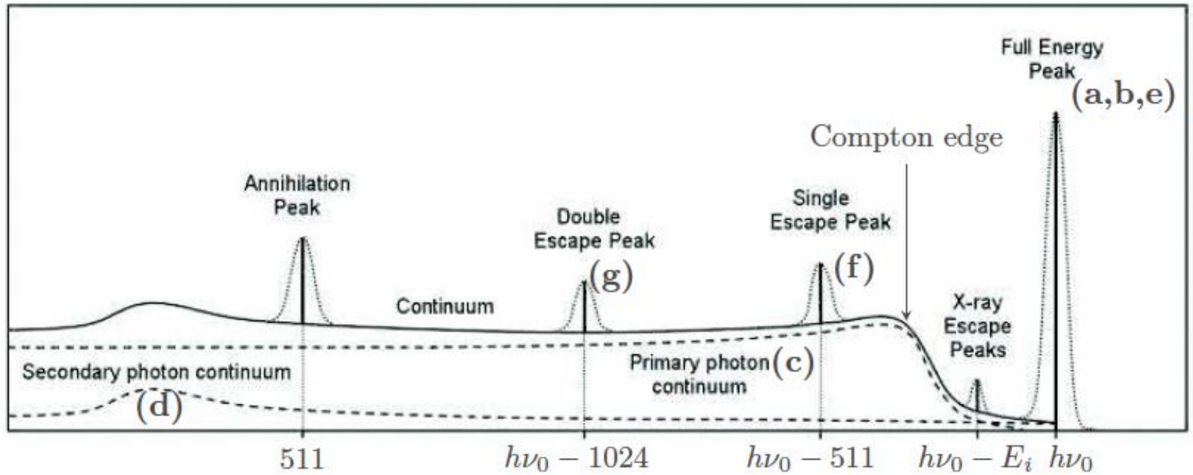

PHOTO-ELECTRIC EFFECT

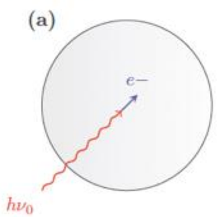

Figure 1.3: Effect of interaction processes on the predicted detector response function for mono-energetic γ-rays with $h\nu_0 >> 1.022MeV$.

COMPTON SCATTERING

PAIR CREATION

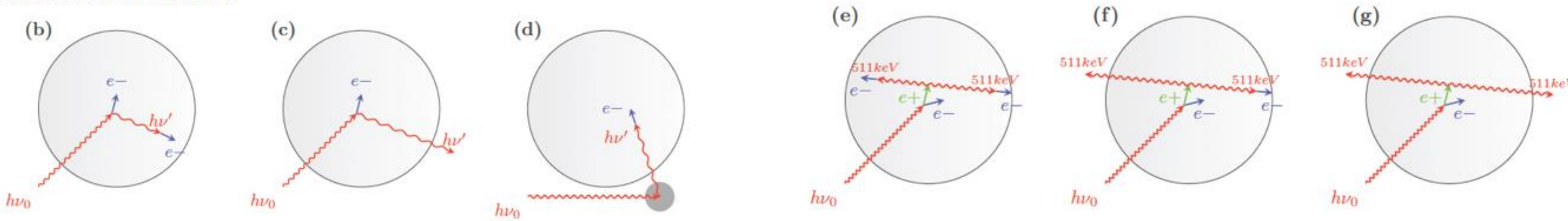

Ulrich.Goerlach@iphc.cnrs.fr, ASP Particle detectors

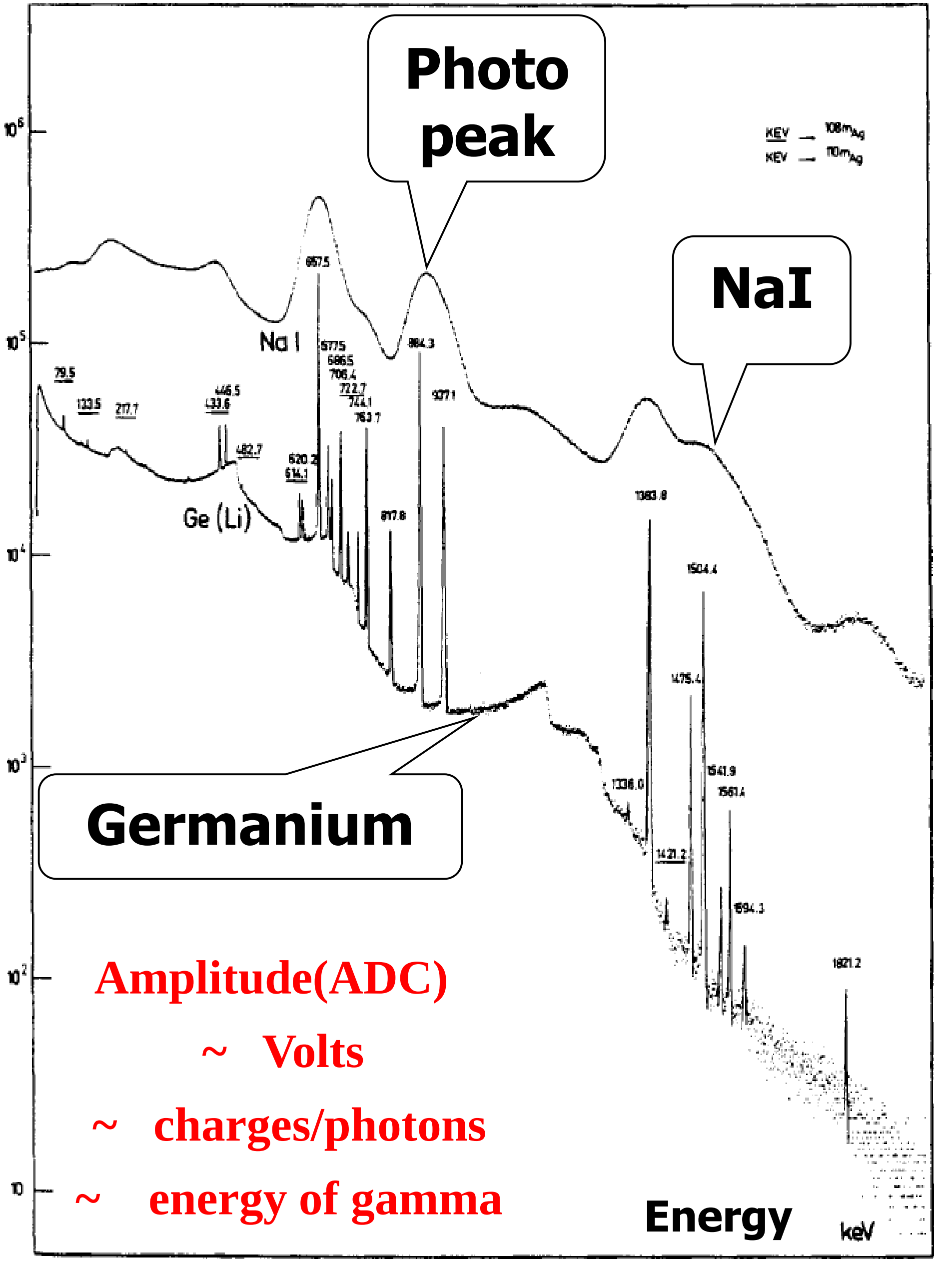

Large volume semi-conductor detector

Semi-conductor detectors

Material	E_g [eV]	w [eV]	Mobility (velocity/E)		τ_e [s]	τ_h [s]	density	Z [a.m.u]
			μ_e [cm^2/Vs]	μ_h [cm^2/Vs]			g/cm^3	
C (diamond)	5.5	13	1800	1200	$2\ 10^{-9}$	$2\ 10^{-9}$	3.515	6
Si	1.12	3.61	1350	480	$5\ 10^{-3}$	$5\ 10^{-3}$	2.33	14
Ge	0.67	2.98	3900	1900	$2\ 10^{-5}$	$2\ 10^{-5}$	5.32	32
GaAs	1.42	4.70	8500	450	$5\ 10^{-8}$	$5\ 10^{-8}$	5.32	31,33
CdTe	1.56	4.43	1050	100	$1\ 10^{-6}$	$1\ 10^{-6}$		48,52
HgI_2	2.13	4.20	100	_	$1\ 10^{-6}$	$2\ 10^{-6}$		53,80

$$\frac{dN}{N} = \frac{1}{\sqrt{N}} \;;\; E \sim N; \quad N = \text{numb. of (e,h))}$$

Parameters Values for Materials Used in Fabricating Semiconductor Radiation Sensors [3]

Université de Strasbourg

Inverse Polarisation

$$d\Big|_{V_{bias}} = x_n + x_p = \sqrt{\frac{2\varepsilon\left(\phi_0 + V_{bias}\right)}{e}\frac{\left(N_A + N_D\right)}{N_A N_D}}$$

Holes move to « - »

electrons move to contact "+"

$$N_A \gg N_D$$

depletion in n-type

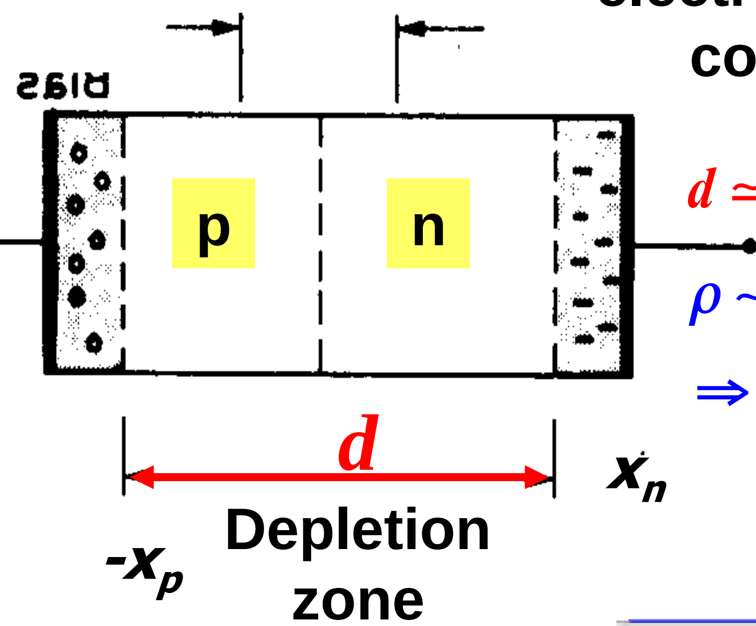

$$d \simeq x_n \approx 0.53\sqrt{\rho_n \phi_0}\ \mu m$$

$$\rho \sim 2 \cdot 10^4\ \Omega cm,\ \phi_0 \sim 1V$$

$$\Rightarrow d \sim 75\ \mu m$$

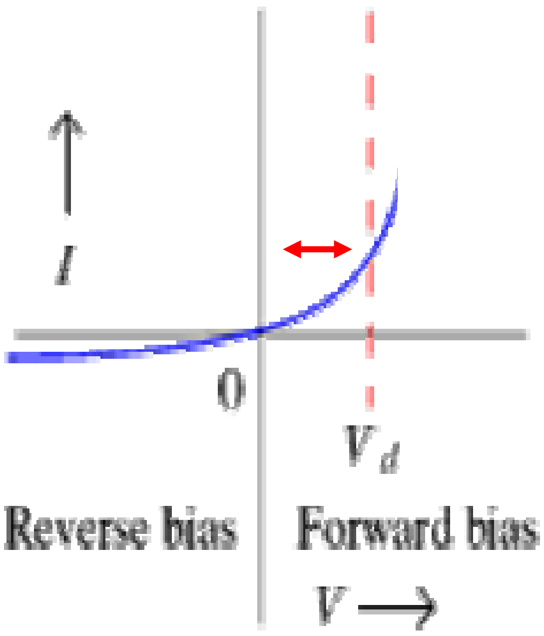

Real Diode

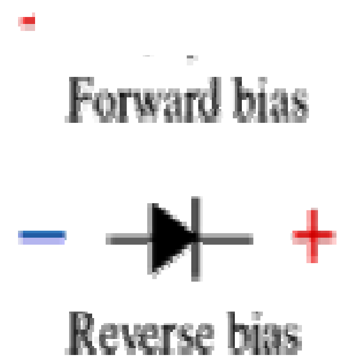

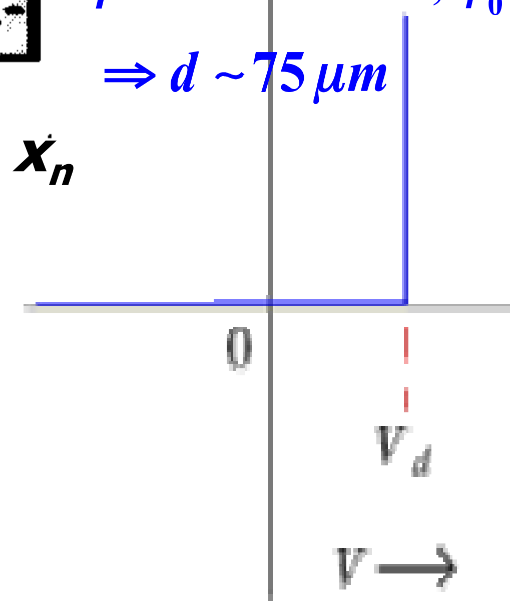

'Ideal' Diode

Large volume detectors

- **Depletion zone :**

$$d\Big|_{V_{bias}} = x_n + x_p = \sqrt{\frac{2\varepsilon\left(\phi_0 + V_{bias}\right)}{e}\frac{\left(N_A + N_D\right)}{N_A N_D}}$$

$$N = N_A \ll N_D;\ \ \phi_0 \ll V_{bias}$$

$$d\Big|_{V_{bias}} = \sqrt{\frac{2\varepsilon V_{bias}}{eN}}\ ;\ N = N_A \text{ ou } N_D = \text{net impurity of material}$$

$$N = 10^{+13}\,atoms/cm^3;\ V_{bias} = 3000\,Volt;$$

$$d\Big|_{V_{bias}=3000\,Volt} = 2.2\,mm$$

- **High purity :**

$$N_A\ ou\ \ N_D = 10^{+10}\,atoms/cm^3;\ V_{bias} = 1000\,Volt;\ \varepsilon = 16\cdot\varepsilon_0;$$

$$\varepsilon_0 = 8.85\cdot 10^{-12}\,F/m;\ F = Coulomb/Volt\ ;\ e = 1.6\cdot 10^{-19}\,Coulomb$$

$$d\Big|_{V_{bias}=1000\,Volt} = 1.8\,cm$$

$$d\Big|_{V_{bias}=2000\,Volt} = 2.5\,cm$$

$$d\Big|_{V_{bias}=3000\,Volt} = 3.1\,cm$$

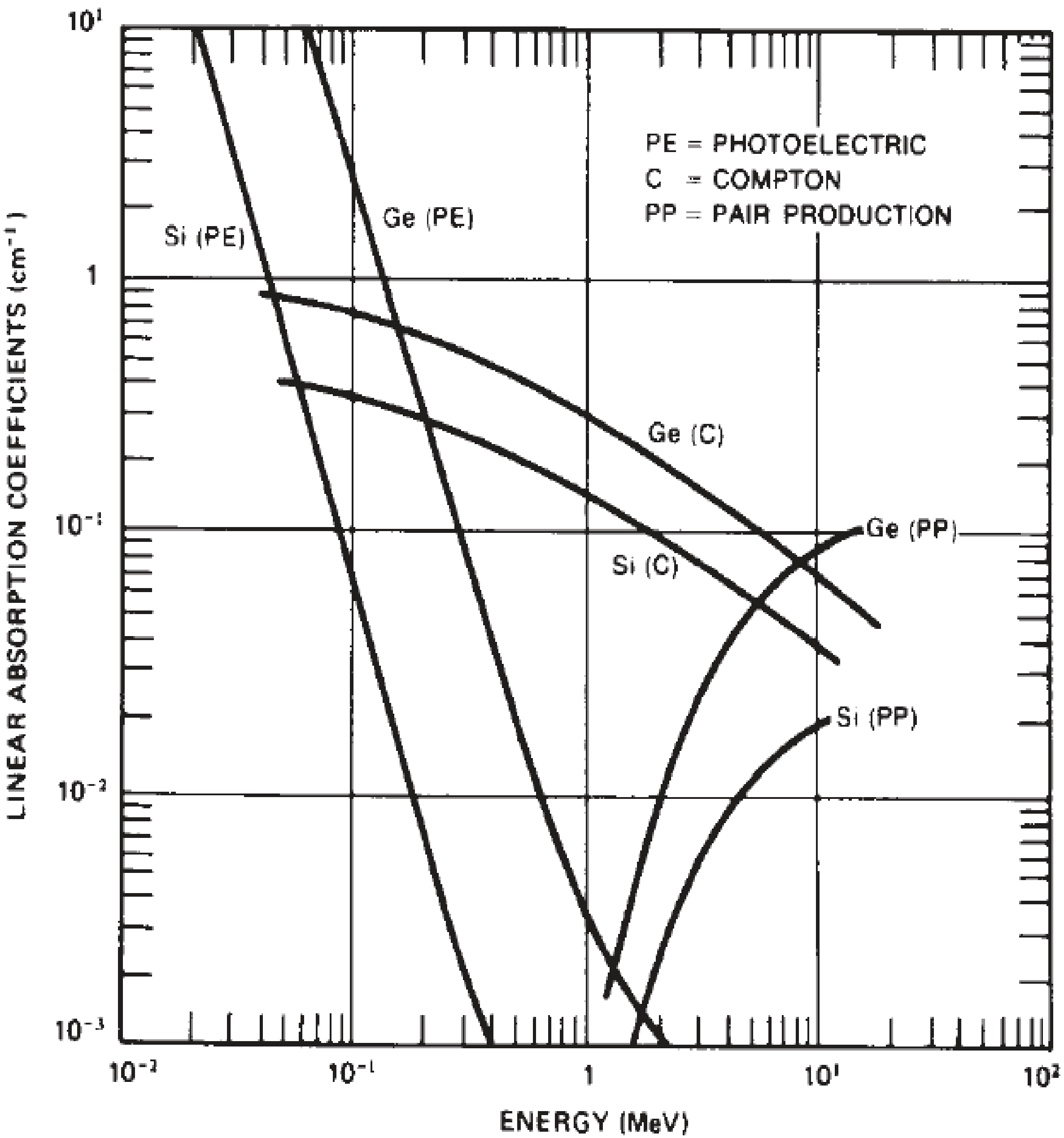

High Purity Germanium

Energy measurement of gammas

($|N_A - N_D| \cong 10^{10}$ cm^{-3}):

- E_{gap} = 0.74 eV ⇒ operation temperature : T= 77K
- w_{eh}=2.98 eV ⇒excellent resolution
  - E_γ = 1 MeV, dE ≅ 1 keV
  - “High” photo peak efficiency

Germanium detectors

Operation temperature: T= 77K (Liquid Nitrogen)

Configuration : co-axial

Electronics is mounted very close to the Crystal

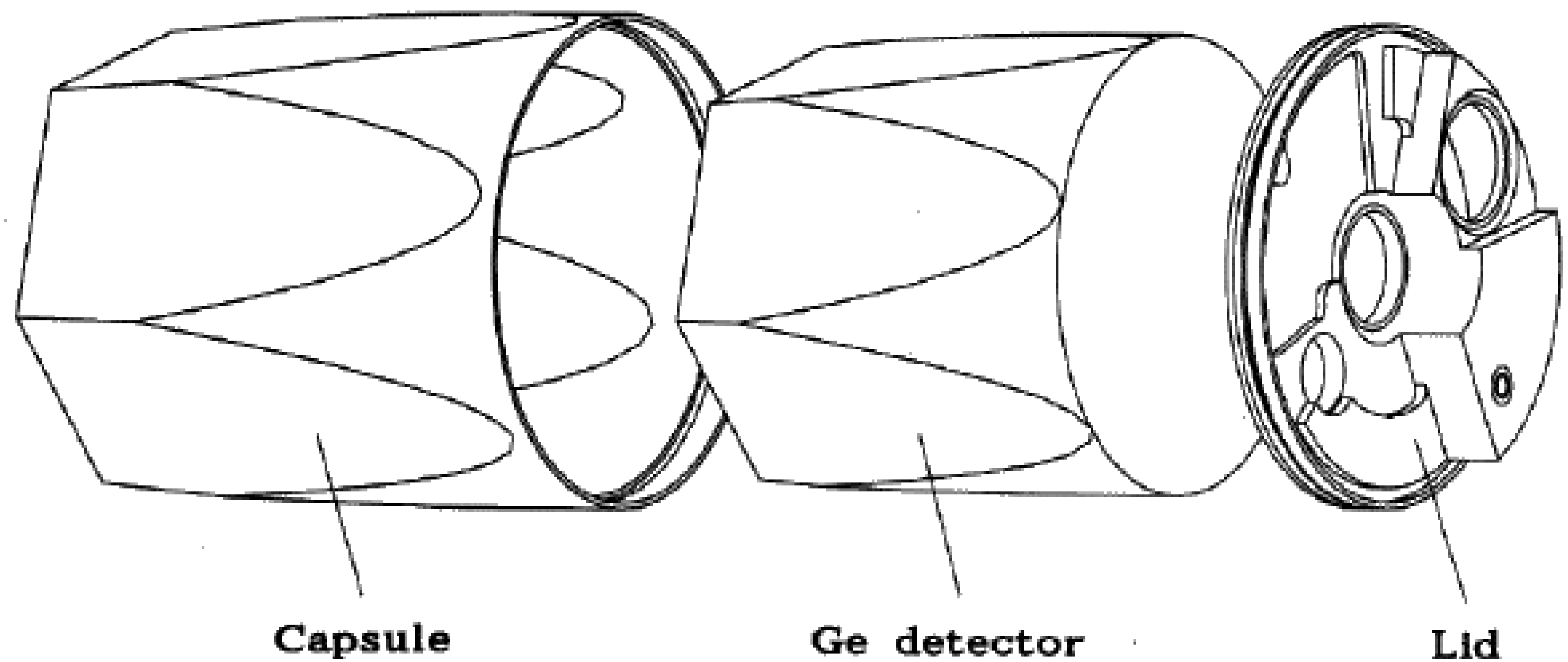

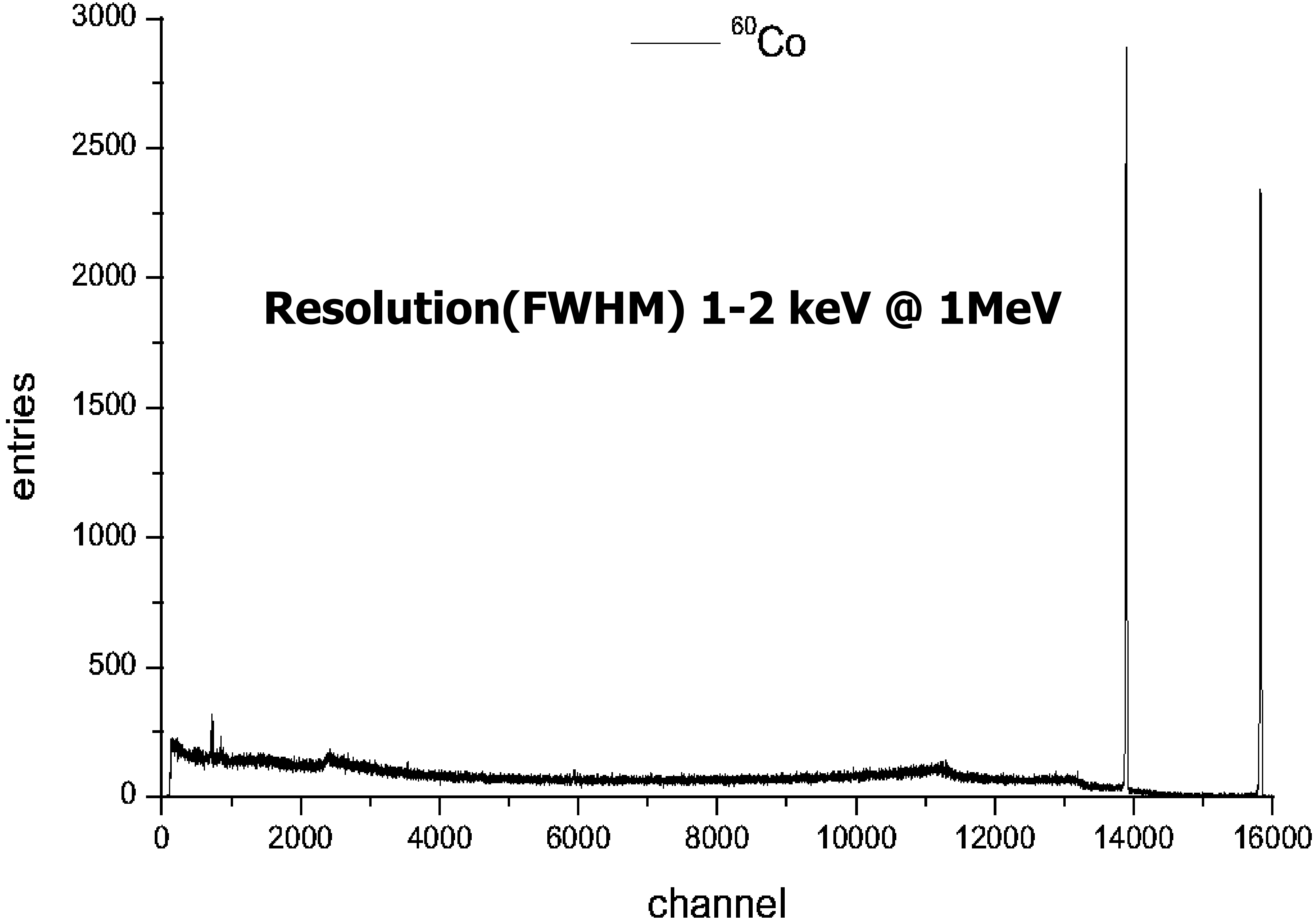

3000
2500
2000
1500
1000
500
0
entries
60Co
Resolution(FWHM) 1-2 keV @ 1MeV
0
2000
4000
6000
8000
10000
12000
14000
16000
channel

incidence : système anti-Compton

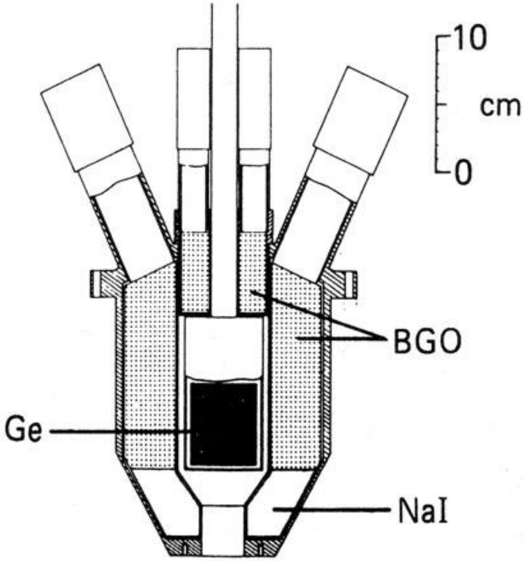

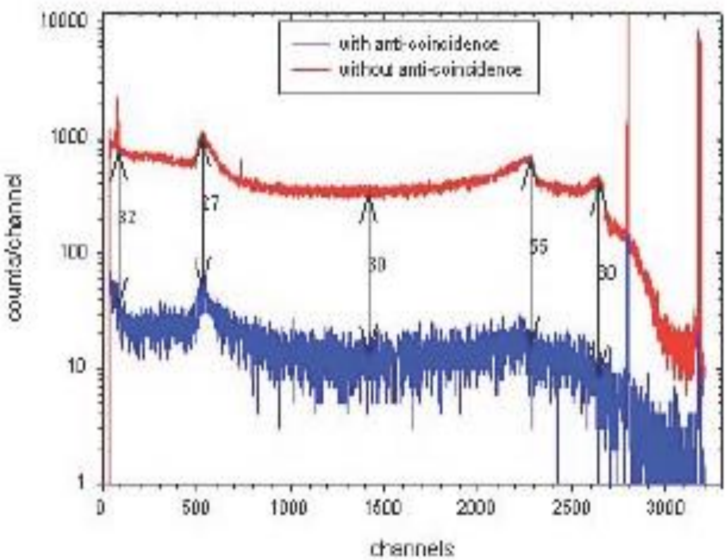

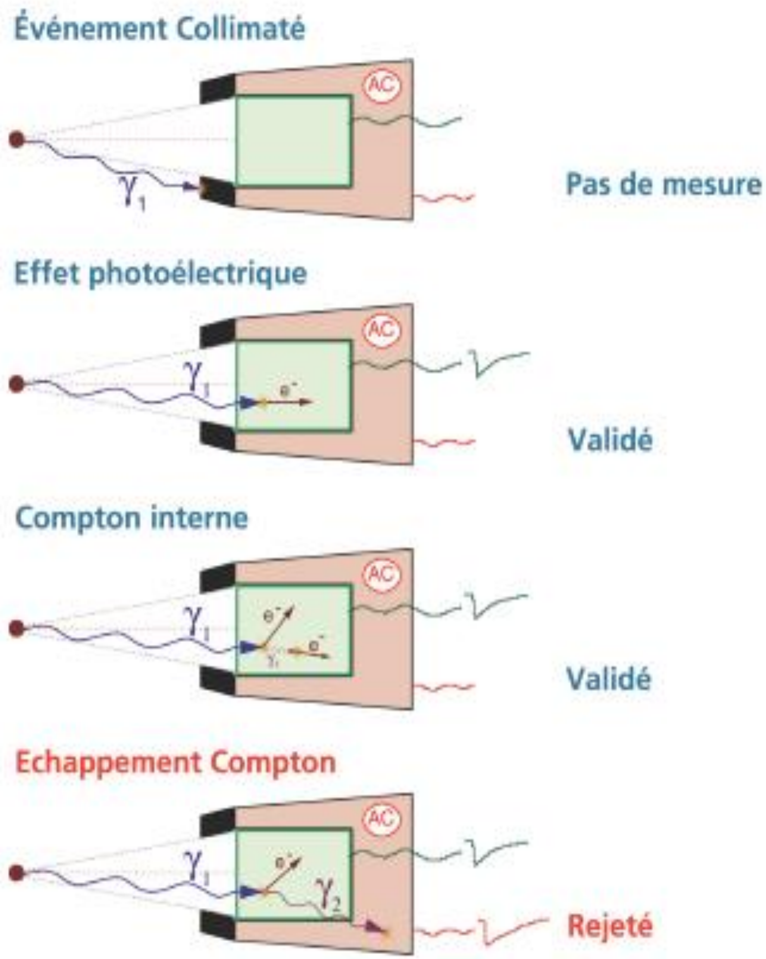

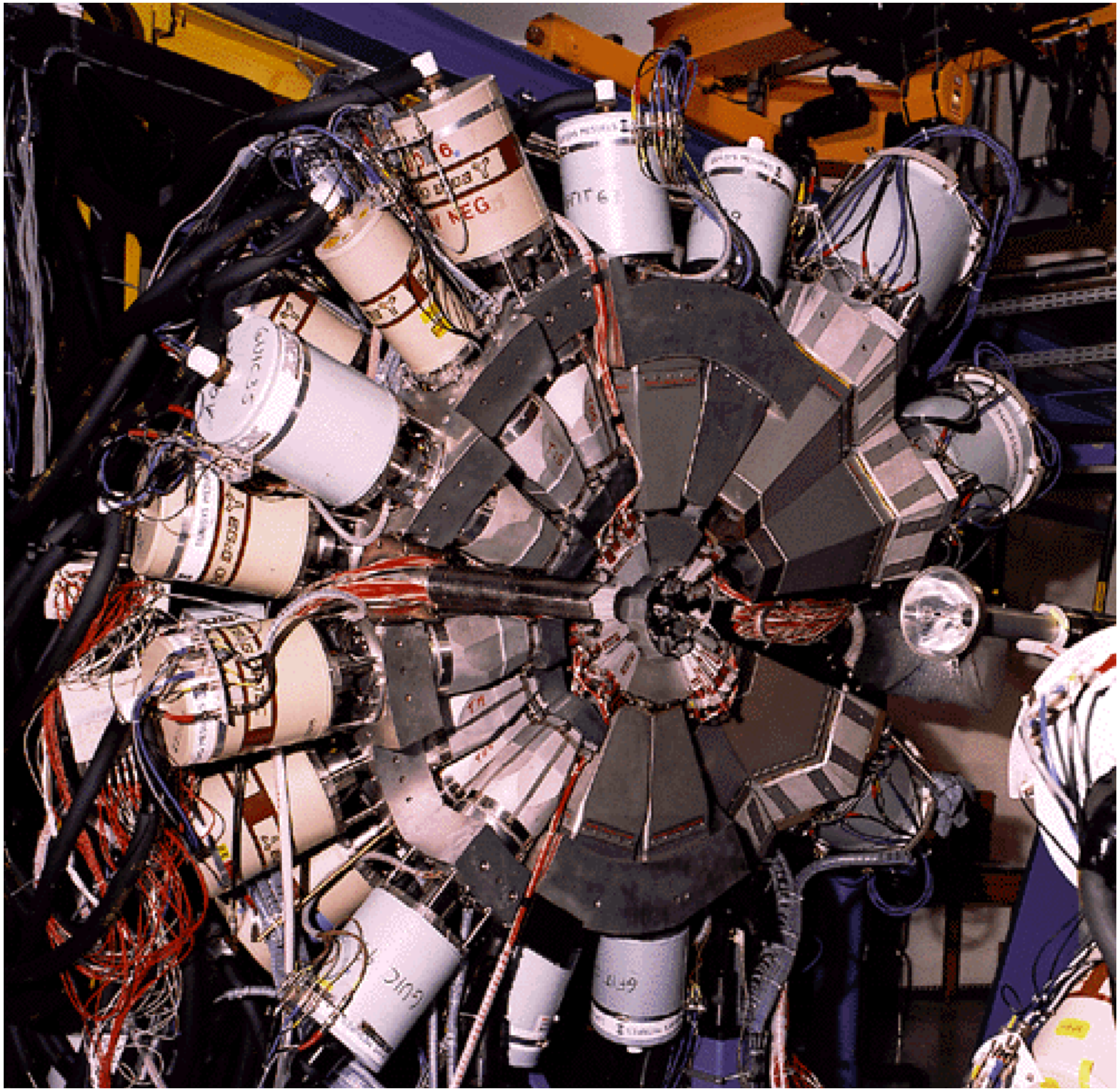

Euroball à Strasbourg

Il y a quelques années

Challenges in Nuclear Structure Physics

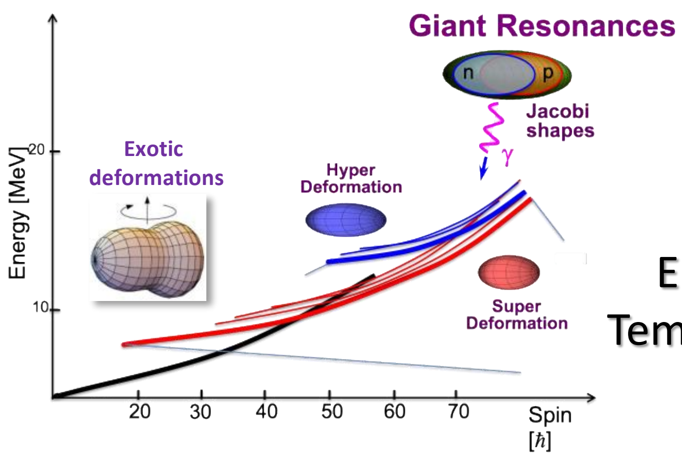

Properties of excited states

- γ-ray spectroscopy

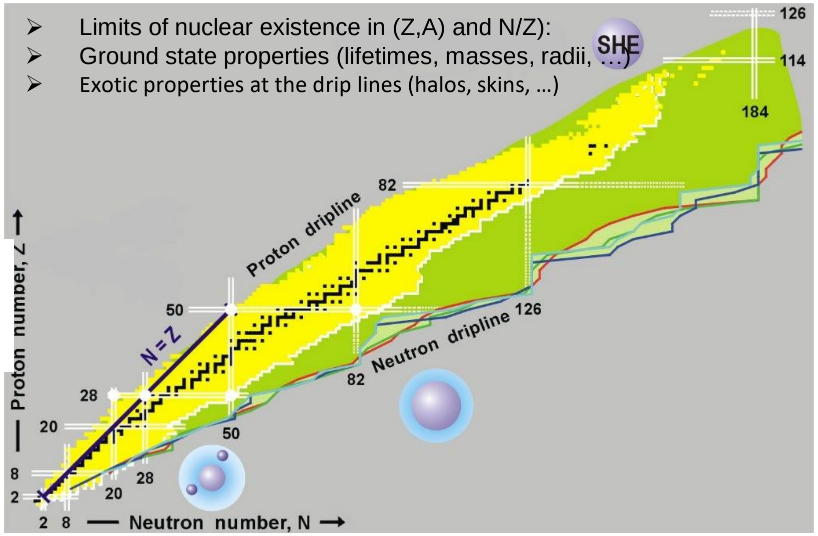

Energy/ Temperature

N/Z - isospin

Spin

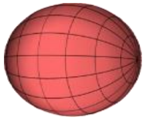

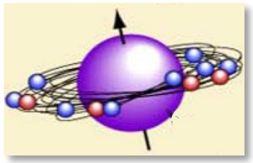

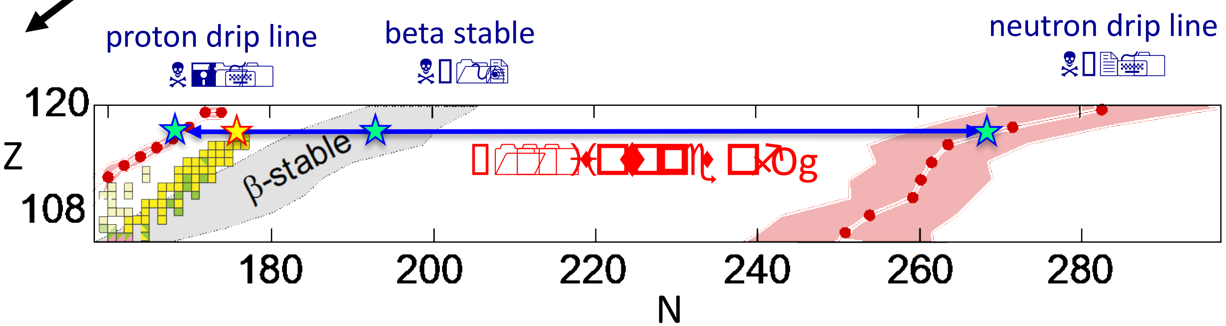

The idea of γ-ray tracking

Compton Shielded Ge

ε_{ph} ~ 10%
N_{det} ~ 100

Ω ~ 40%
θ ~ 8°

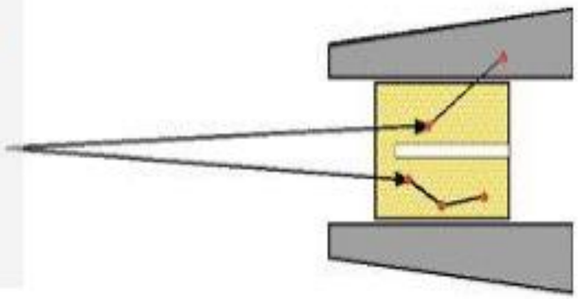

large opening angle means poor energy resolution at high recoil velocity.

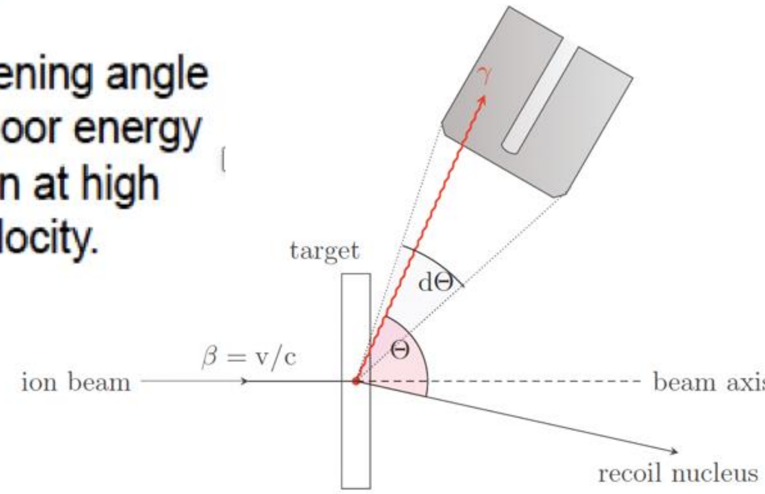

Figure 1.12: Doppler broadening

Previously scattered gammas were wasted.
Technology is available now to track them.

Ge Tracking Array

ε_{ph} ~ 50%
N_{det} ~ 100

Ω ~ 80%
θ ~ 1°

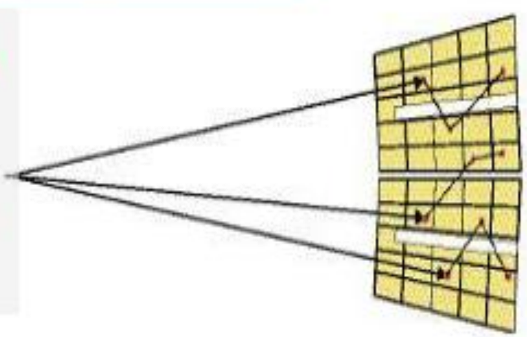

Combination of:

- segmented detectors
- digital electronics
- pulse processing
- tracking the γ-rays

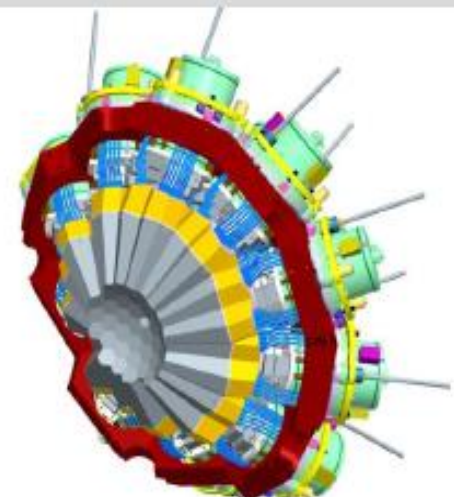

What is AGATA?

13 Countries, > 40 Institutions

AGATA Definition: NIM A 668 (2012) 26

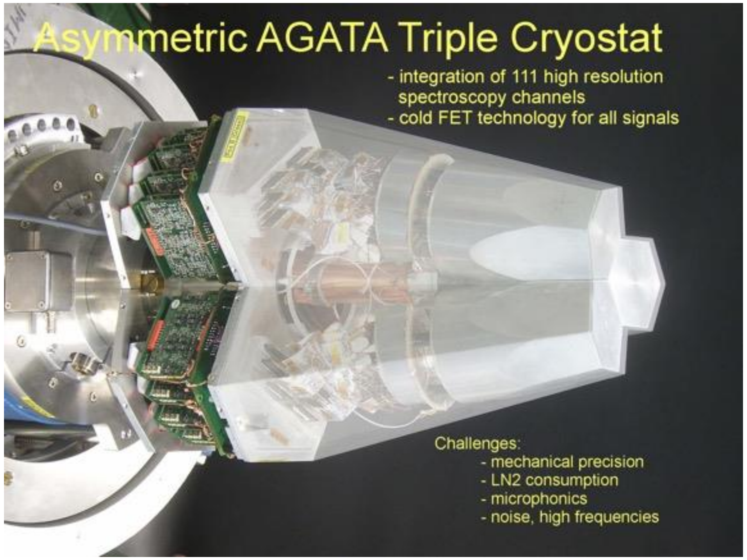

- Solid Sphere of Ge material: Solid angle coverage ~ 82 %
- 36-fold segmentation of crystal
- Track each gamma interaction through the crystal
- Reconstruct and disentangle gammas

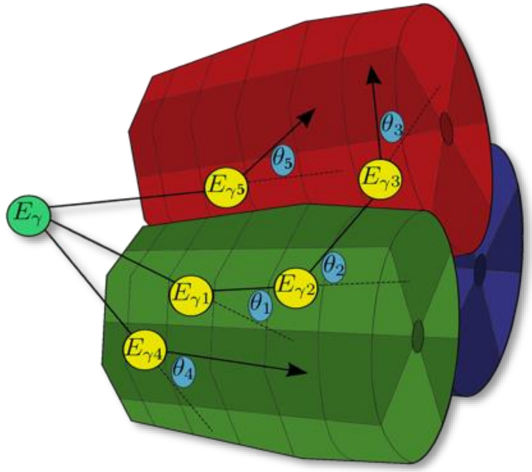

Rates	3 MHz (Mγ= 1)	300 kHz (Mγ= 30)
Efficiency	43% (Mγ= 1)	28% (Mγ = 30)
Peak/Total	58% (Mγ= 1)	49% (Mγ = 30)
Angular Resolution	~1º	
FWHM (1MeV), v/c = 50%	~6keV	

180 hexagonal crystals:	3 shapes
3 fold clusters (cold FET):	60 all equal
Inner radius (Ge):	23.5 cm
Amount of germanium:	362 kg
36-fold segmentation	6480 segments

signal formation in

Ge-HP

Cylindrical geometry

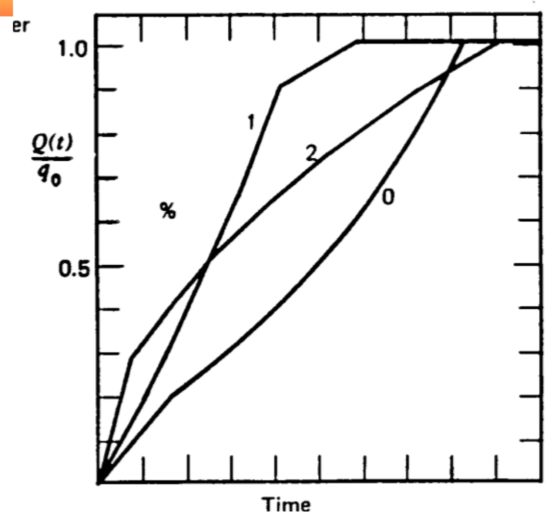

Gamma interactions

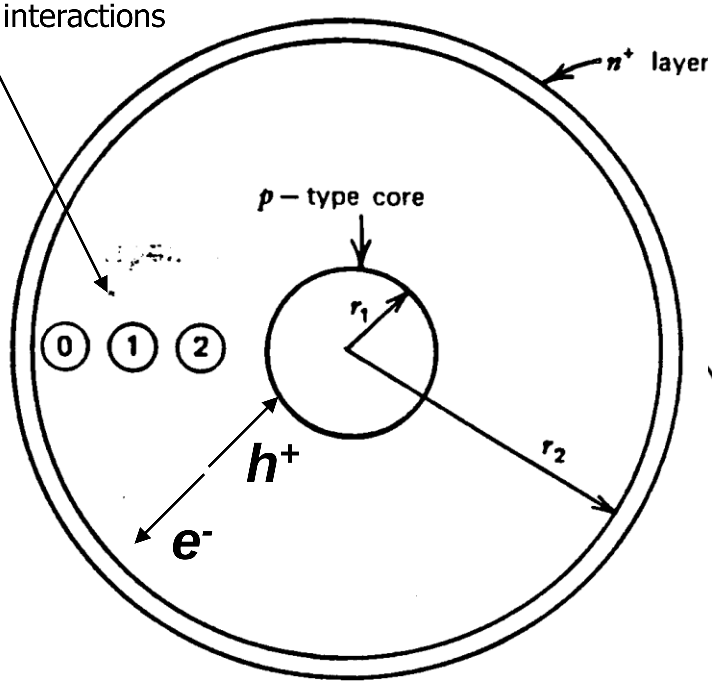

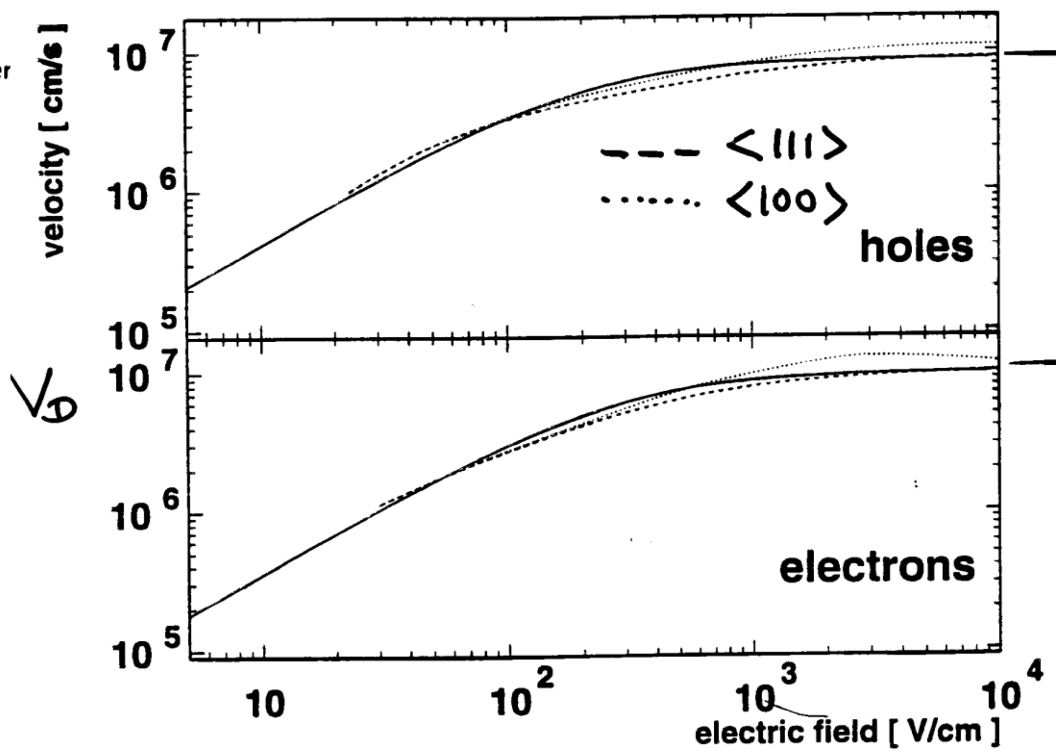

Segmentation of High Purity Ge crystal

Divide the electrodes on the surface of the detector

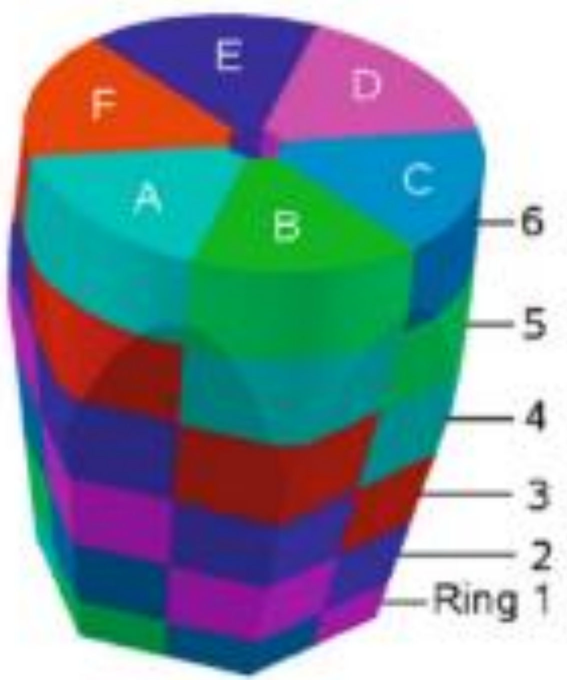

Weighting field shows how the segmentation works

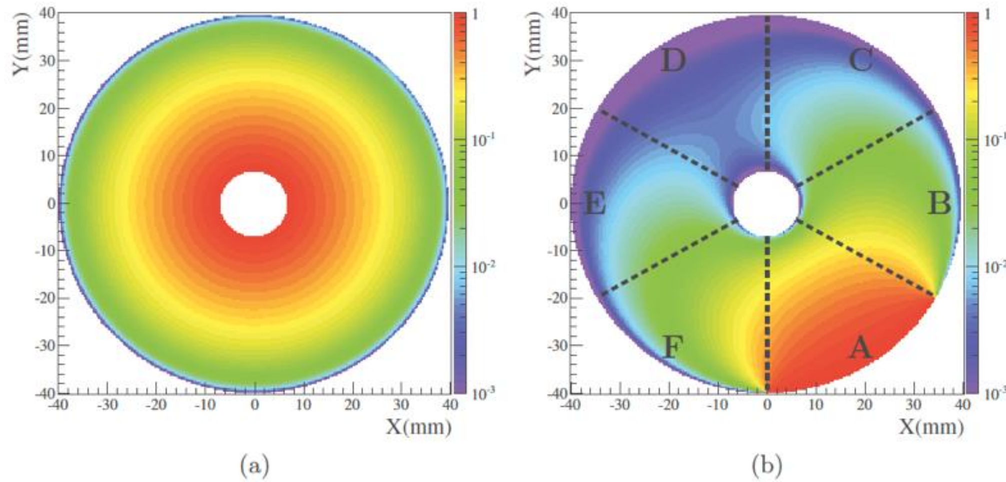

Figure 2.2: Weighting-potential distributions of the Core (a) and of segment A (b). Calculation conditions are the following: readout electrode at unit potential, all other electrode at zero potential, no space charge inside the material.

$$Q(t) = -q \cdot [\phi_w(x_h(t)) - \phi_w(x_e(t))]$$

$$i(t) = q \cdot [E_w(x_h(t)) \cdot v_h(t) - E_w(x_e(t)) \cdot v_e(t)]$$

ϕ_w and E_w are the weighting potential and the weighting field.

Michaël Ginsz, PhD thesis 2017

AGATA Tracking Concept

1

Highly segmented

HPGe detectors

γ

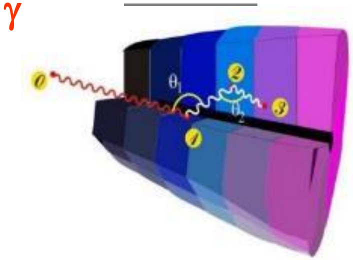

2

Digital electronics

to record and process signals

3

Pulse Shape Analysis to decompose recorded waves

$(x,y,z,E,t)_i$

Identified interaction points

4

Evaluation of permutations of interaction points

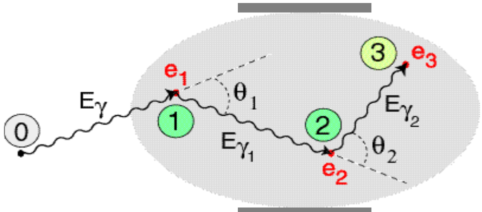

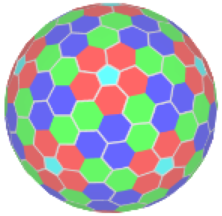

Reconstructed γ rays

Pulse Shape Analysis Concept

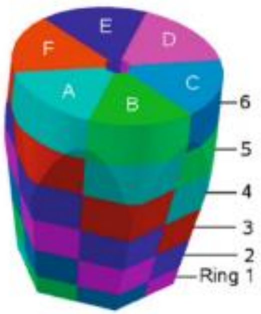

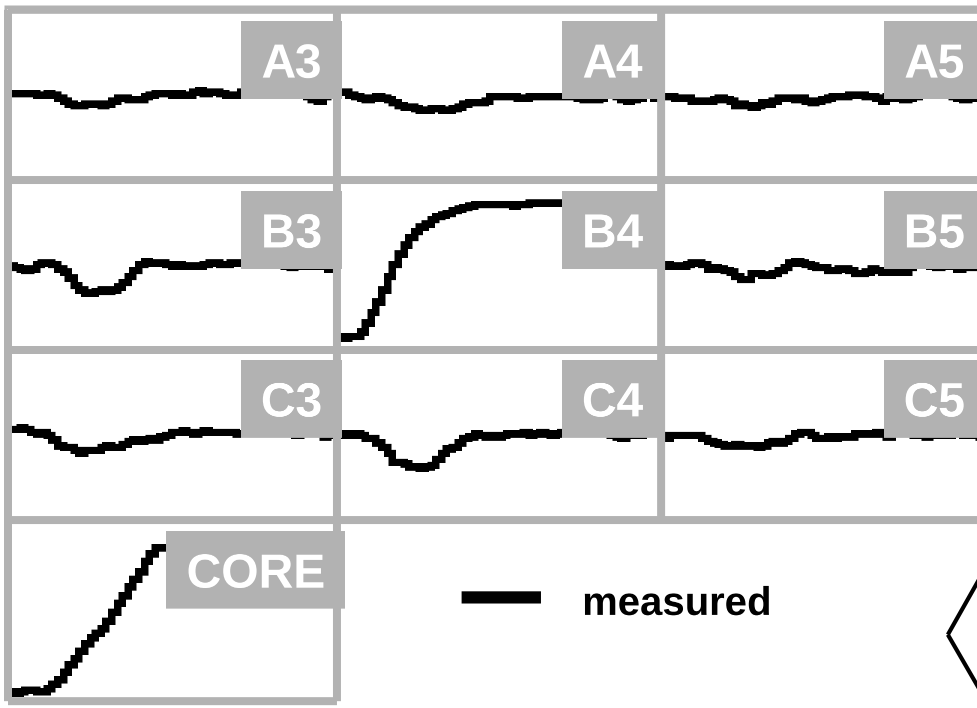

791 keV deposited in segment B4

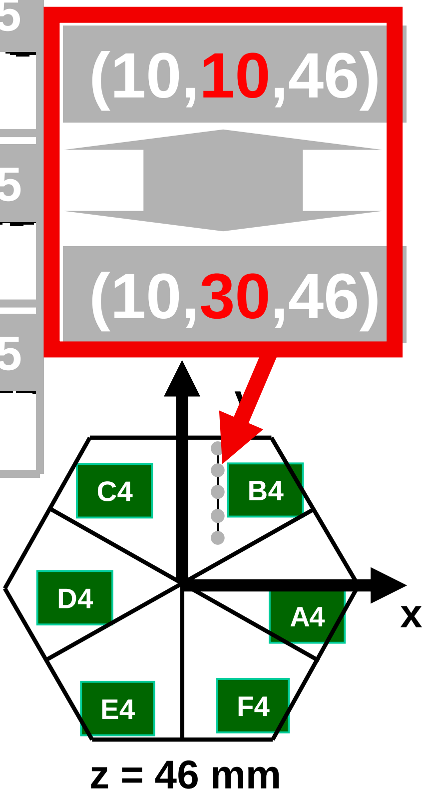

Pulse Shape Analysis Concept

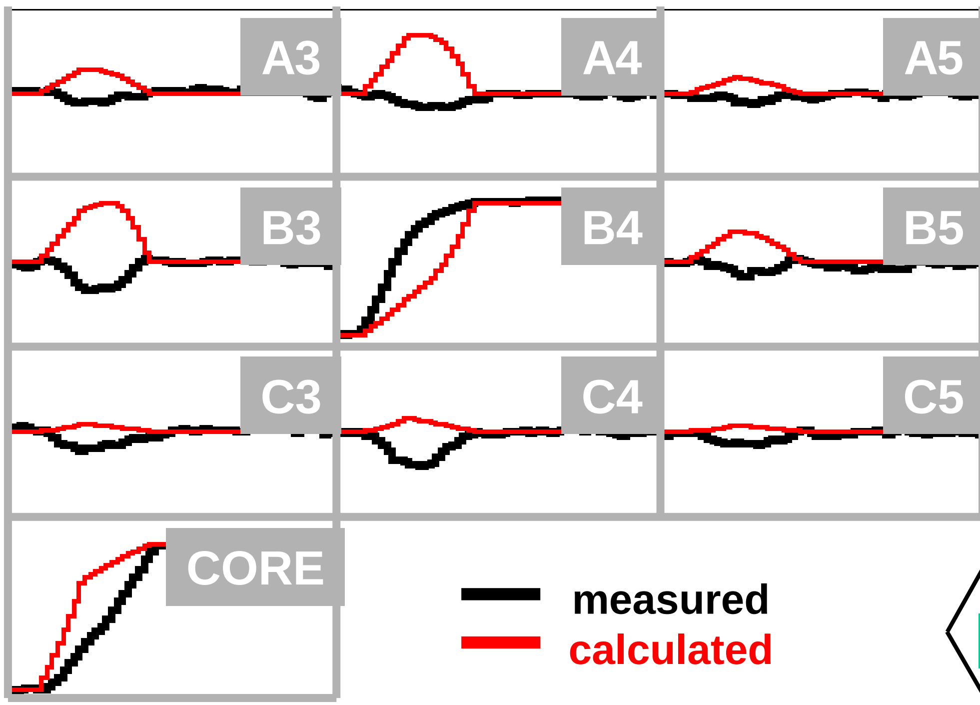

791 keV deposited in segment B4

Calculated from Electric field simulation

(10,10,46)

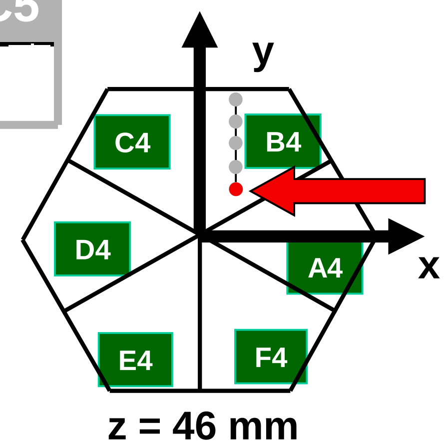

z = 46 mm

Université de Strasbourg

Pulse Shape Analysis Concept

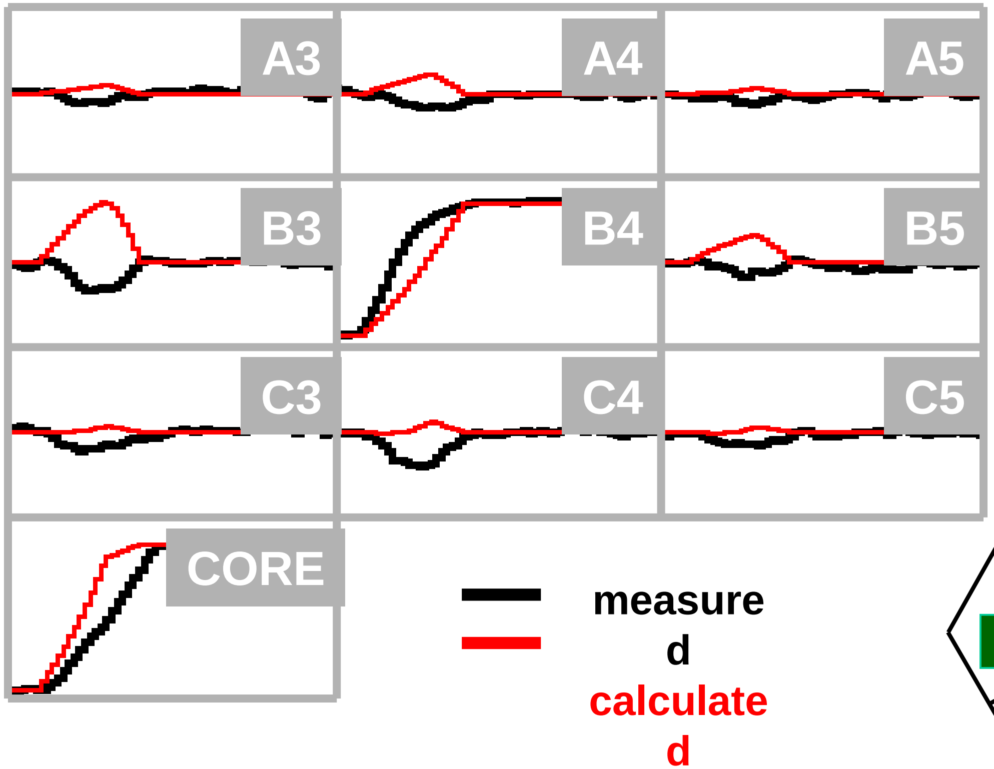

791 keV deposited in segment B4

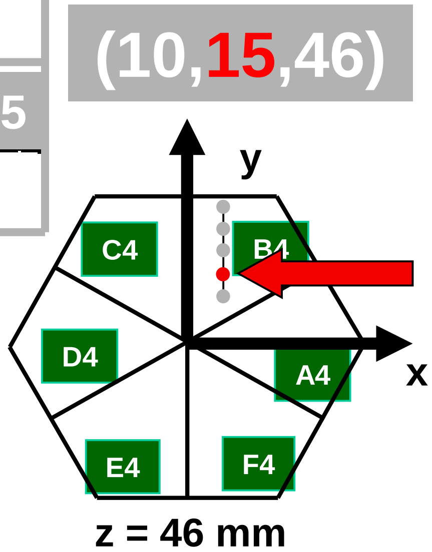

Pulse Shape Analysis Concept

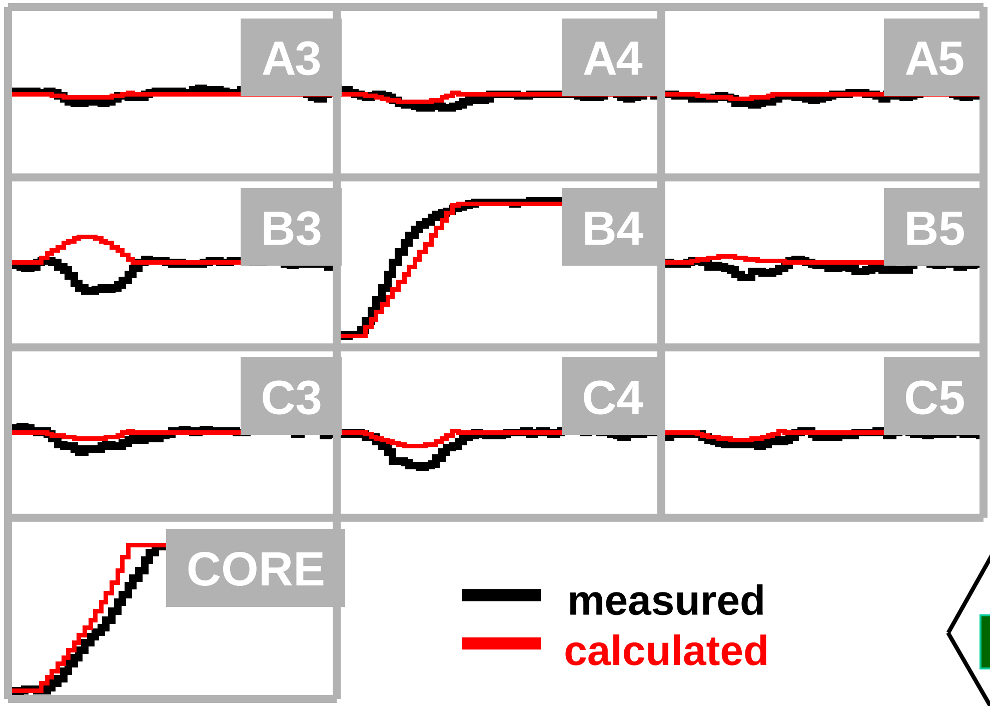

791 keV deposited in segment B4

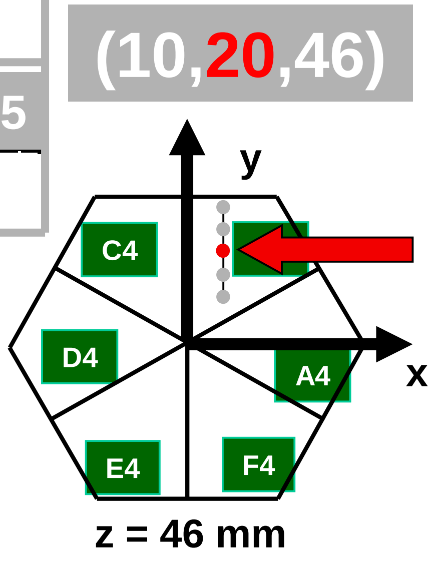

Université de Strasbourg

Pulse Shape Analysis Concept

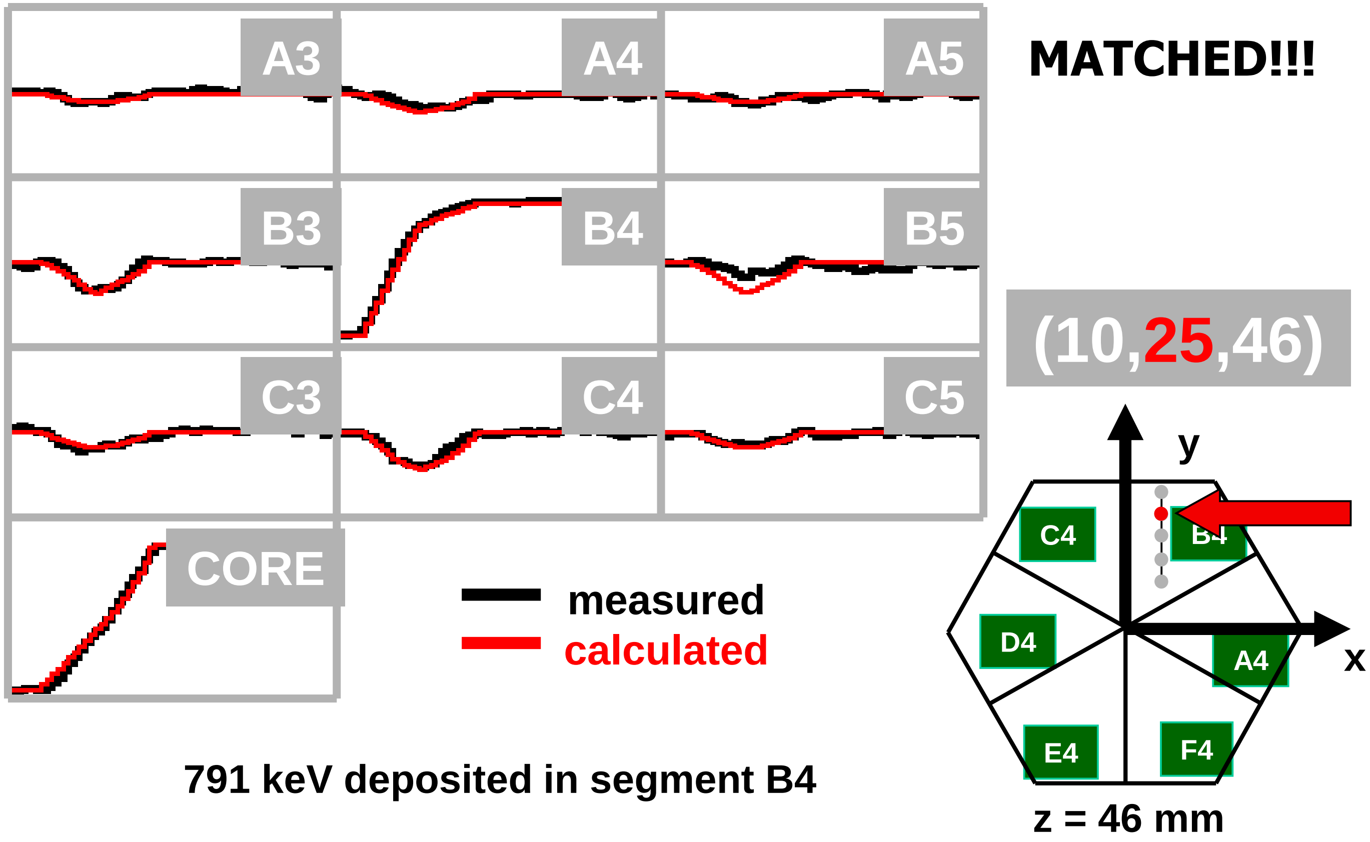

791 keV deposited in segment B4

Pulse Shape Analysis Concept

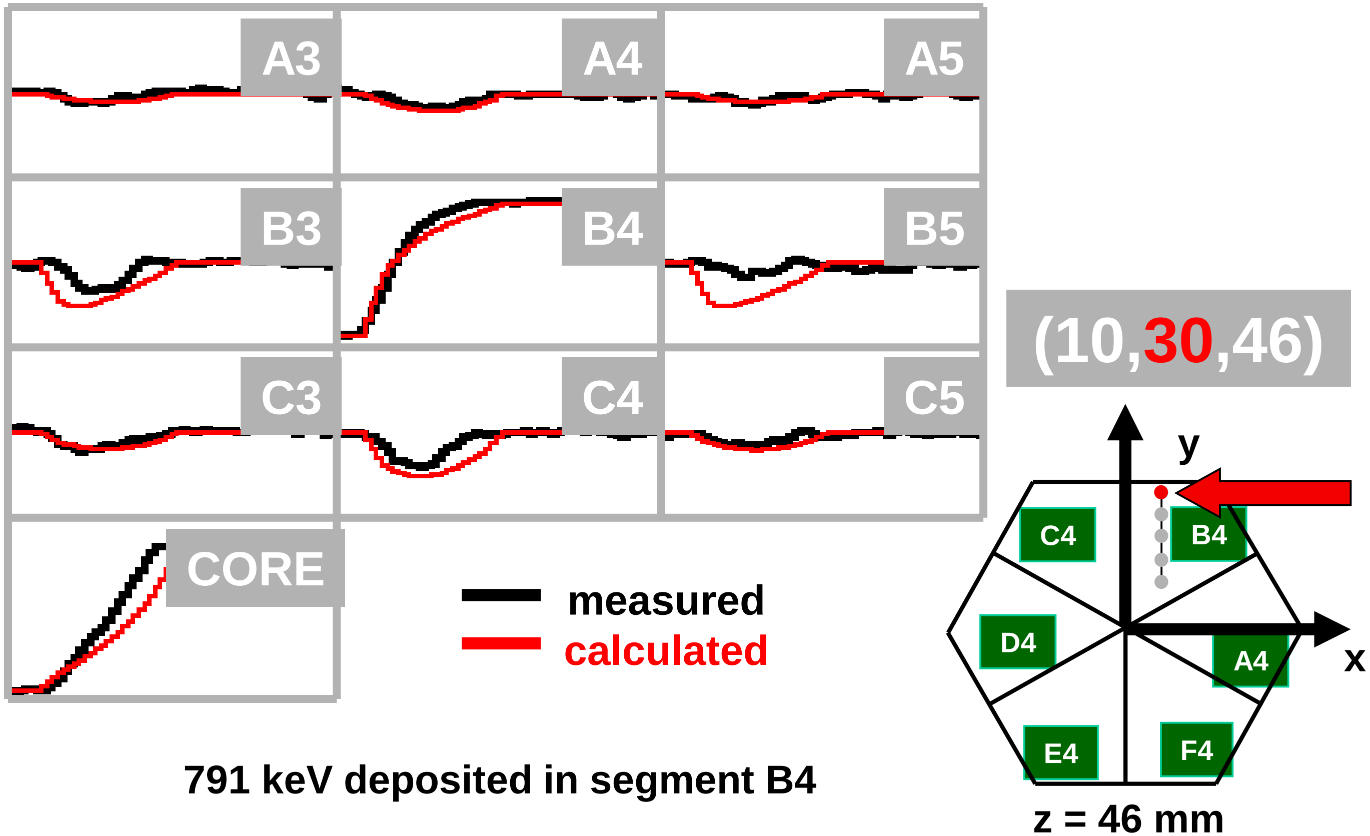

791 keV deposited in segment B4

Pulse Shape Analysis Concept

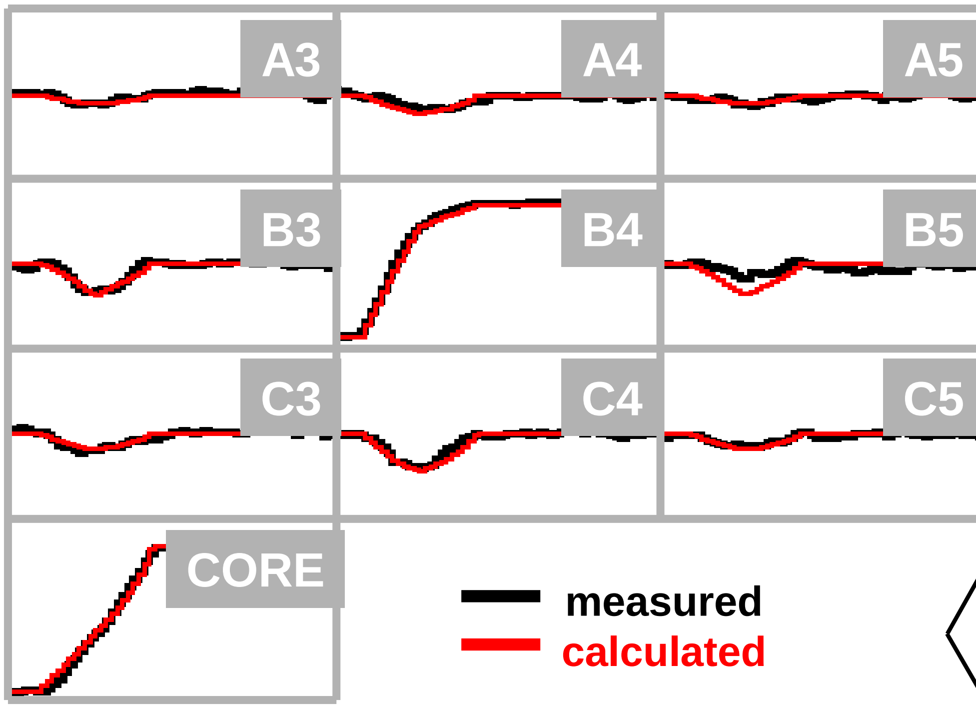

measured
calculated

791 keV deposited in segment B4

Result of *Grid Search* algorithm

(10,25,46)

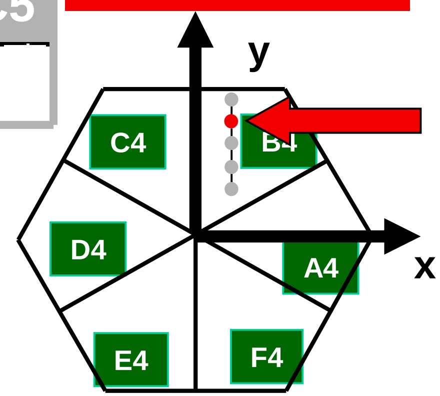

z = 46 mm

Evolution of AGATA

2012-2014
GSI, Germany
~25 detectors

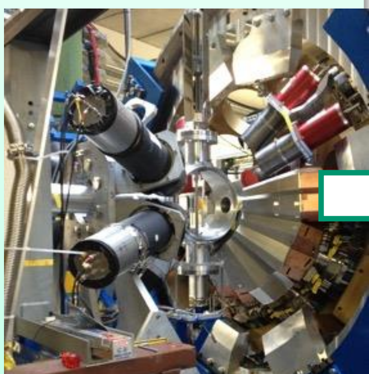

AGATA at GSI

2014-2021
GANIL, France
45 -> detectors

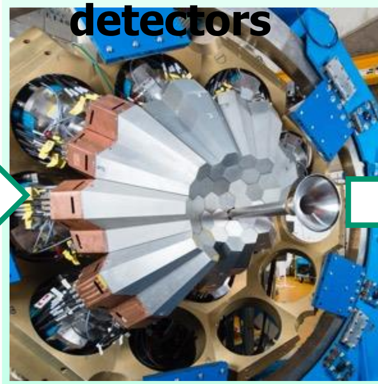

AGATA at GANIL

2021-2024
Legnaro, Italy
60 -> detectors

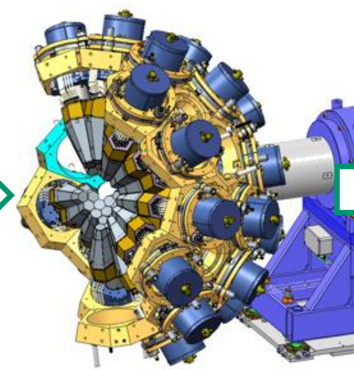

AGATA at LNL

2025 ->
FAIR, Germany
80-90 detectors

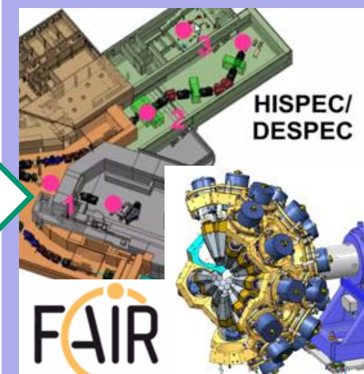

AGATA at NUSTAR

Reaccelerated RIBs:
- **Coulomb Excitation, Direct Reactions, Deep Inelastic, Fusion**
- **Direct and inverse kinematics β ~ 10%**

In-flight RIBs:
- **Relativistic Coulomb Excitation, Knockout, Fragmentation.**
- **β ~ 50%**

They think to have 60 detectors for AGATA by end 2023

Evolution of AGATA

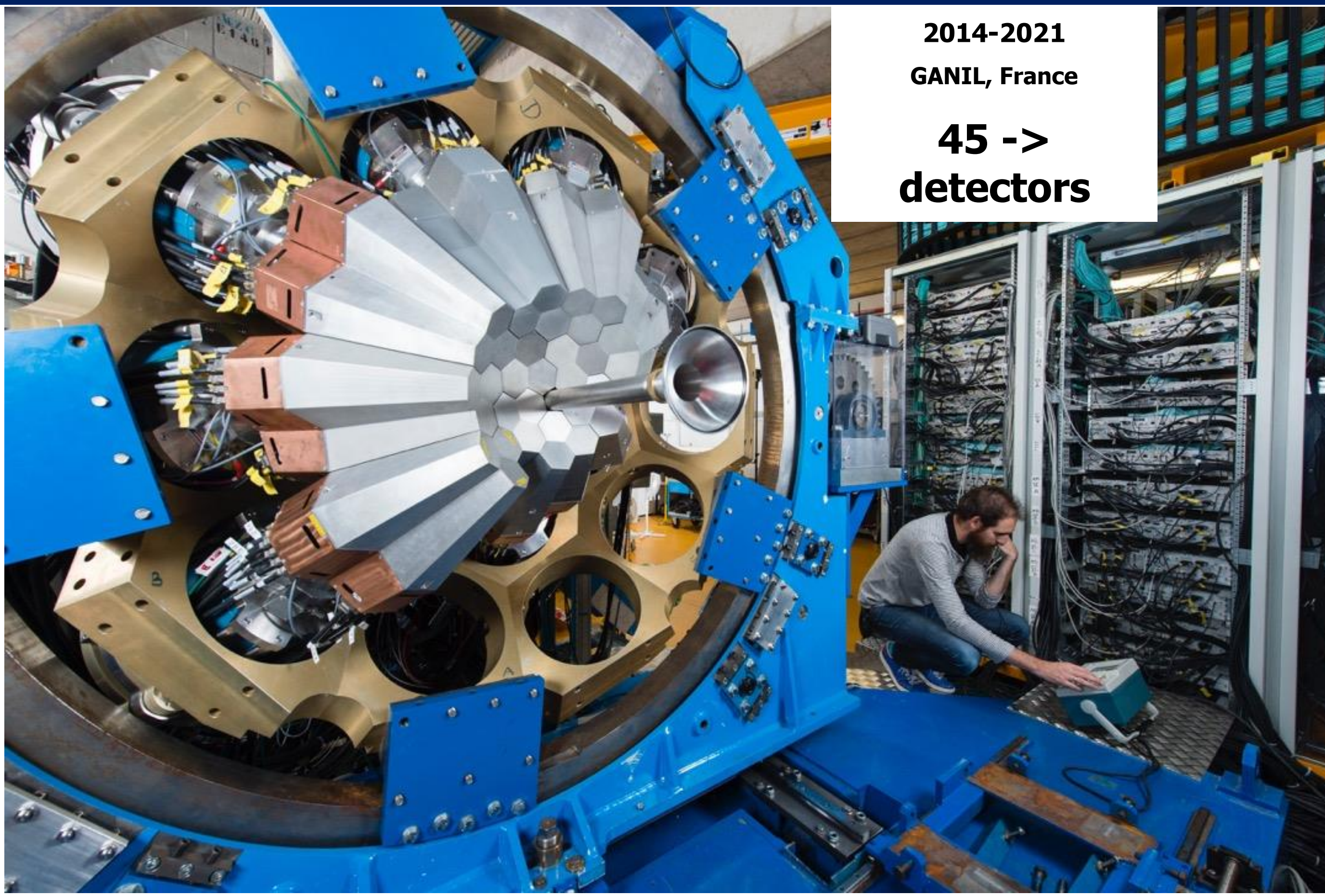

2014-2021

GANIL, France

45 -> detectors

2021-2024

Legnaro, Italy

60 -> detectors

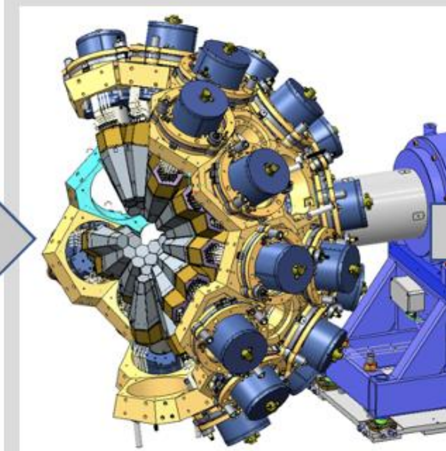

AGATA at LNL

Université de Strasbourg

Conclusions
(nuclear detectors)

- High Z Scintillators are used for gamma spectroscopy, particular for anti Compton spectrometers
- Low Z (organic)-Scintillators used for particle detection/stopping
- Semiconductors: Si used for charged particle spectroscopy (alpha, protons, ... Fission fragments)
- Semiconductors: HP-Ge for high resolution and high efficient Gamma spectroscopy

Le LHC

Grand Collisionneur de Hadrons

7 TeV protons + 7 TeV protons

CMS

Large Hadron Collider

- Pr rculate 11,245 times/sec
- 100’s of millions of proton-proton collisions/second
- Collisions are a billion times hotter han the centre of the sun and create ew particles ($E = mc^2$)

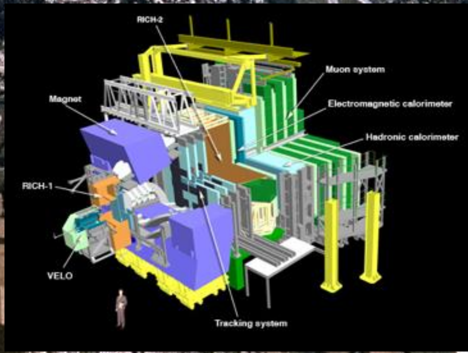

ALICE

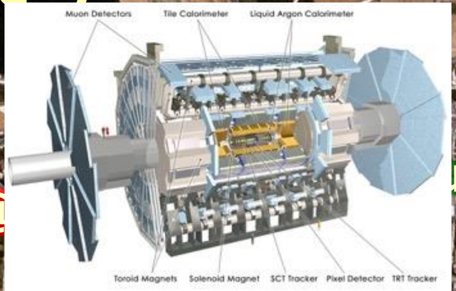

CMS Centre @

uter Centre

ucas Taylor, 2012

How huge are ATLAS and CMS?

ATLAS superimposed to the 5 floors of building 40

CMS

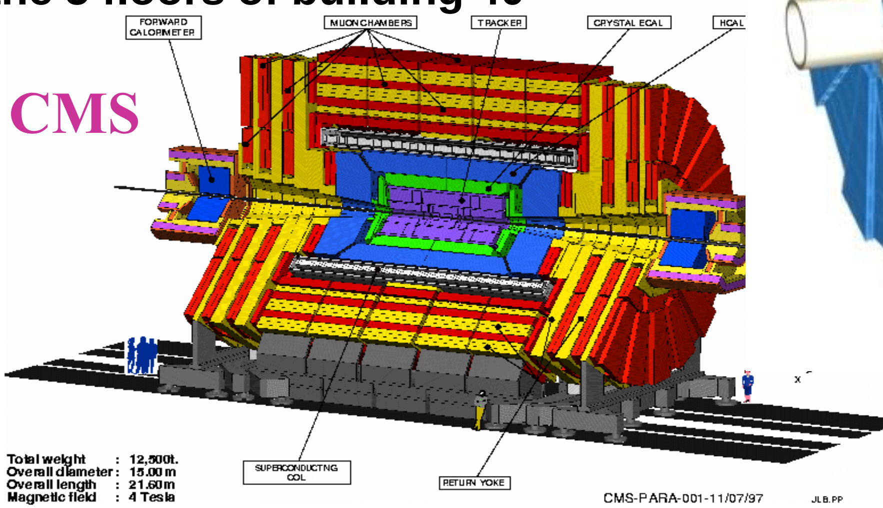

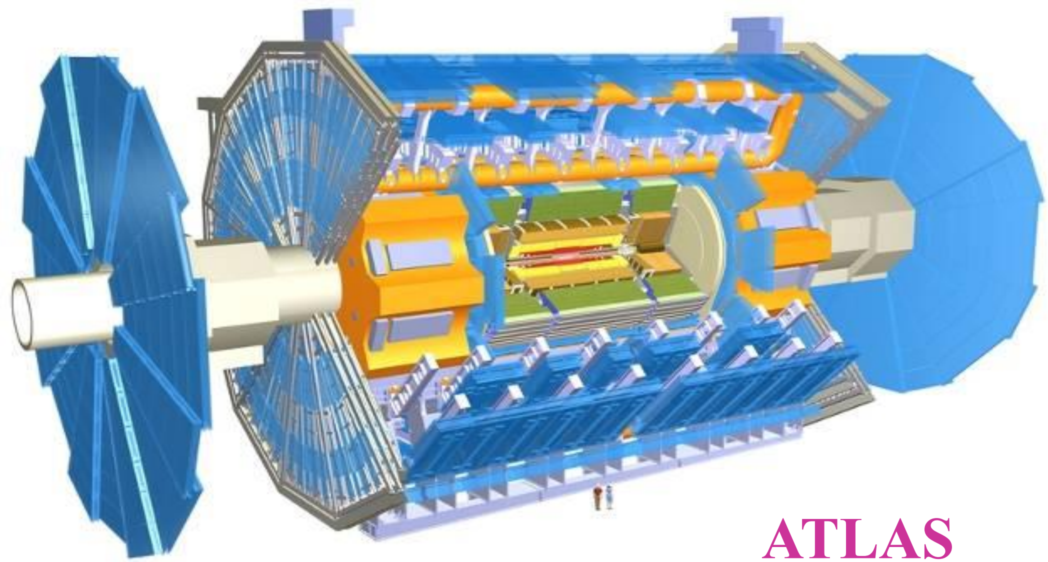

ATLAS

	ATLAS	CMS
Overall weight (tons)	*7000*	*12500*
Diameter	*22 m*	*15 m*
Length	*46 m*	*22 m*
Solenoid field	*2 T*	*4 T*

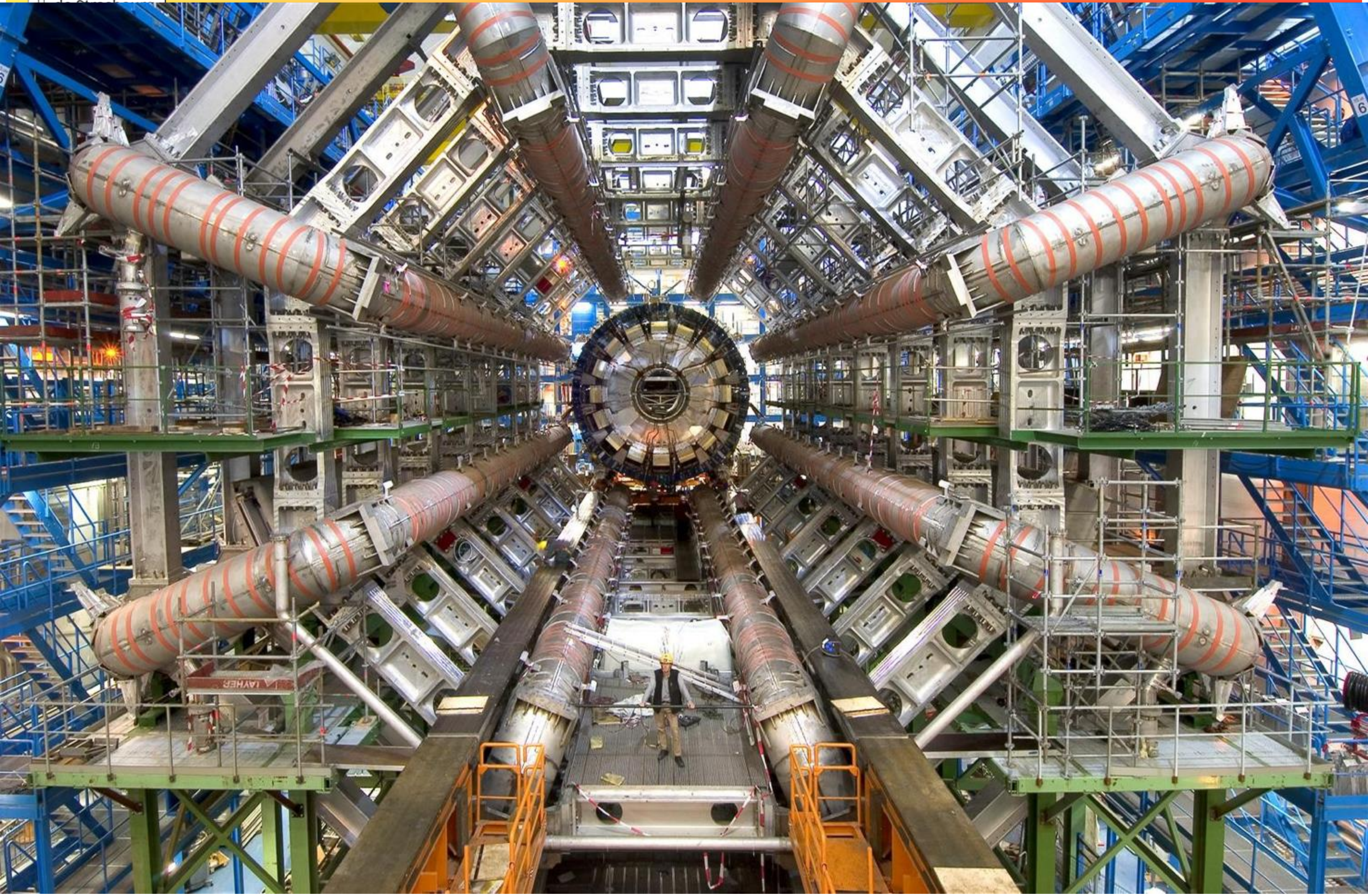
LAYHER

ALICE

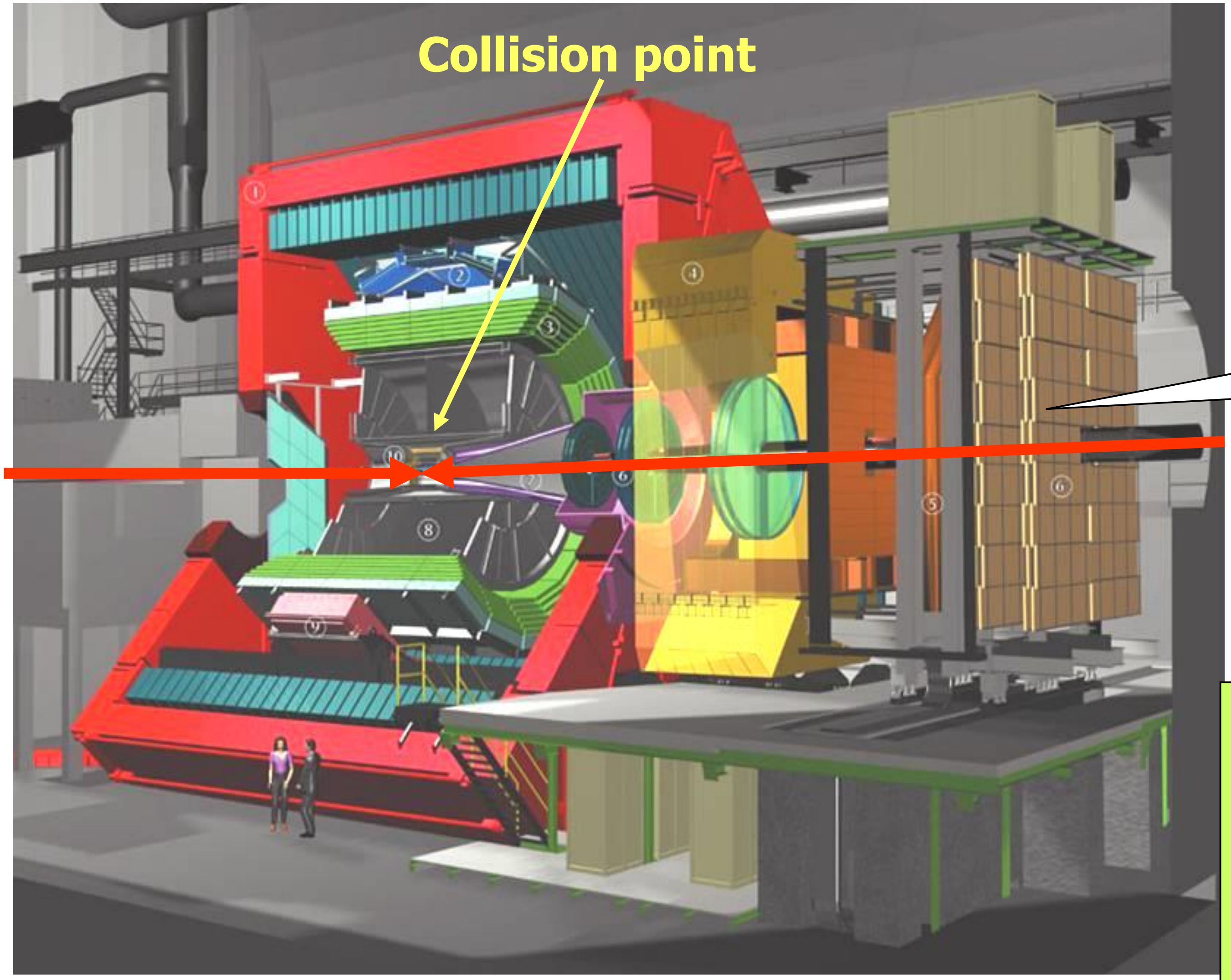

Over 1000 physicists

Muon spectrometer

Dimensions :

Length : 26m.

- **Hight : 16m.**
- **Weight : 10000 tonnes.**

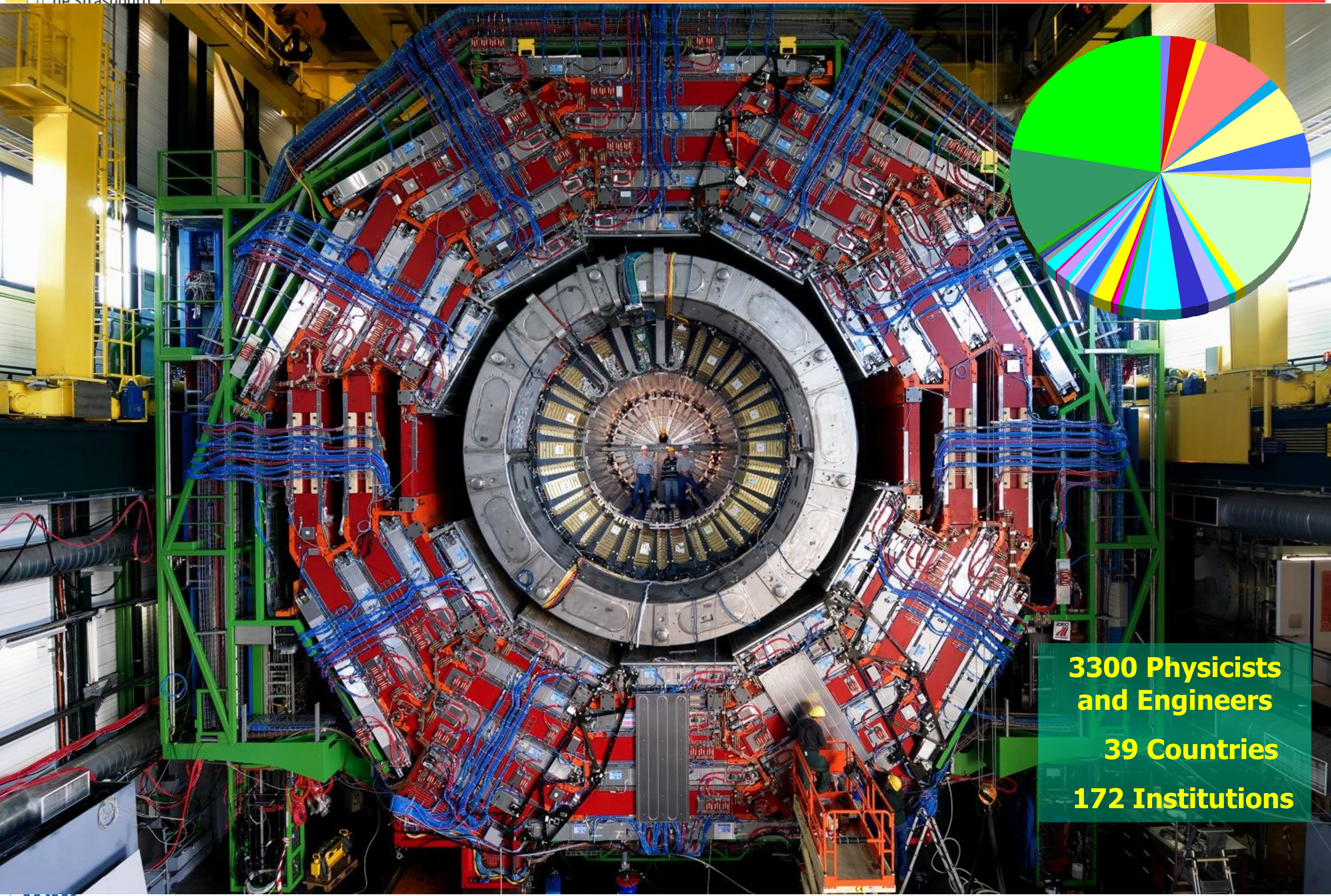
3300 Physicists
and Engineers
39 Countries
172 Institutions

Université de Strasbourg

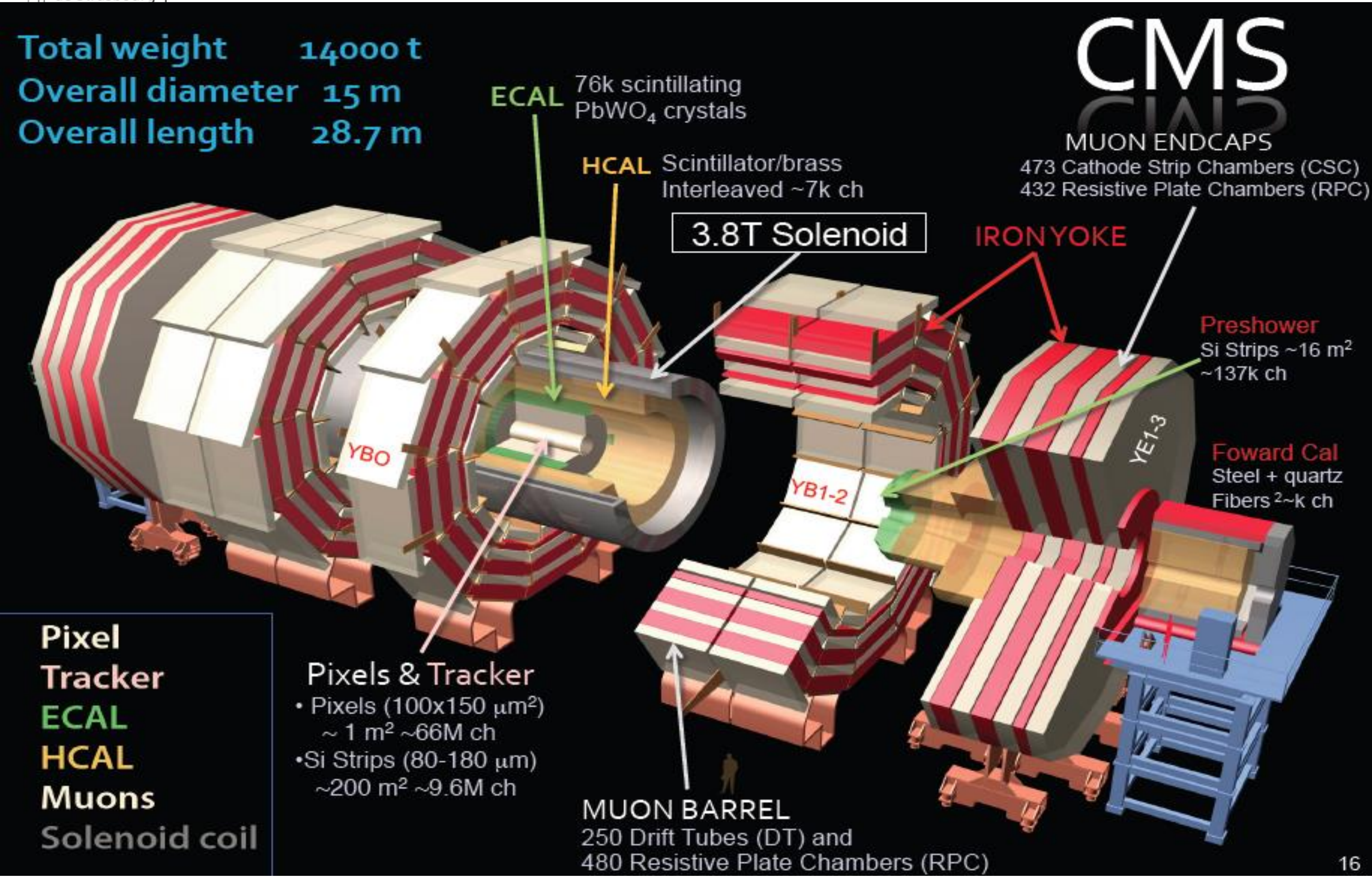

iPHC Institut Pluridisciplinaire Hubert CURIEN STRASBOURG

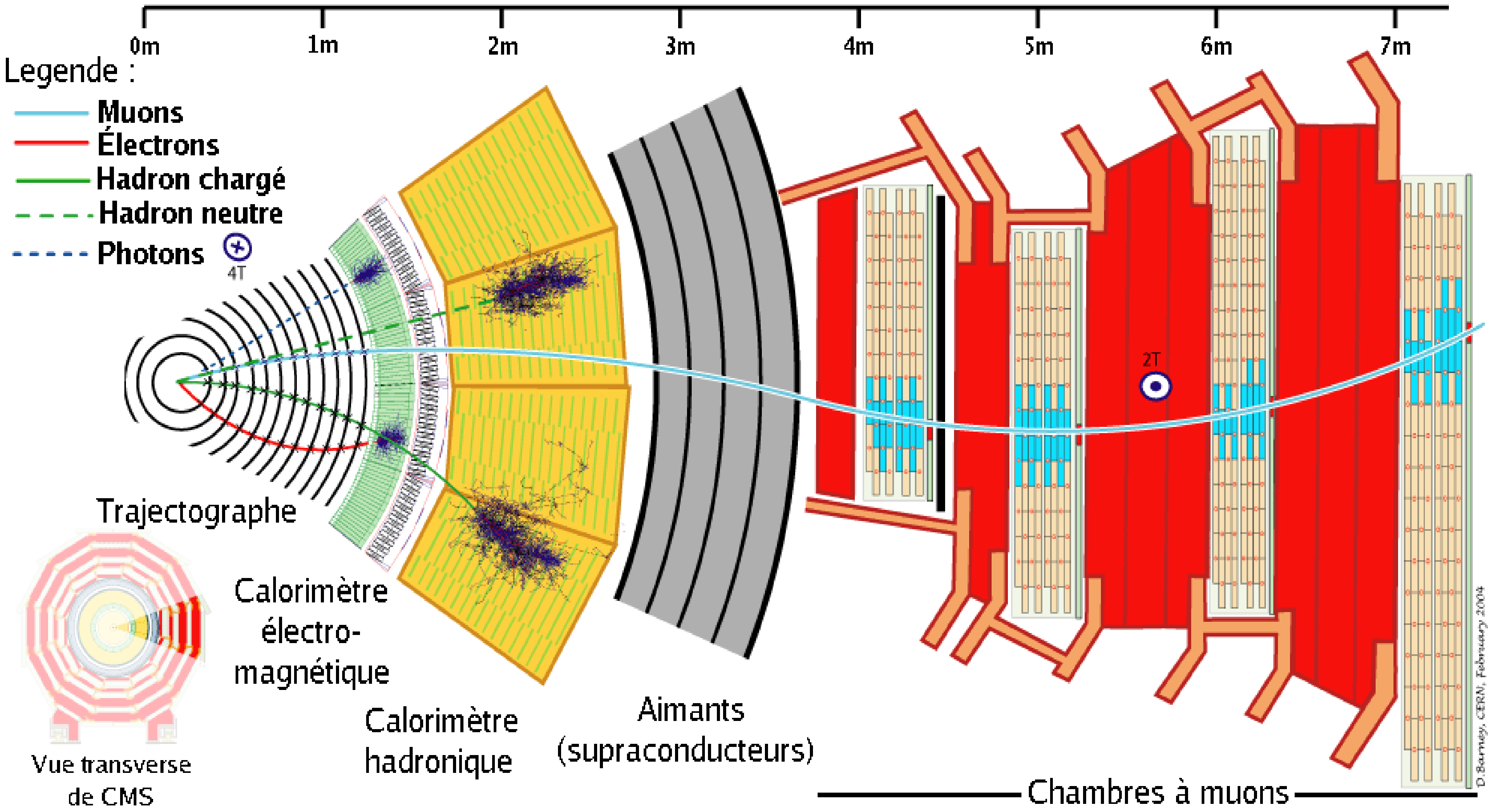

Transverse slice through CMS detector

3-jet event in CMS

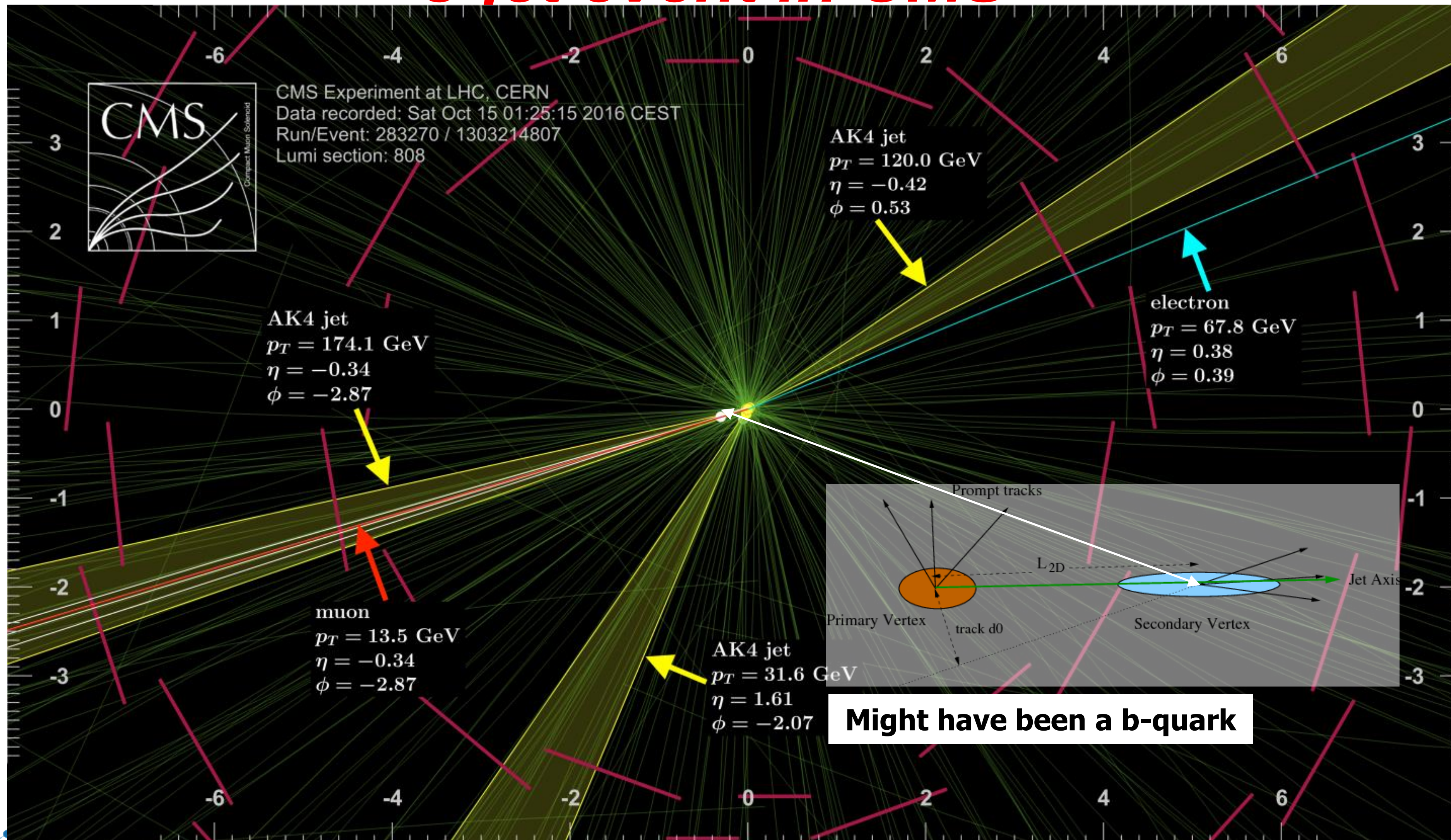

CMOS Pixel detectors

- **MAPS = Monolithic Active Pixel Sensors**

- **For high resolution tracking**

CMOS (Complementary metal-oxide-semiconductor) Detectors

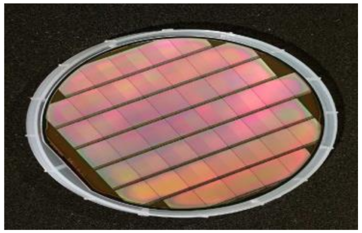

Avantages of CMOS VLSI technology:

- μ-circuits integrated but still
- 100% fill factor
- Small sensitive volume (≈ épitaxial layer) ≈10 μm thick detectors can be very thin
- Industrial production standards ⇒ « modestes » costs,

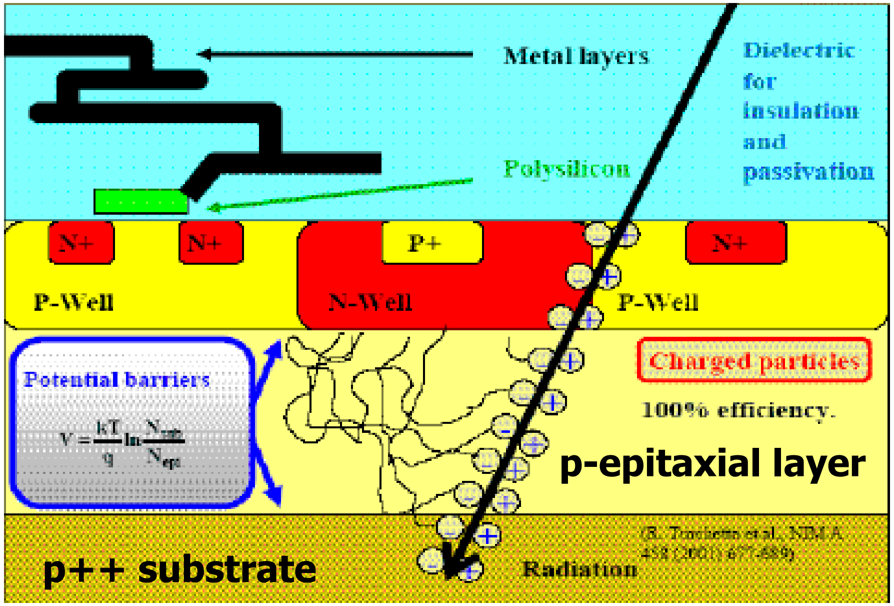

- Signal is created in p-epitaxial layer (lower doping):

  $Q \approx 80$ e-h / μm ⇒ signal < 1000 e^-

- e^- diffusent (thermiquement) to the jonction helped by reflexions at the boundaries formed by the p-weel and the substrat (higher doping)
- Diffusion time < 100ns
- Charge is collected by the diode formed by the jonction n-well/p-epitaxial layer

<u>Short coming</u>:

Circuitry of the electronic circuit is limited to only NMOS transistors.

ALPIDE — the Monolithic Active Pixel Sensor (MAPS) for ITS2

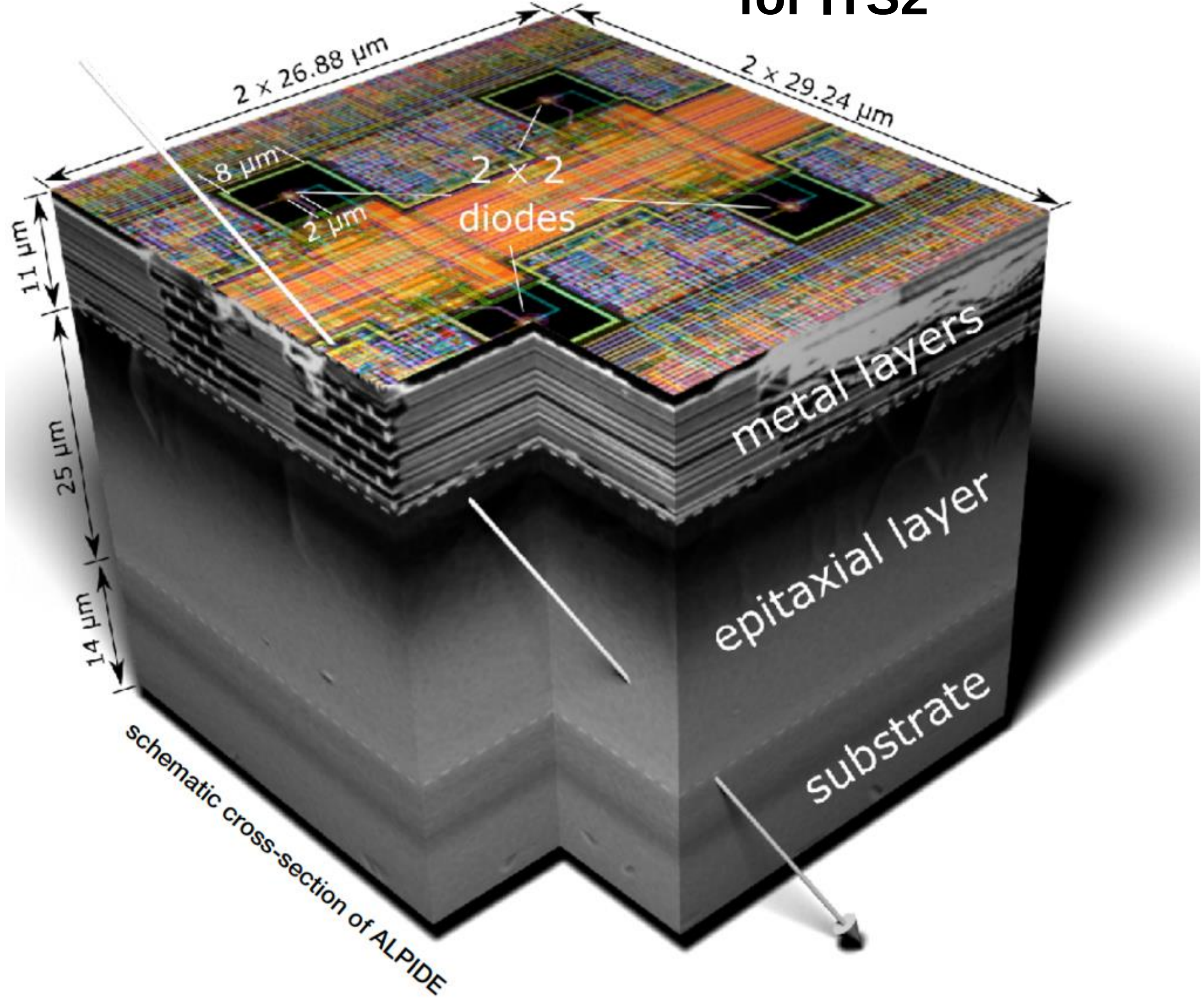

Ulrich.Goerlach@iphc.cnrs.fr, ASP Particle detectors

Characteristics:

- Pixel detector could be made very thin, low material budget!
- Thin epitaxial layer → Small signals
- Small pixel size possible (10x10μm^2) to obtain very good spatial resolution, but then limited space for electronic circuit available
- Only n-well Transistors
- Simple on pixel-cell electronics → slow Read Out (next slide)

Basic Read-Out Architecture
only 3 transistors

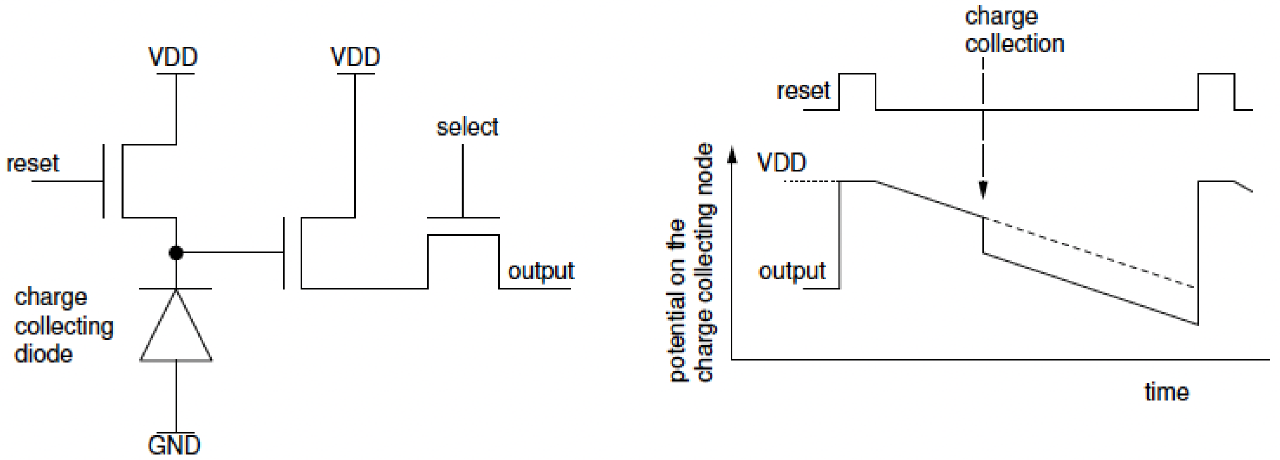

Figure 3.8: Three transistor cell, (a) with a timing diagram showing the signal shape after passage of a particle, (b).

Tomasz Hemperek, PhD thesis

Overview of Rolling Shutter Architecture

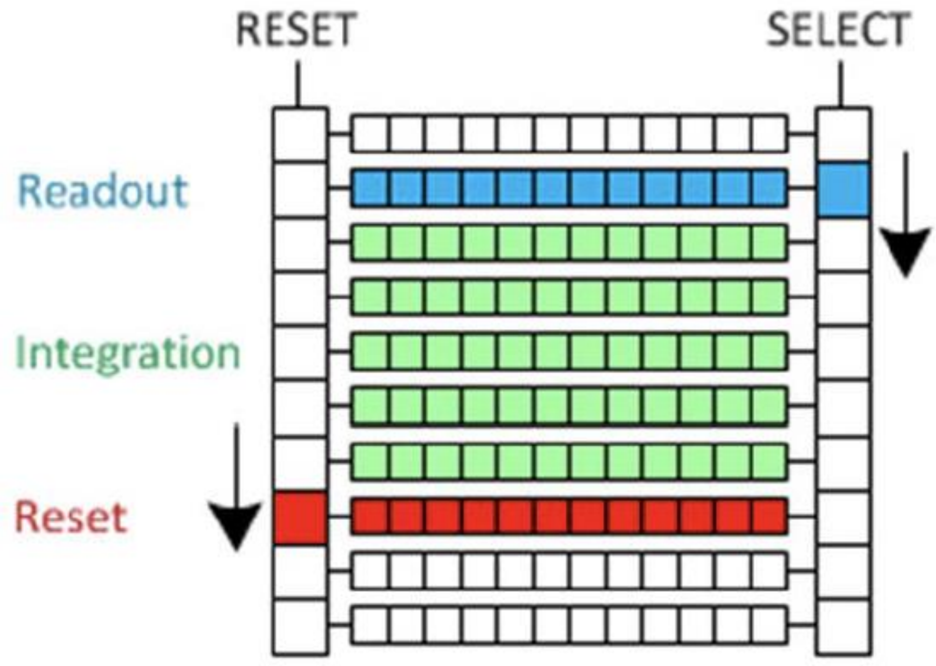

Rolling shutter readout concept where the integrated signal is read out and reset row by row:

- **In his case all pixel outputs in the column are connected.**
- **Only one row of pixels is selected at a time for readout and/or reset.**
- **The column outputs can be multiplexed at the periphery in case of limited analog outputs.**
- **The recorded values can be digitized by external or internal components**

Tomasz Hemperek, PhD thesis

Université de Strasbourg

Typical layout of a MAPS chip

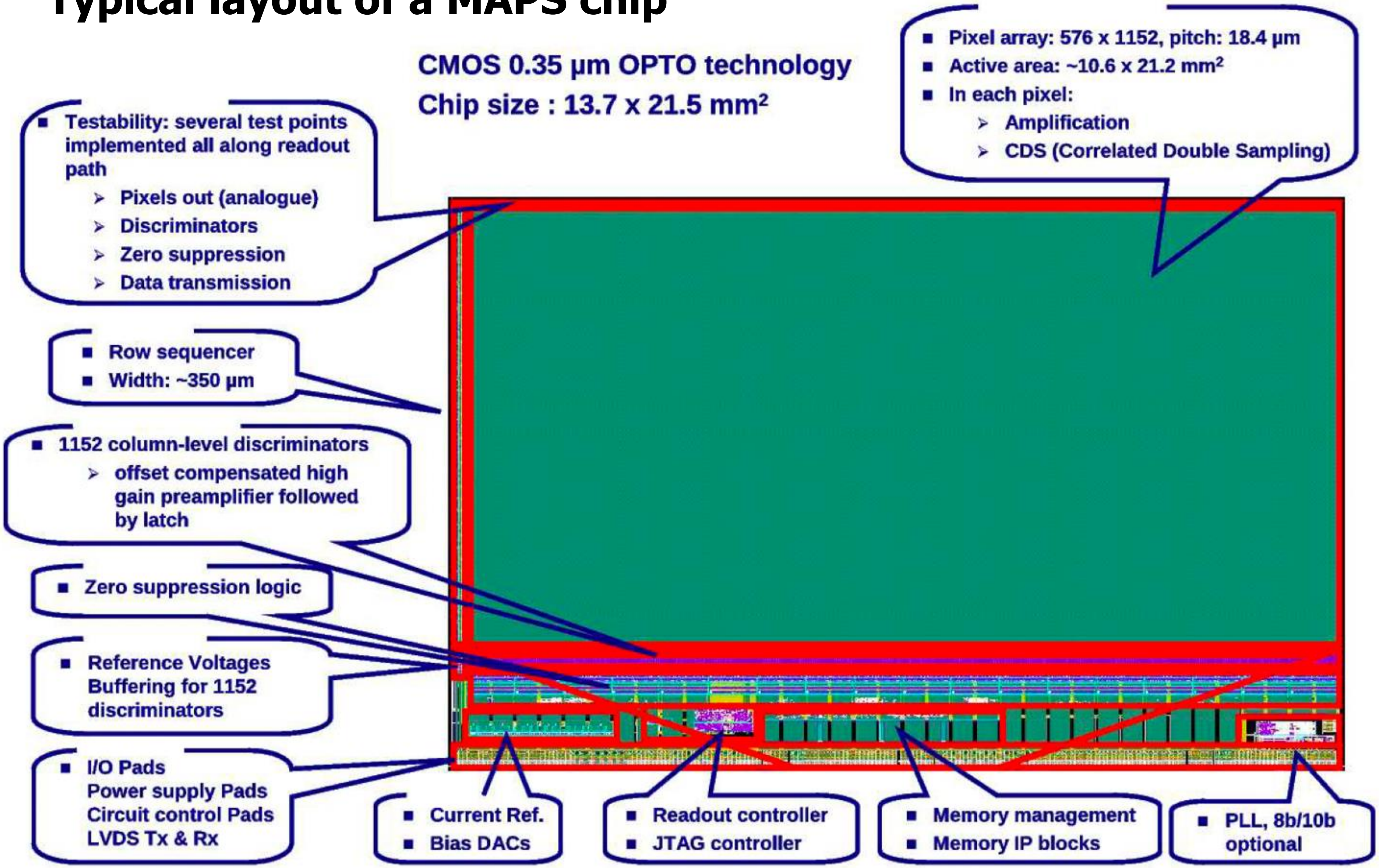

courtesy of Ch. Hu-Guo / TWEPP-2010

Developments to improve performance for different experiments

- Several labs develop CMOS pixel sensors : Italy (INFN, Univ.), UK (RAL), CERN, France (IPHC, Saclay), USA, ...
- Increase and speed up collected charge by drift in depleted silicon
- Use of high resistivity silicon wafers
- Use of different (more complicated) CMOS processes
- Change layout to use the complete design potential (use of p-MOS transistors)
- Speed up Read Out architecture
- Large area (wafer size) devices (stitching)
- Curved thin detector layers without additional support material
- ….

Depleted Monolithic Active Pixels (HV-MAPS or D-MAPS)

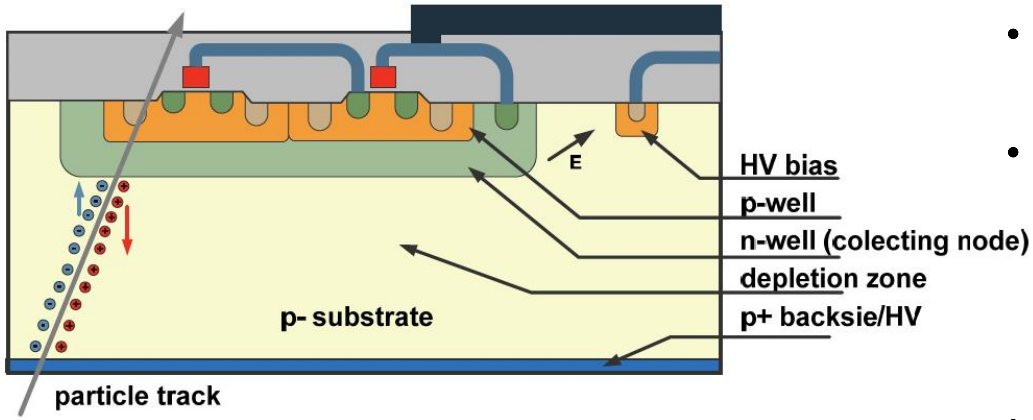

Figure 1-4 Cross section of a depleted MAPS detector with fully depleted bulk with backside contact where charge is collected by drift.

Tomasz Hemperek, PhD thesis

Goals:

- large signals
- fast charge collection by drift in a 50μm – 200μm thick depleted layer
- the use of PMOS and NMOS transistors in the pixel cell (full CMOS),
- The entire CMOS pixel electronics is placed inside the deep n-well.
- This way, the pixel contains only one deep n-well without any inactive secondary wells that could attract the signal charge and cause detection inefficiency.
- it is reversely biased with respect to the substrate from the front side.
- By applying high voltage reverse bias (>60V) it is possible to create a depletion depth of a few to tens of microns
- implementation in a commercial technology

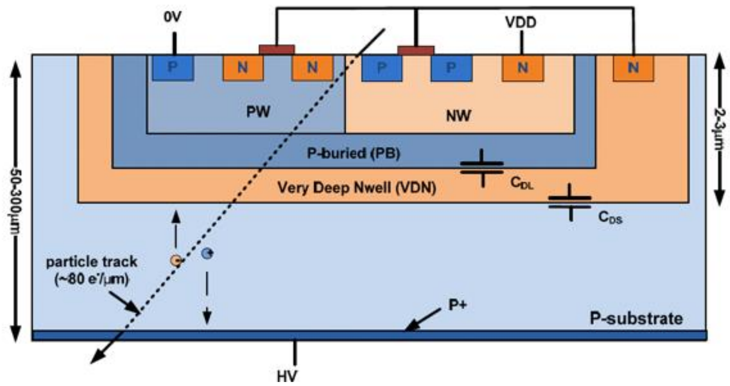

Depleted MAPS, logic inside collecting node

Many different designs are being explored and tested

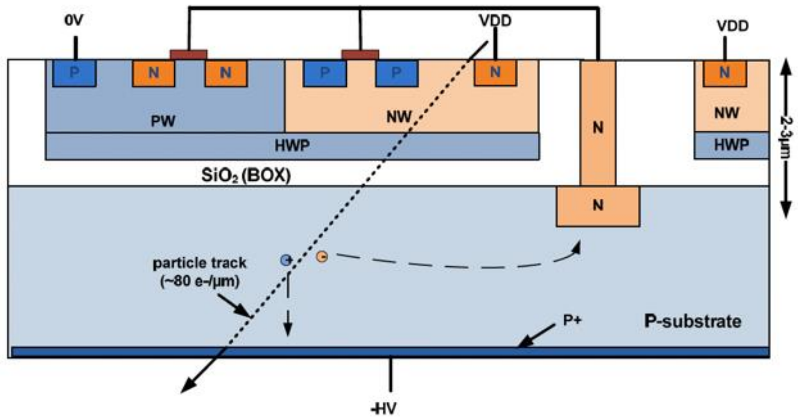

Depleted MAPS, HV-SOI

(BOX = buried layer of silicon oxide)

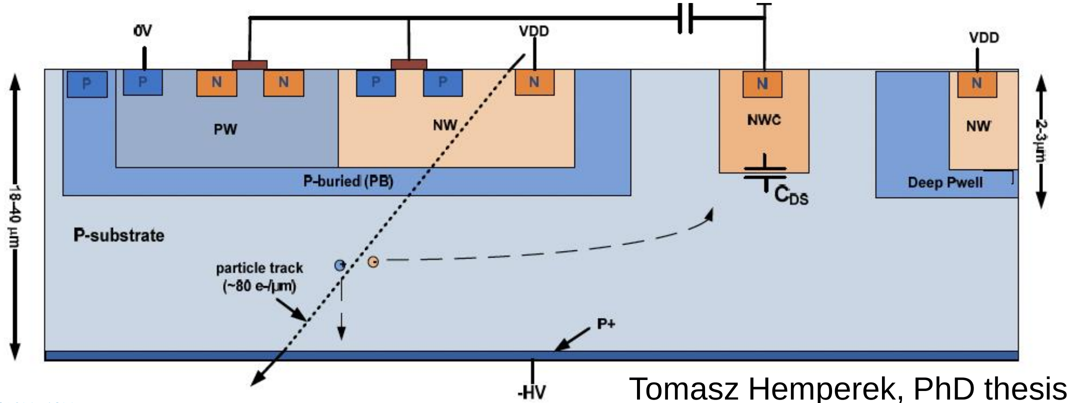

Depleted MAPS,

Logic located outside collecting node

Tomasz Hemperek, PhD thesis

Building Vertex detectors with MAPS

STAR experiment at RHIC, BNL

First large scale application of MAPS in an experiement

- 2 layers of MAPS for pixel vertex detector

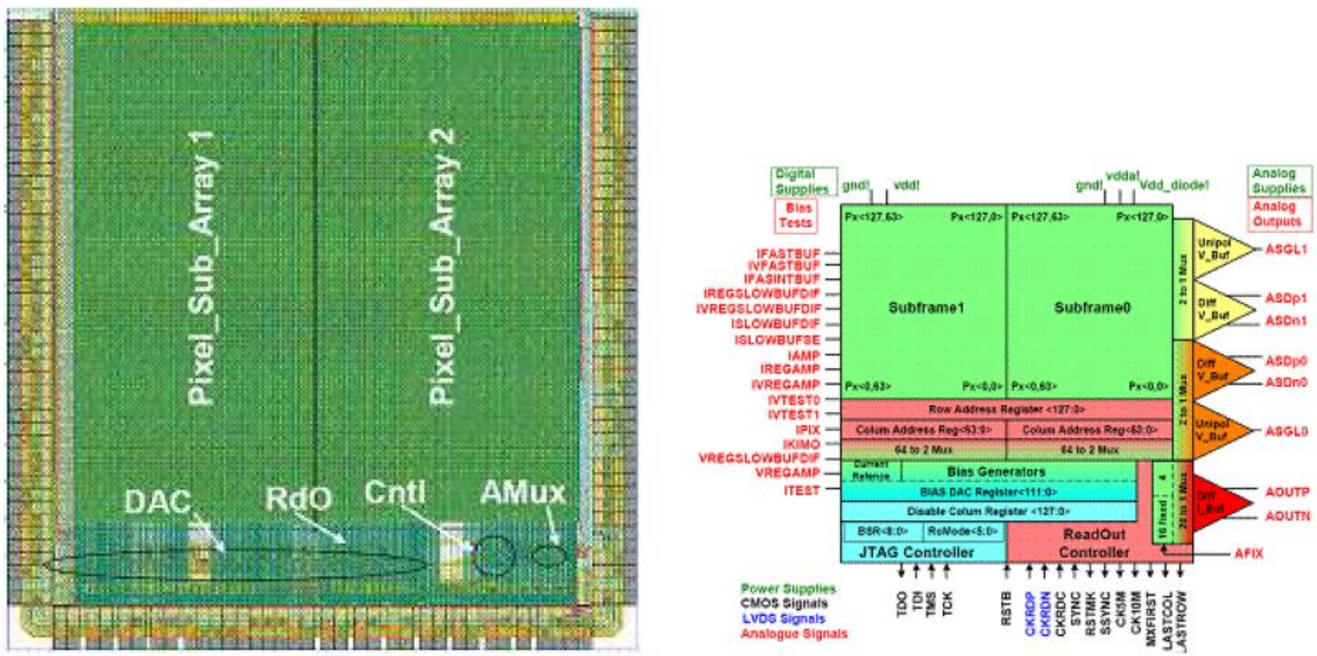

(a) chip layout (b) functional diagram of the chip

M. A. Szelezniak PhD thesis 2008

Figure 6.3: MIMOSTAR chip - layout, (a), and a functional schematic diagram, (b).

STAR experiment at RHIC, BNL

First large scale application of MAPS in an experiement

- 2 layers of MAPS for pixel vertex detector

356 M pixels in 2 layers ~0.16 m^2
R=28mm, 80mm
Pixels size 20.7x20.7 μm^2
X/X_0 = 0.39% for layer 1
Integration time 185.6 μs

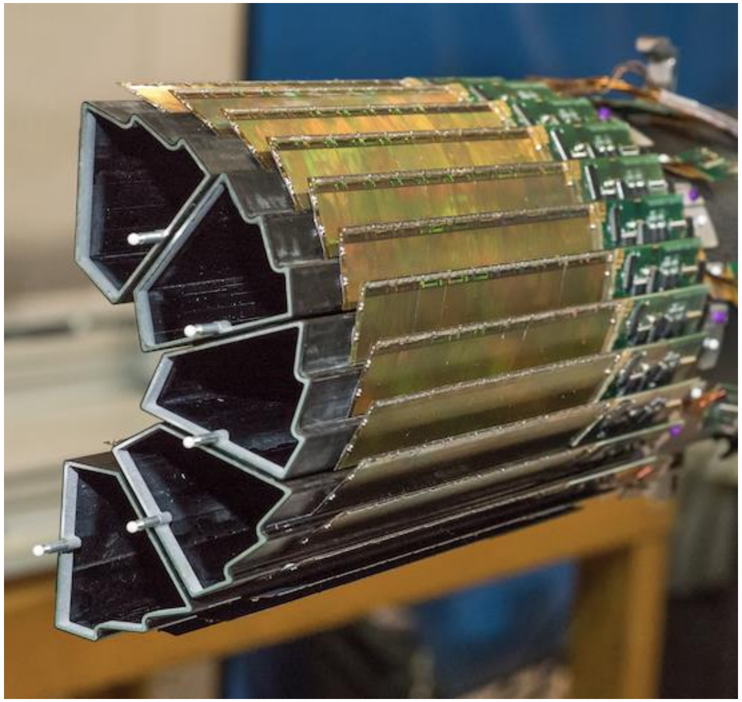

carbon fiber sector tubes (~ 200 μm thick)

Université de Strasbourg

Building Vertex detectors with MAPS

ALICE (LHC-CERN)

A Large Ion Collider Experiment

ITS2 layout

- 7 layers (inner/middle/outer): 3/2/2 from R = 23 mm to R = 400 mm
- 192 staves (IL/ML/OL): 48/54/90
- Ultra-lightweight support structure and cooling

10 m² active silicon area, 12.5×10⁹ pixels

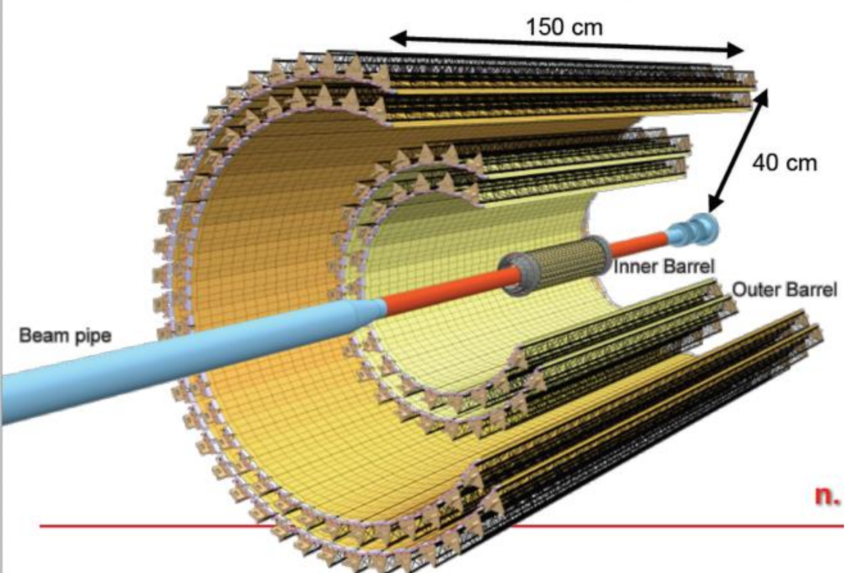

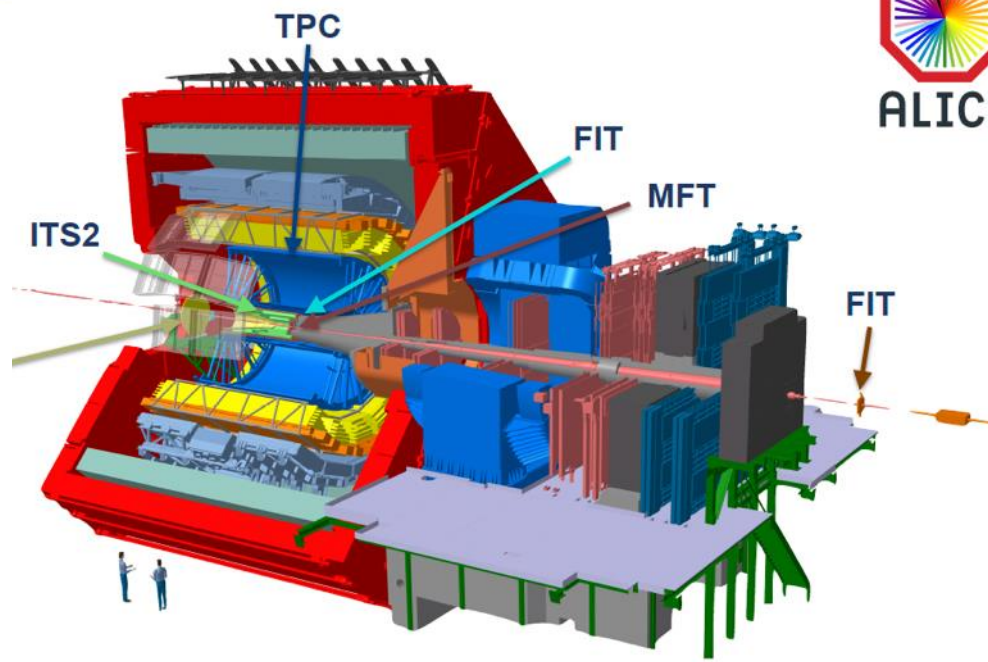

ALICE

CMOS MAPS:

Spatial resolution ≈ 5 µm

Integration time < 10 µs

high-resistivity silicon epitaxial layer

Ulrich.Goerlach@iphc.cnrs.fr, ASP Particle detectors

UNIVERSITY OF OXFORD

ALICE: MAPS

- Improve impact parameter resolution by a factor of ~3 in (r-ϕ) and ~5 in (z)
  - Closer to IP: 39 mm → 21 mm (layer 0)
  - Reduce beampipe radius: 29 mm → 18.2 mm
  - Reduce pixel size: (50 μm x 425 μm) → O(30 μm x 30 μm)
  - Reduce material budget: 1.14 % X_0 → 0.3 % X_0 (inner layers)

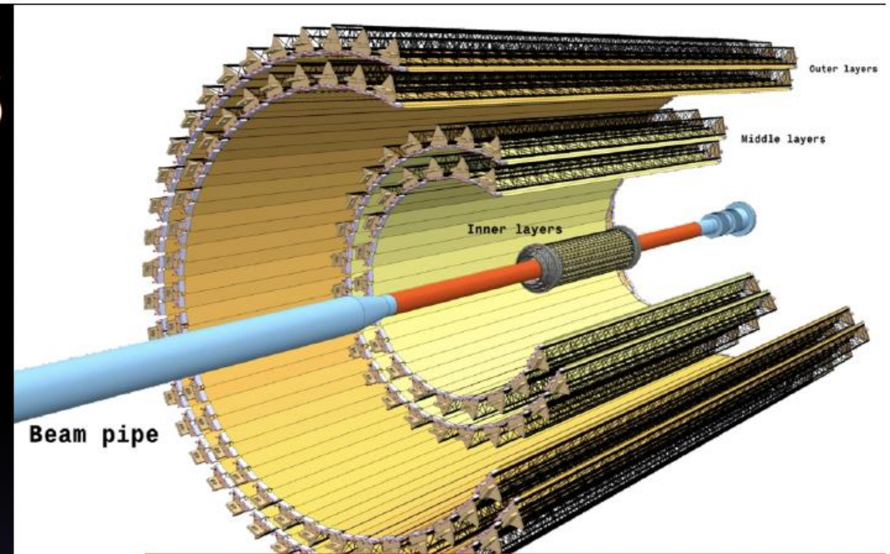

~ 10 m^2 12.5 G pixel

- High tracking efficiency and p_T resolution
  - Increase granularity and radial extension → 7 pixel layers
- Fast readout of Pb-Pb interactions at 50 kHz (now 1kHz) and 400 kHz in p-p interactions
- Rad hard to TID: 2.7 Mrad, NIEL: 1.7 x 10^{13} 1 MeV n_{eq} cm^{-2} (safety factor 10)
- Fast insertion/removal for maintenance

P. Riedler

Building Vertex detectors with MAPS

ALICE (LHC-CERN)

A Large Ion Collider Experiment

ALICE

ALPIDE — the Monolithic Active Pixel Sensor (MAPS) for ITS2

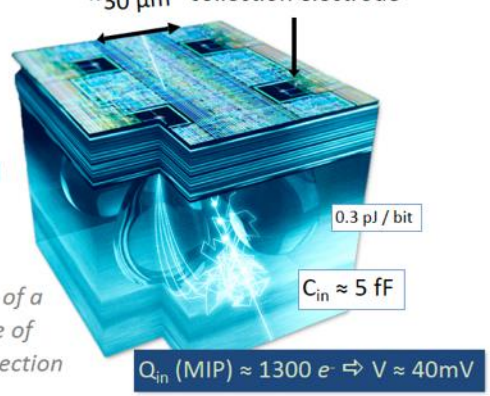

2 x 2 pixel volume

Artistic view of a SEM picture of ALPIDE cross section

- Developed within the ITS2 project

Technology

Technology now used in other applications

- TowerJazz 180 nm CMOS Imaging Process
- High-resistivity (> 1kΩ cm) p-type epitaxial layer (25 μm) on p-type substrate
- Small n-well diode (2 μm diameter), ~100 times smaller than pixel (~30 μm)
  ➔ low capacitance (~fF)
- Reverse bias voltage ($-6\ V < V_{BB} < 0\ V$) to substrate to increase depletion zone around NWELL collection diode
- Deep PWELL shields NWELL of PMOS transistors
  ➔ full CMOS circuitry within active area

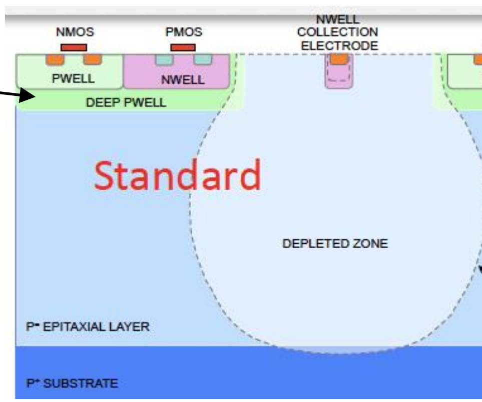

Key features

- In-pixel amplification and shaping, discrimination and Multiple-Event Buffers (MEB)
- In-matrix data sparsification
- On-chip high-speed link (1.2 Gbps)
- Low total power consumption < 40 mW/cm²

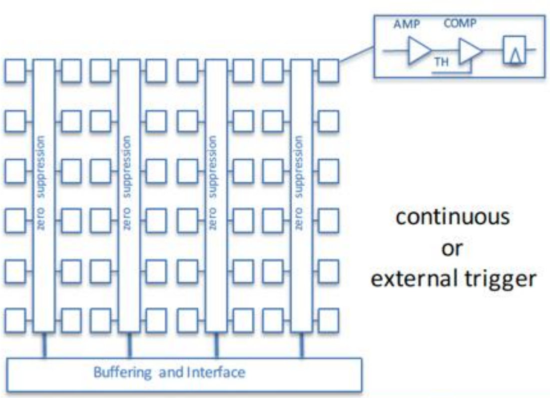

continuous or external trigger

ESE Electronics seminar by T. Kugathasan

Capture d'écran

ALICE ITS2 | CERN Detector Seminar | October 21st, 2022 | Felix Reidt (CERN) 11

INMAPS

UNIVERSITY OF OXFORD

- TowerJazz and the *Detector Systems Centre* (Rutherford Appleton Laboratory)
  - Deep P-layer to shield the PMOS transistors from epi layer
    - No charge loss occurs
    - Full CMOS ➠ Smart pixels possible
    - Not a CMOS standard process
  - Disadvantages
    - limited number of producers and non-standard CMOS process

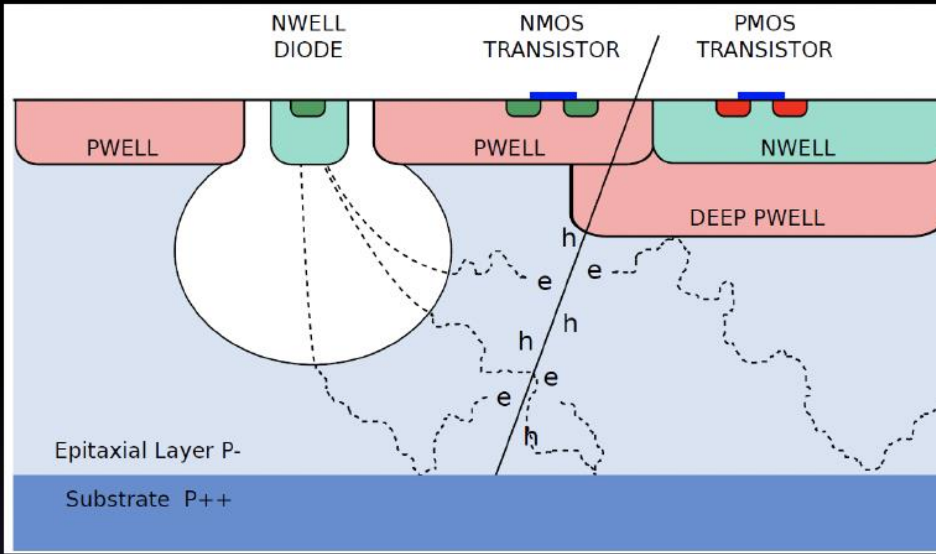

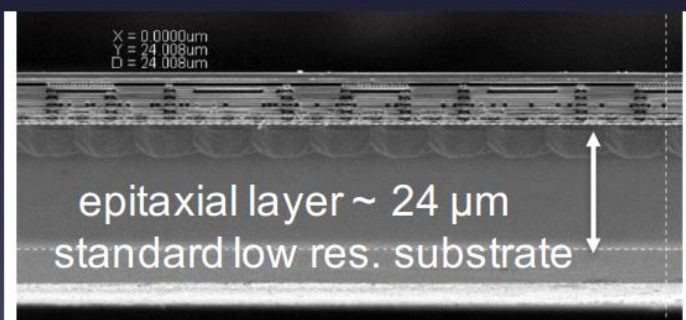

ALICE ITS, SEM picture of prototype chip

Application in HEP: ALICE

- INMAPS on High Resistivity resistivity (> 1kΩ cm) p-type epi-layer 18-40 µm thick
  - Moderate reverse bias to back bias to increase depletion zone around NWELL diode → some charge collection by drift
  - Small n-well collecting diodes small ➠ C_{in}
  - Radiation tolerance (TID) to 700 krad (= 1/1500 of HL-LHC-pp)

R. Turchetta, W. Snoeys

Université de Strasbourg

ALICE (LHC-CERN) ITS 2

A Large Ion Collider Experiment

ALICE

On-surface commissioning

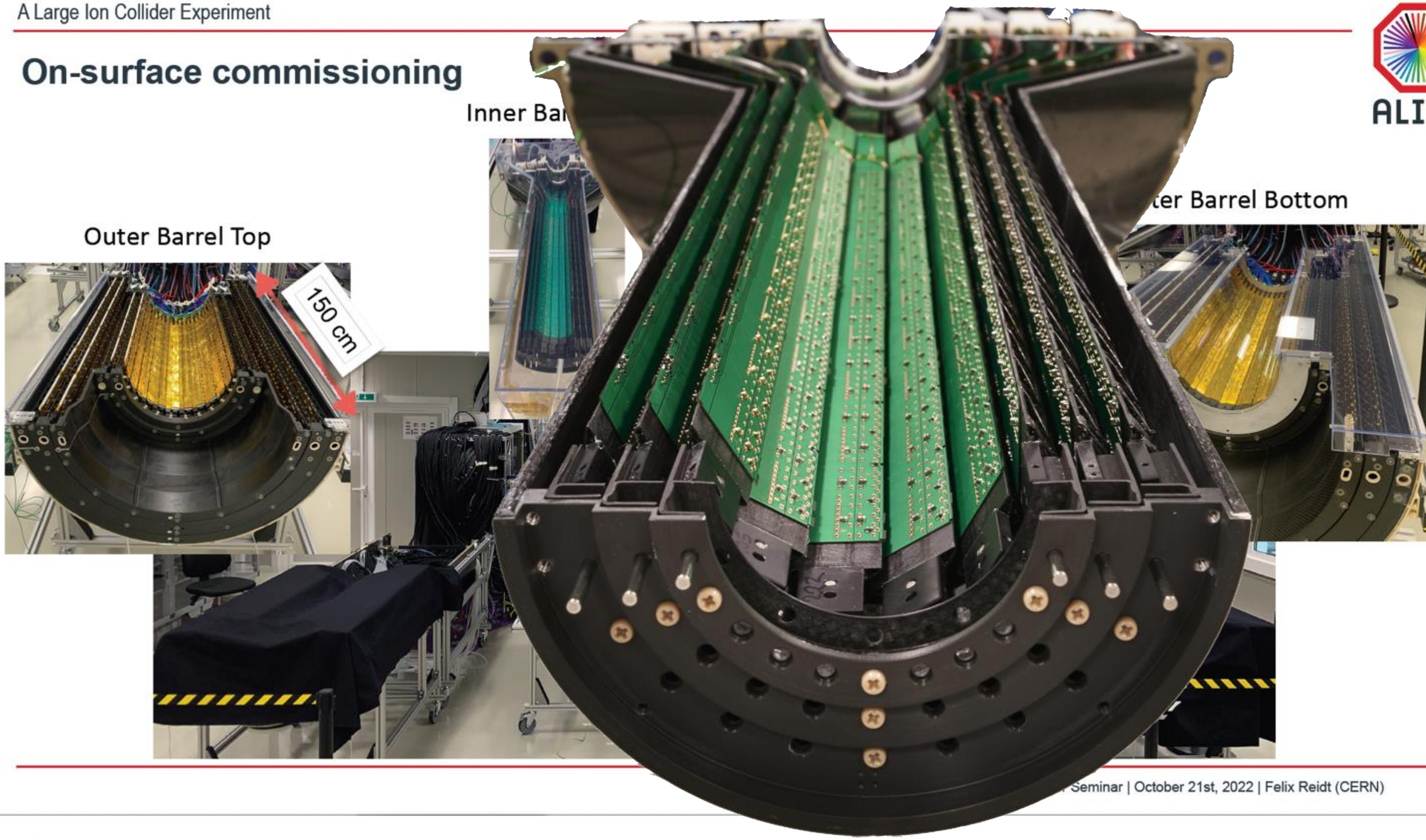

Seminar | October 21st, 2022 | Felix Reidt (CERN) 25

Université de Strasbourg

ITS3

the idea (1): make use of the flexible nature of thin silicon

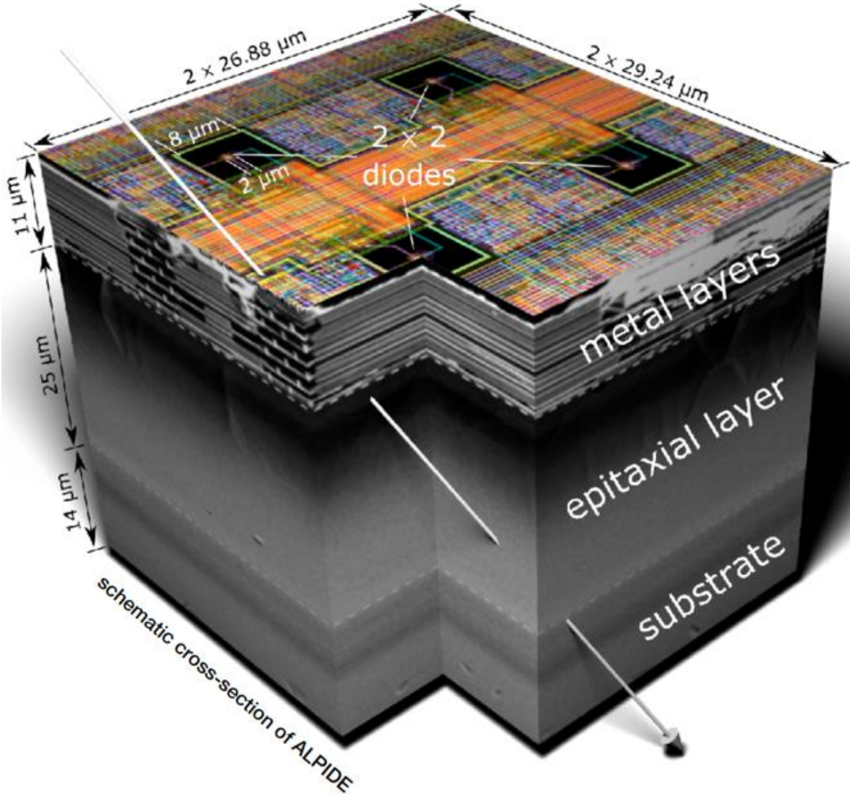

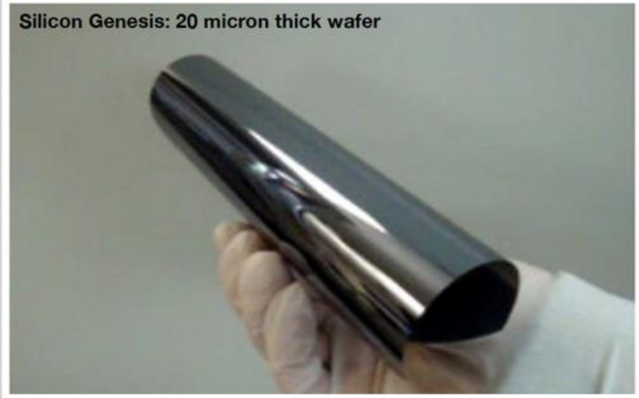

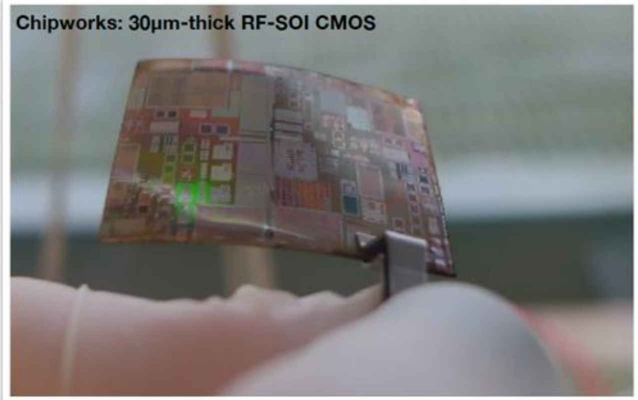

Magnus Mager (CERN) | ALICE ITS3 | CERN detector seminar | 24.09.2021 | 9

Layer assembly

Layer 2 | Layers 2+1 | Layers 2+1+0

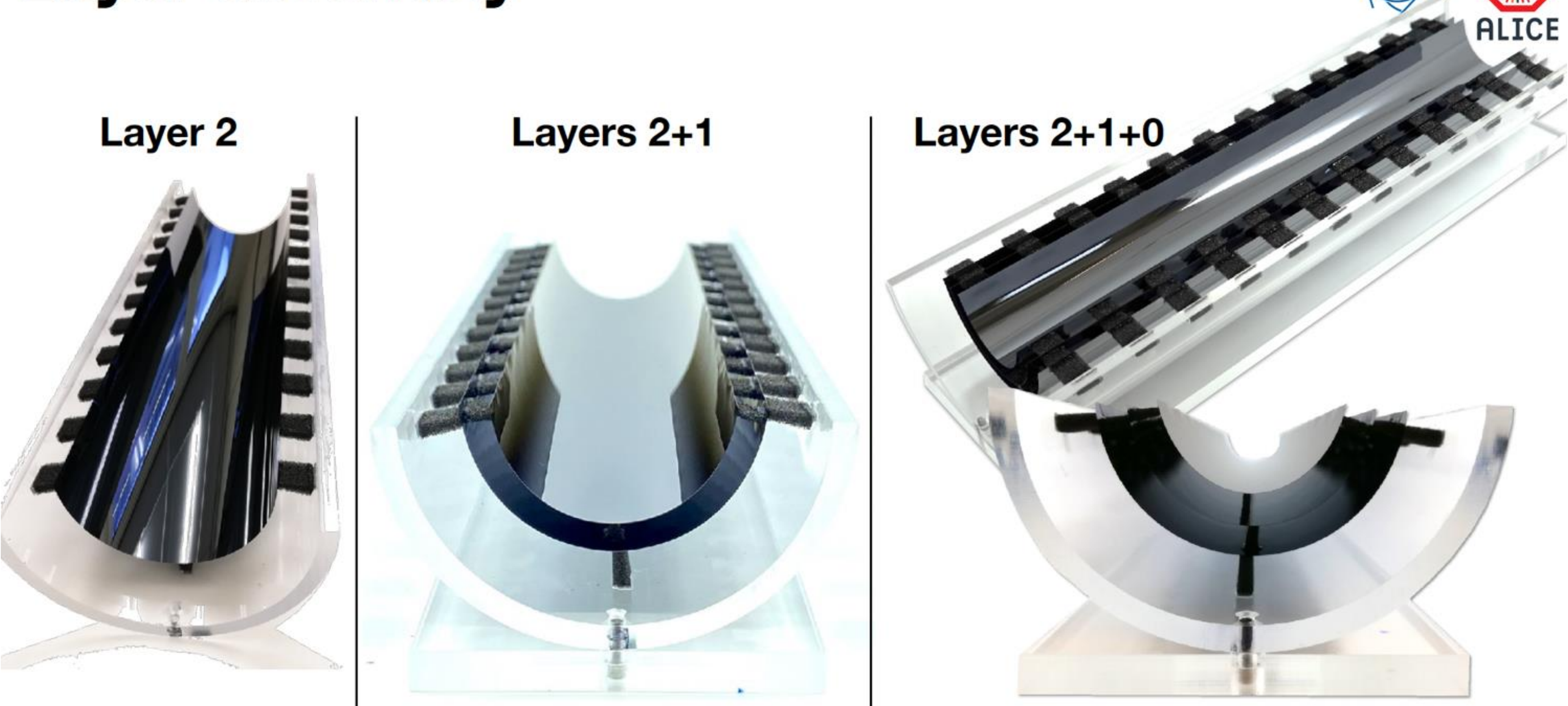

3-layer integration successful!

Magnus Mager (CERN) | ALICE ITS3 | CERN detector seminar | 24.09.2021 | 26

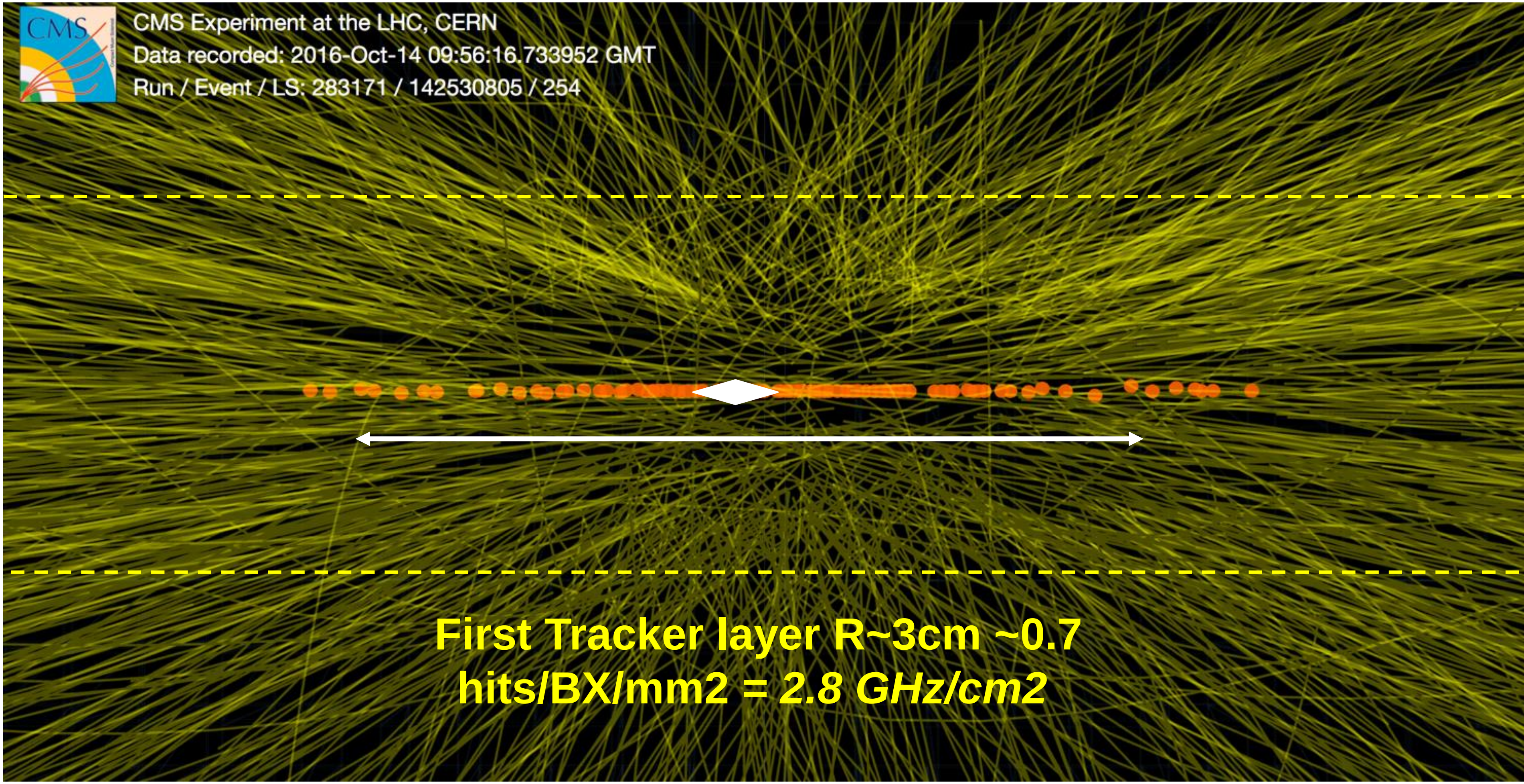
CMS Experiment at the LHC, CERN
Data recorded: 2016-Oct-14 09:56:16.733952 GMT
Run / Event / LS: 283171 / 142530805 / 254
First Tracker layer R~3cm ~0.7
hits/BX/mm2 = *2.8 GHz/cm2*

3D sensors

UNIVERSITY OF OXFORD

- Advantages
  - Decouple thickness from electrode distance
  - Lower depletion voltage, less power dissipation
  - Smaller drift distance, less trapping
- Disadvantage
  - More complex production process
  - Lower yield, higher costs
  - Higher capacitance (more noise)

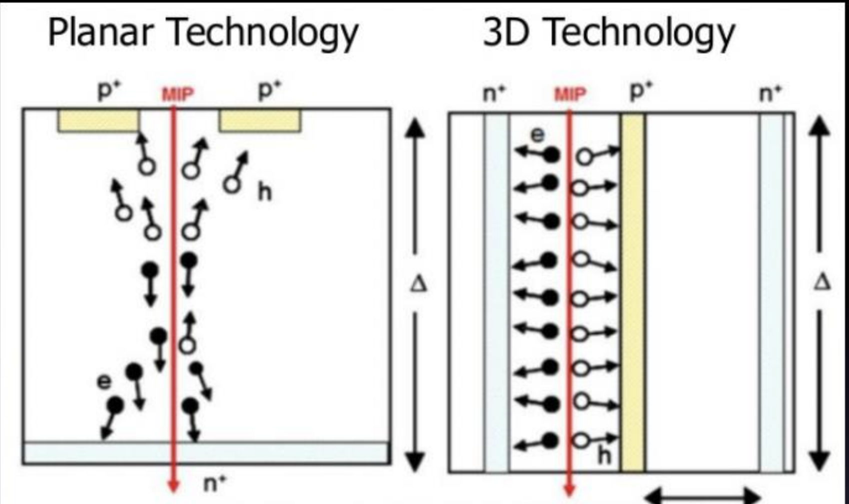

C. Da Via et al., NIM A 694 (2012) 321

- 3D is the most radiation hard technology to-day
- Similar performance than planar sensors, but less demanding in terms of bias voltage and cooling.
- For the HL-LHC we need :
  - More radiation hard (innermost layer(s), 1-2E16 n_{eq}/cm^2)
  - Smaller pixels (compatible with new readout chip, 50 µm – 25 µm)
  - Thinner (reduce cluster size/merging, 200 µm – 100 µm)

S. Parker and C. Kenney

3D Silicon

Silicon pixels: 3D **FBK** — single-side

Column diameter **~5 µm**

High Resistivity layer
- Active layer thickness **~150 µm**
- Resistivity > 3 kOhm•cm

Low Resistivity layer
- Resistivity 0.1-1 Ohm•cm
- Initial wafer thickness **~500 µm**
- Residual wafer thickness after thinning **50-100 µm**

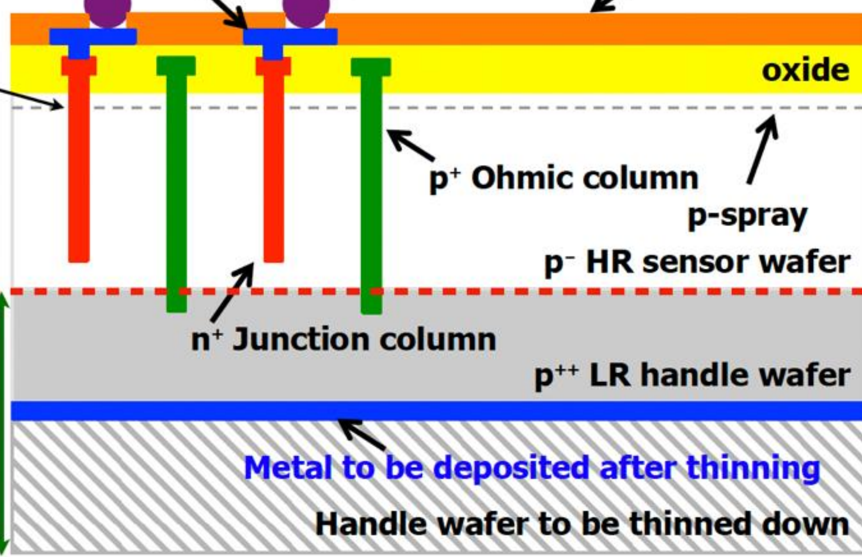

G.F. Dalla Betta et al., NIMA 824 (2016) 386

Two wafers:
High-**R**esistivity and **L**ow-**R**esistivity, bonded with **D**irect **W**afer **B**ond - **DWB** technique by IceMos Technology, Belfast

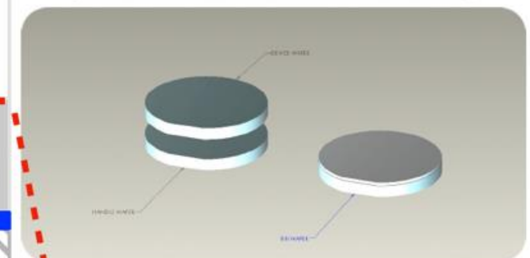

Divide between layers →

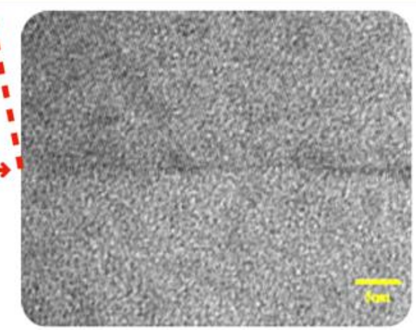

High resolution TEM image of two bonded wafers cross section

Columns produced by:
single-side **D**eep **R**eactive **I**on **E**tching - **DRIE** process optimised by ***FBK*** (less expensive than double-side process)

4D Detectors (x,y,z and time)

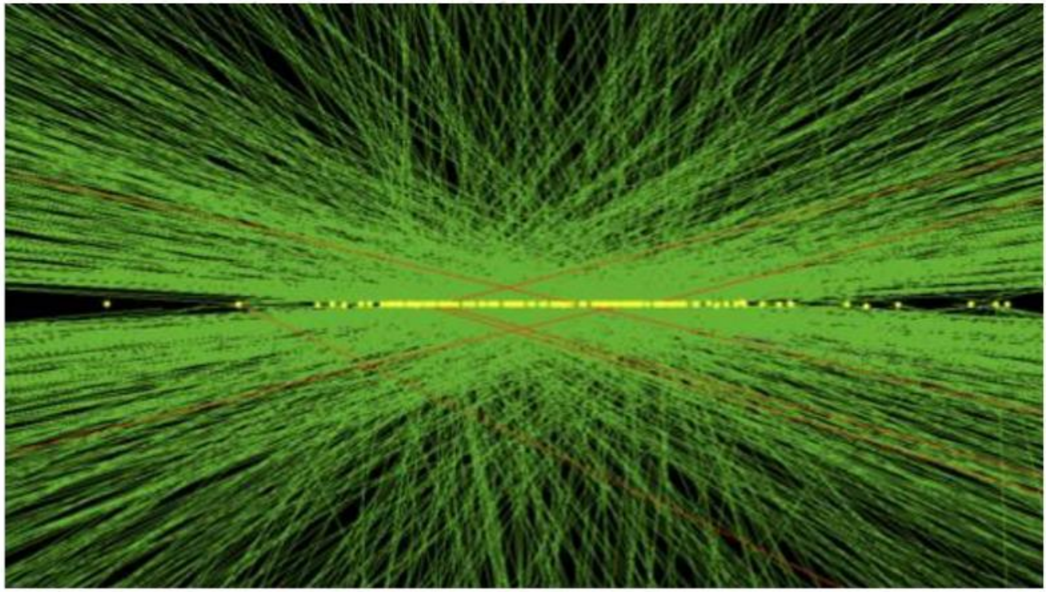

Tracking z-resolution can be larger than vertex-separation: Ambiguous Track-to-vertex association

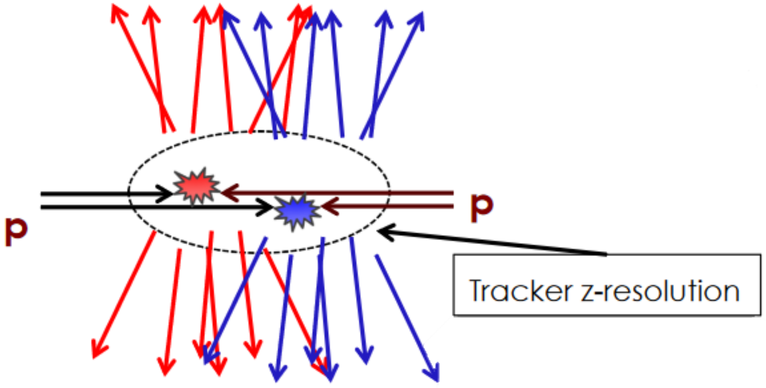

N. Cartiglia, INFN, Hiroshima Conference 2017

Timing at each point along the track:

- **Massive simplification of patter recognition**
- **Faster tracking algorithm**
- **Even in very dense environments by using only "time compatible points »**

The Time Structure of Crossing Bunches

- In addition to extent in z, there is an extent of the bunch crossing in time
- For nominal HL-LHC optics the core of the bunches pass through each other in ~300 ps
- When bunches overlap entirely, achieve maximum spread in z and maximum pileup density
- Normally an experiment only sees the integral of this distribution over time

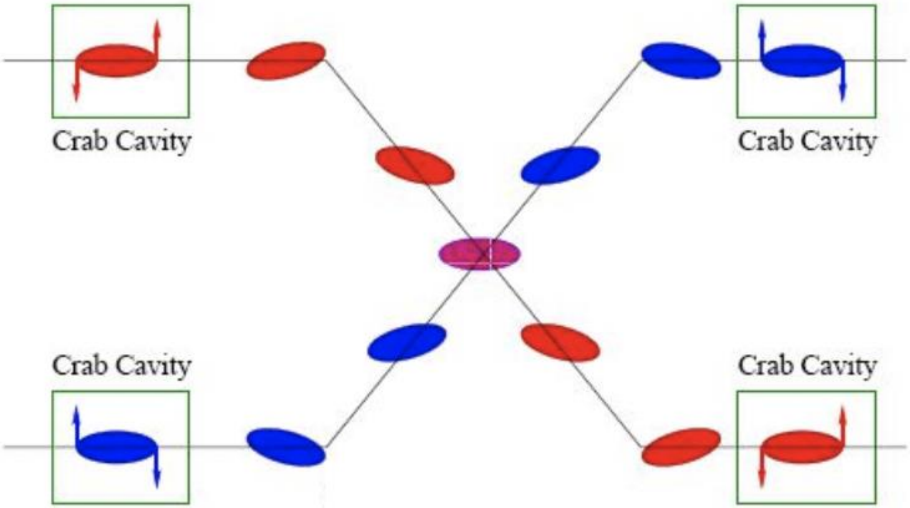

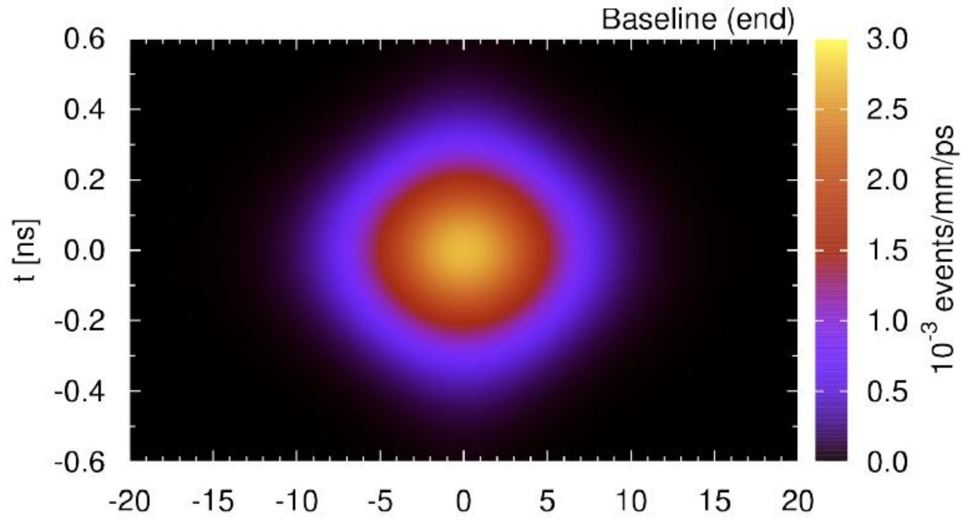

Need to discriminate vertices with time spread of ~180 ps, must have time track timing resolution significantly smaller than beamspot spread so that tracks cluster in time.

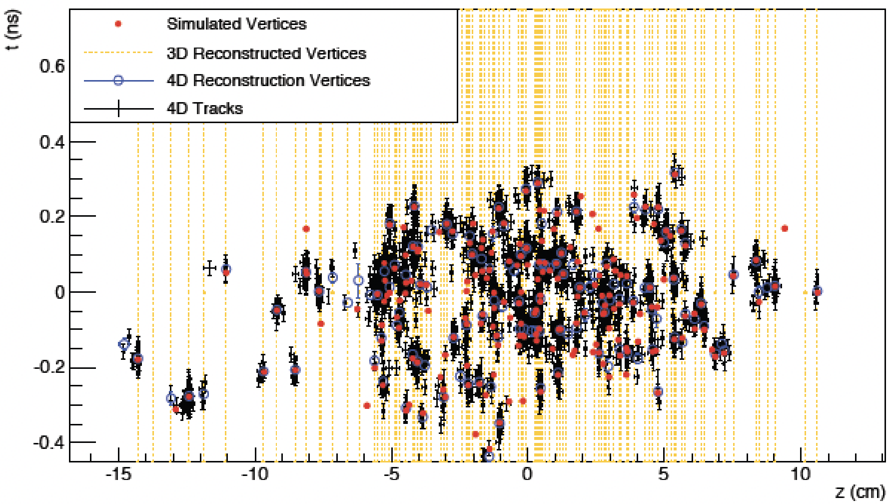

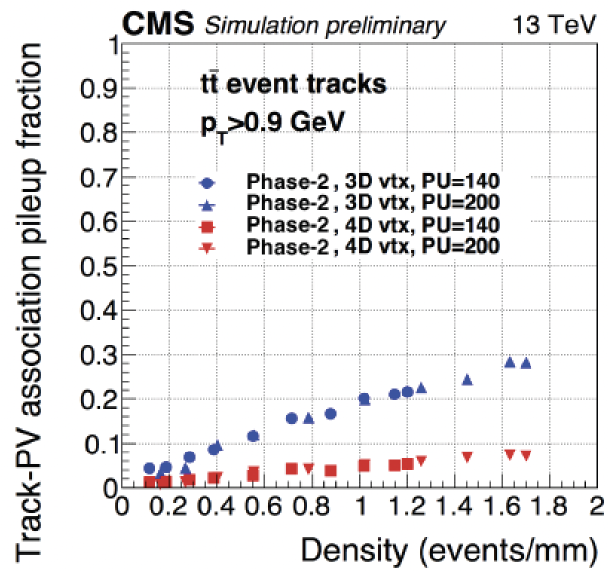

Figure 1.2: Left: Simulated and reconstructed vertices in a 200 pileup event assuming a MIP timing detector covering the barrel and endcaps. The vertical lines indicate 3D-reconstructed vertices, with instances of vertex merging visible throughout the event display. Right: Rate of tracks from pileup vertices incorrectly associated with the primary vertex of the hard interaction normalized to the total number of tracks in the vertex.

Using the Time-at-vertex in Reconstruction

- With the track-time at distance of closest approach it becomes possible to cluster tracks in 2D into vertices
- This significantly increases the distance between vertices and hence makes them harder to confuse
- Expect 5-10x improvement in vertex merging rate (achieved 9x)
- Expect 3-5x reduction in track-vertex association false positives (achieve ~3x)

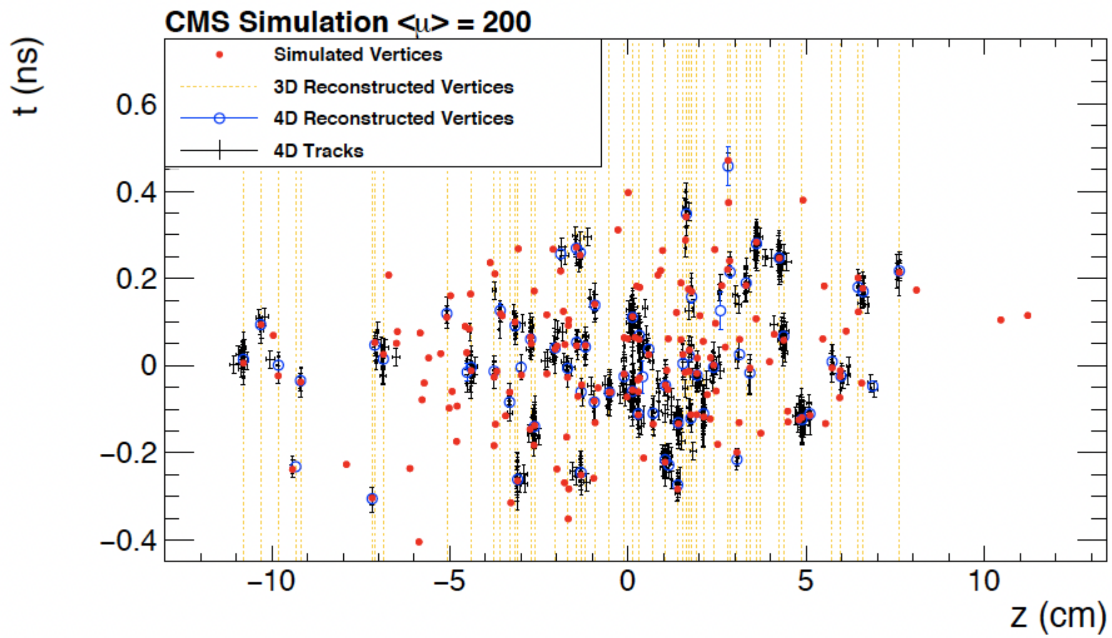

CMS Simulation

<μ>	4D Merged Vertex Fraction	3D Merged Vertex Fraction	Ratio of 3D/4D
50	0.5%	3.3%	6.6
200	1.5%	13.4%	8.9

Crystals

lutetium-yttrium orthosilicate crystals activated with cerium (LYSO:Ce) read out with SiPMs. The

The barrel timing layer will cover the pseudorapidity region up to |h| = 1.48 with a total active surface of about 40 m2.

The fundamental detecting cell will consist of a thin LYSO:Ce crystal with about 12⇥12 mm2 cross-section coupled to a 4x4 mm2 SiPM.

The crystal thickness will vary between about 3.7 mm (|h| < 0.7) and 2.4 mm (|h| > 1.1),

Figure 2.4: Top left: Set of $11 \times 11 \times 3$ mm^3 LYSO:Ce crystals with depolished lateral faces, before and after Teflon wrapping. Bottom left: 6×6 mm^2 HPK SiPMs glued on LYSO crystals. Right: Crystal+SiPM sensors plugged on the NINO board used for test beam studies.

LGADs

Nicolo Cartiglia

- Achieve ≈10 ps timing resolution with Si detectors using charge amplification with Low-Gain Avalanche Detectors

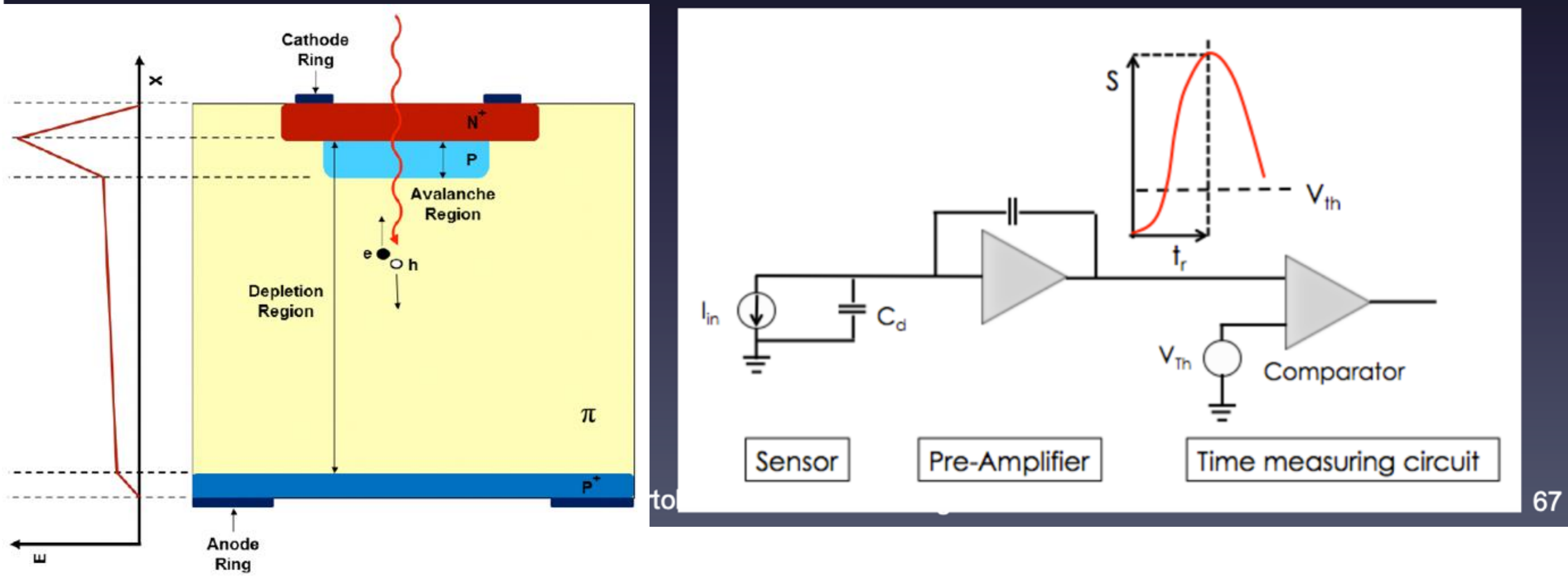

Lots of R&D, DC and AC coupled, chip design, test beams

Both ATLAS and CMS but also for Higgs factories etc

HL-LHC necessitates upgrades to the CMS detector

3

Experimental challenges	LHC		HL-LHC	General mitigation strategy
• inst. luminosity	$2 \times 10^{34}\ s^{-1}\ cm^{-2}$	→	up to $7.5 \times 10^{34}\ s^{-1}\ cm^{-2}$	‣ improved trigger & computing
• detector irradiation	O(10^{14} neq/cm^2)		>O(10^{15} neq/cm^2)	‣ radiation-tolerant sensors & electronics
• pile-up interactions	O(40)		140-200	‣ timing and increased granularity

Compact Muon Solenoid (CMS)
HL-LHC Upgrades

Tracker:
Radiation tolerant, high granularity, less materials, tracks in hardware trigger (L1), coverage up to |η| = 3.8

Barrel Calorimeter:
New BE/FE electronics,
ECAL: lower temp.,
HCAL: partially new scintillator

Muon system:
New electronics
GEM/RPC coverage in $1.5 < |\eta| < 2.8$,
investigate muon tagging at higher η

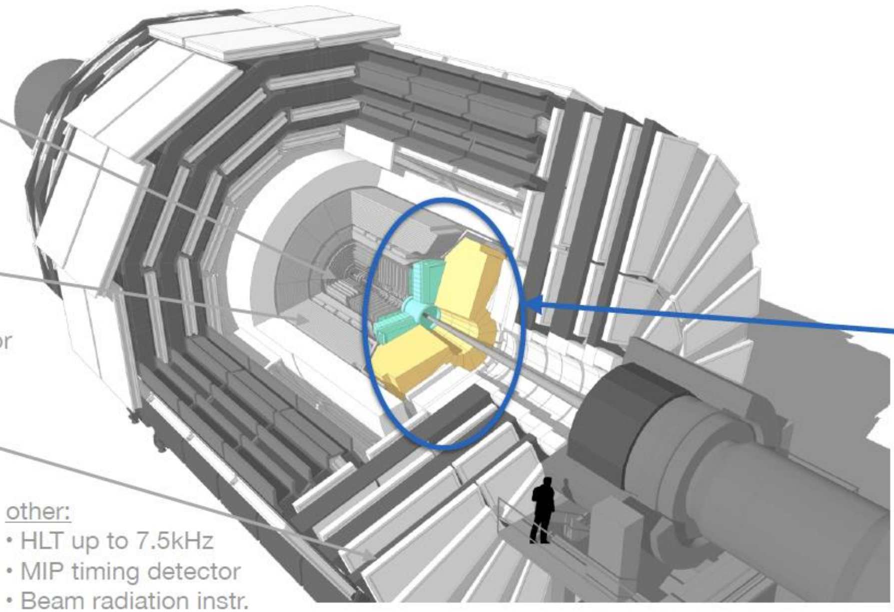

other:
• HLT up to 7.5kHz
• MIP timing detector
• Beam radiation instr. and luminosity

To be replaced for HL-LHC

Endcap Calorimeters:
$1.5 < |\eta| < 3.0$

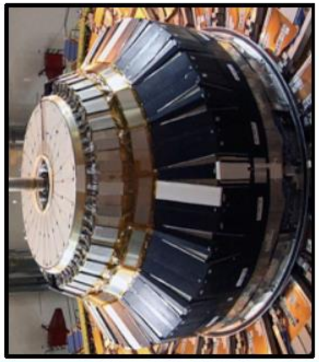

Université de Strasbourg

Calorimeters: HGCAL for the High Luminosity-LHC

High granularity and time resolution

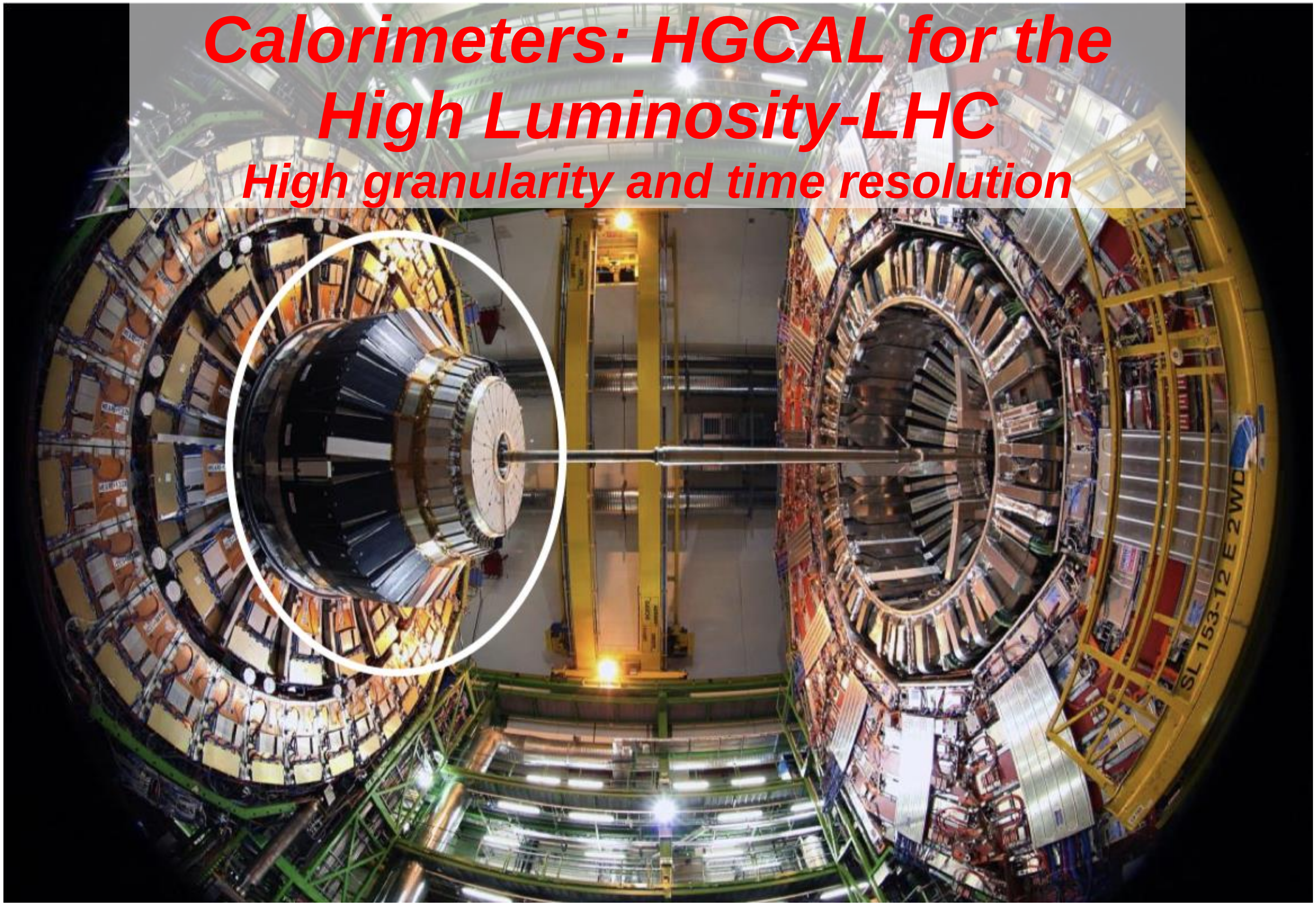

IPHC Institut Pluridisciplinaire Hubert CURIEN STRASBOURG

Technology Choices

Both Endcaps	Silicon	Scintillator
Area	~620 m²	~370 m²
Channel Size	0.5 - 1.2 cm²	4 - 30 cm²
# Channels	~6 M	~240 k
# Modules	~27000	~4000
Op. Temp.	-30 C	-30 C

Per Endcap	CE-E	CE-H	
		Si	Si+Scint
Absorber	Pb, CuW, Cu	Stainless steel, Cu	
Depth	27.7 X_0	10 λ	
Layers	26	7	14
Weight	23 t	205 t	

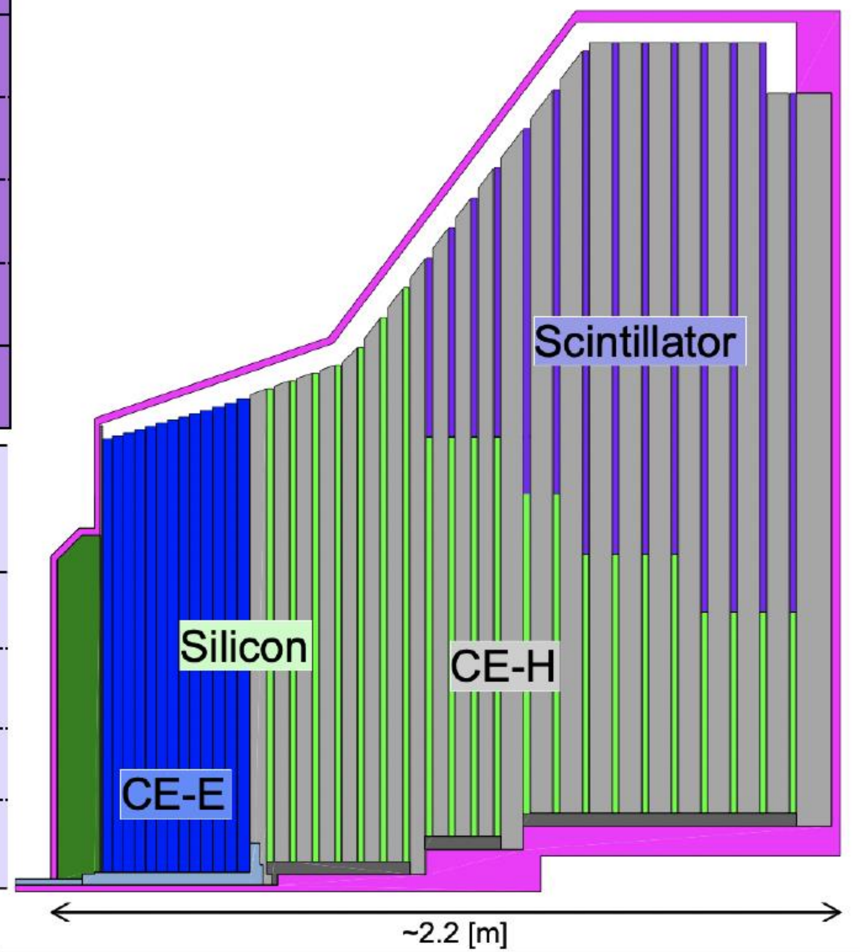

- Dissipated power ~250 kW
- Removed with two-phase CO2 cooling operated at -35 C
- Geometry slightly adjusted since the TDR release

Idea: HGCAL will be 3D imaging calorimeter **with timing capabilities**

VBF H (γγ)

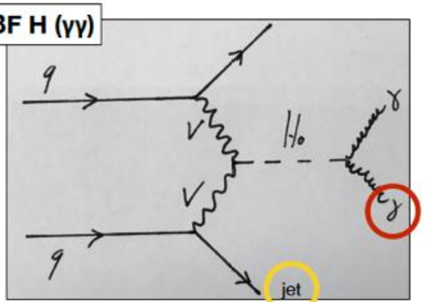

\+ 200 PU

- **Plots show cells with E >~3.5 MIPs, projected to the front face of the endcap calorimeter**
- **Concept: identify high-energy clusters, then make timing cut to retain hits of interest**
- **Design HGCAL to obtain a ~30ps timing measurement for multi-MIP energy deposits**

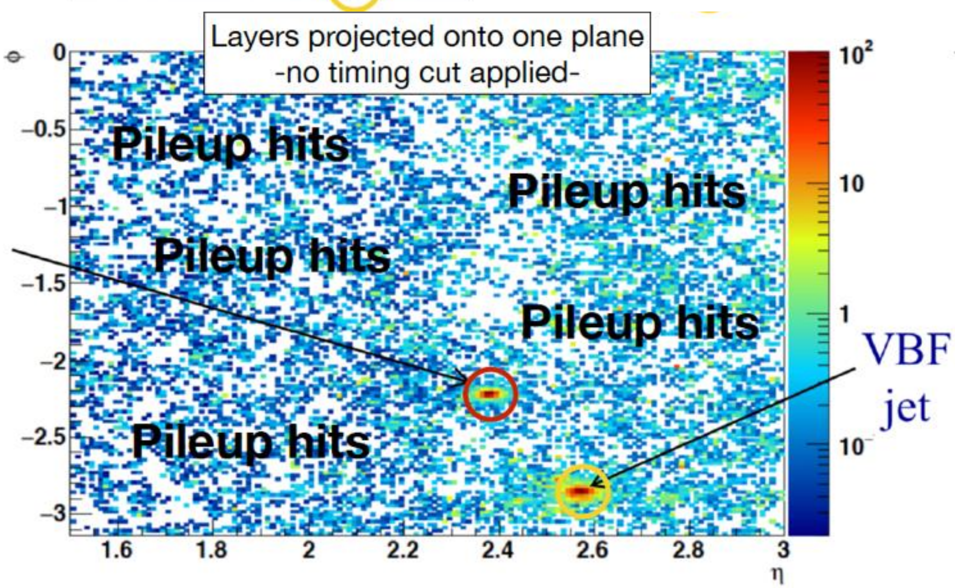

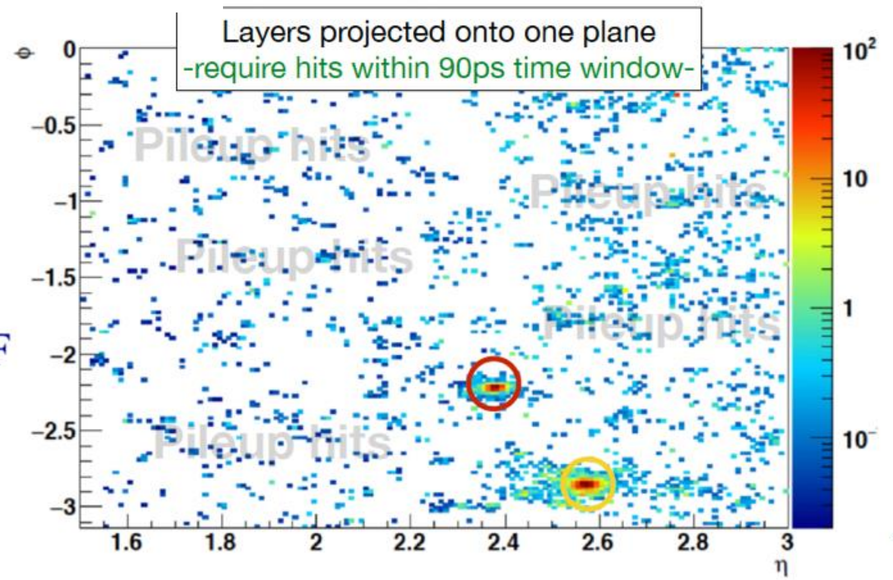

Lateral Structure, Cassettes

- Silicon and scintillator modules assembled into cassettes
- Supported and cooled by copper cooling plate
- Data from modules collected by motherboards
- Cassettes house all services and DC2DC converters

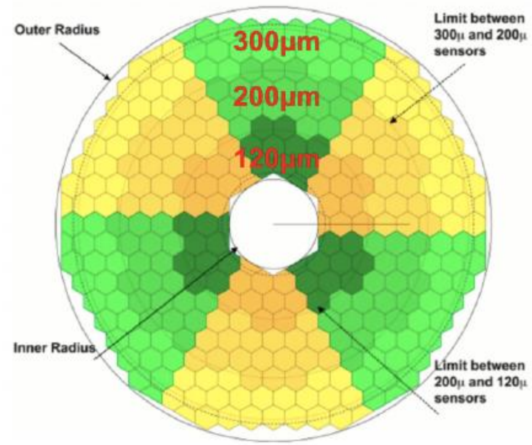

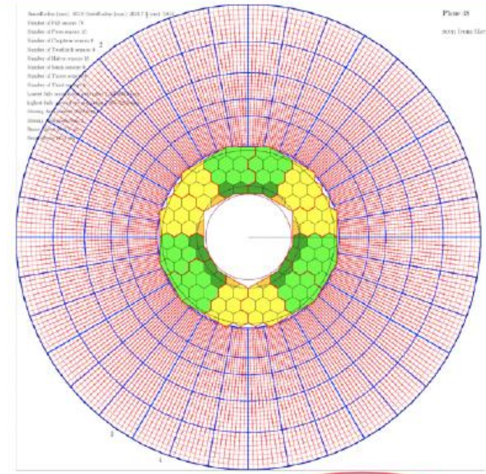

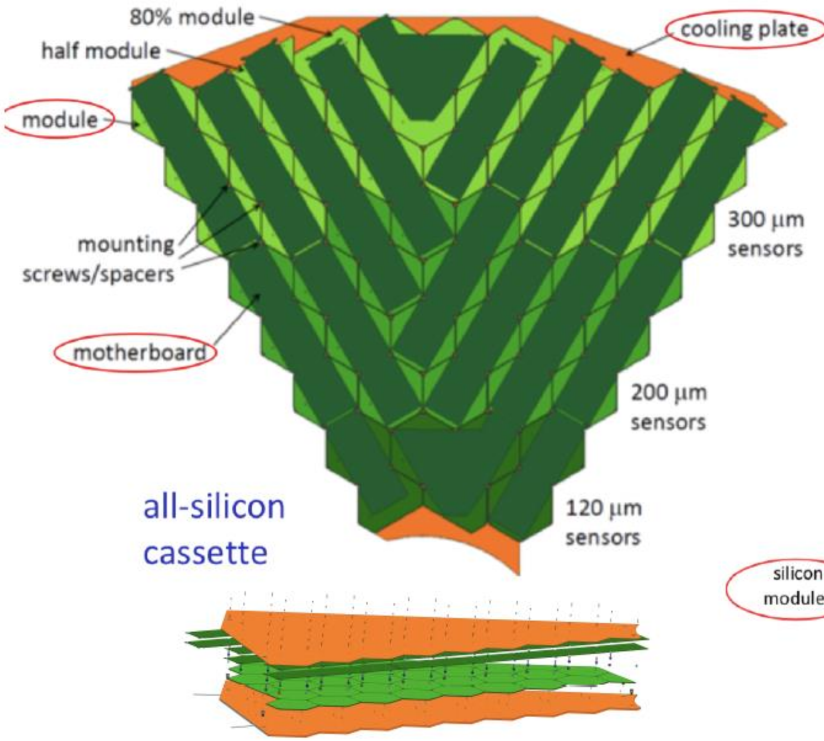

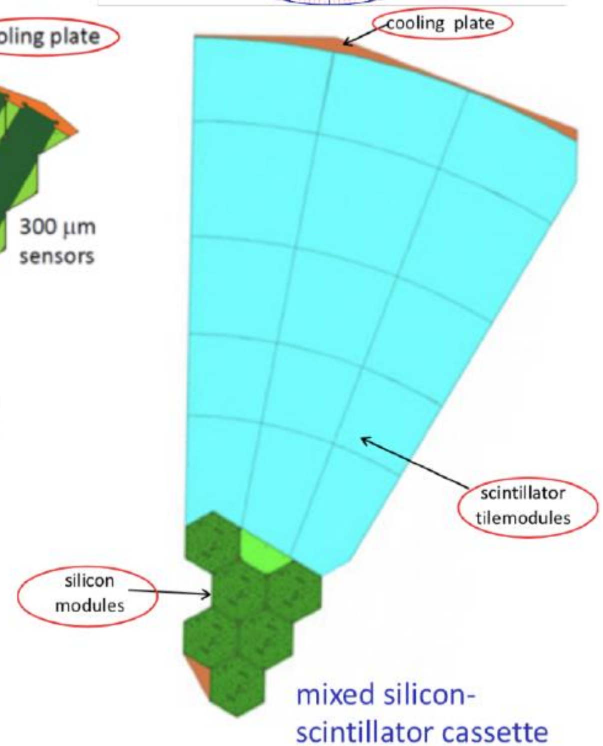

Silicon Modules

- Glued stack of baseplate, sensor and readout hexaboard
- baseplates are made of CuW in CE-E, PCB in CE-H
- Relative alignment within ~50um achieved with gantry based automated assembly
- Electrical connections are done with wire-bonds

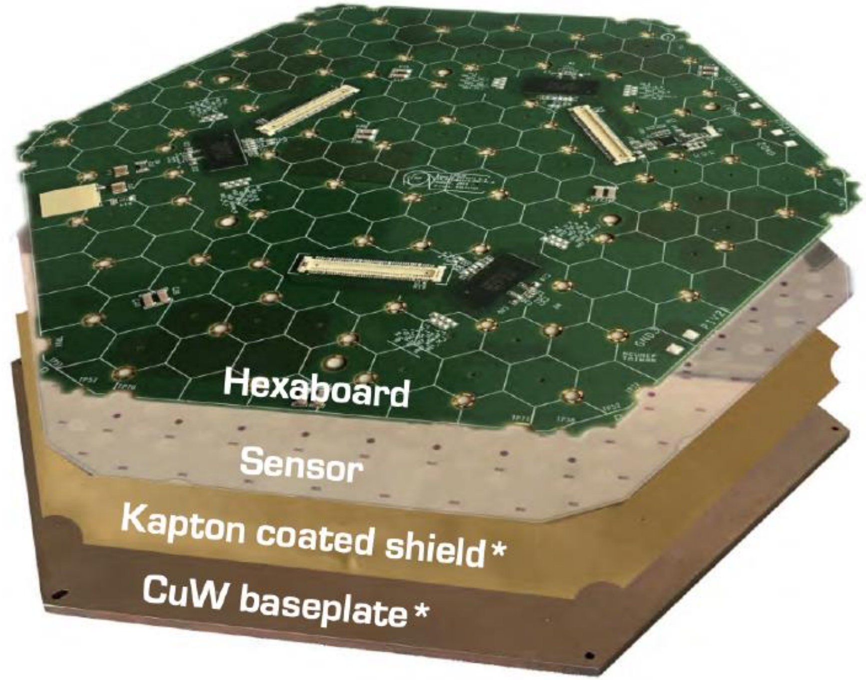

* In CE-H, PCB baseplate with laminated Kapton™

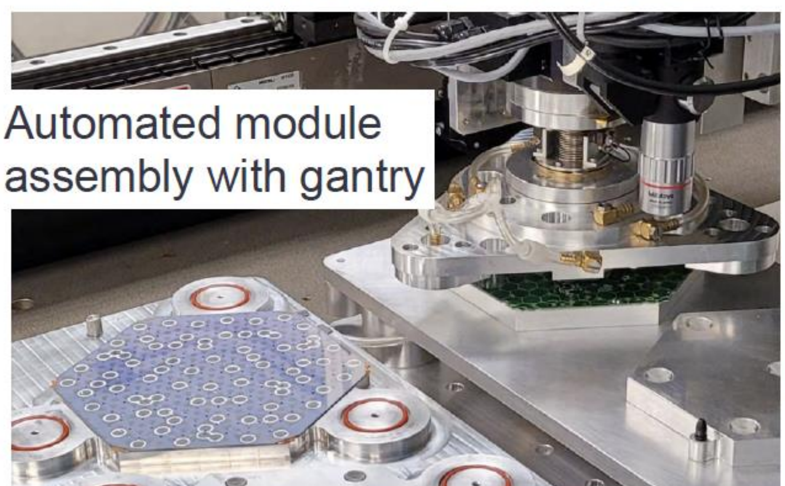

Automated module assembly with gantry

signal bonds

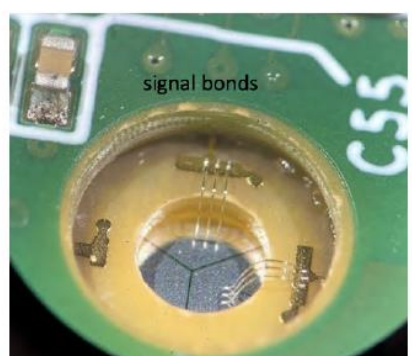

shield bonds

backside HV bonds

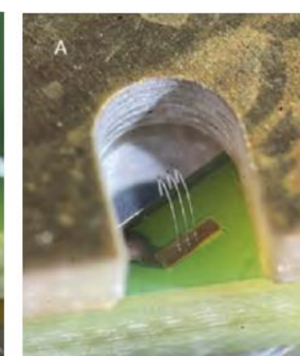

Dreams in space

Université de Strasbourg

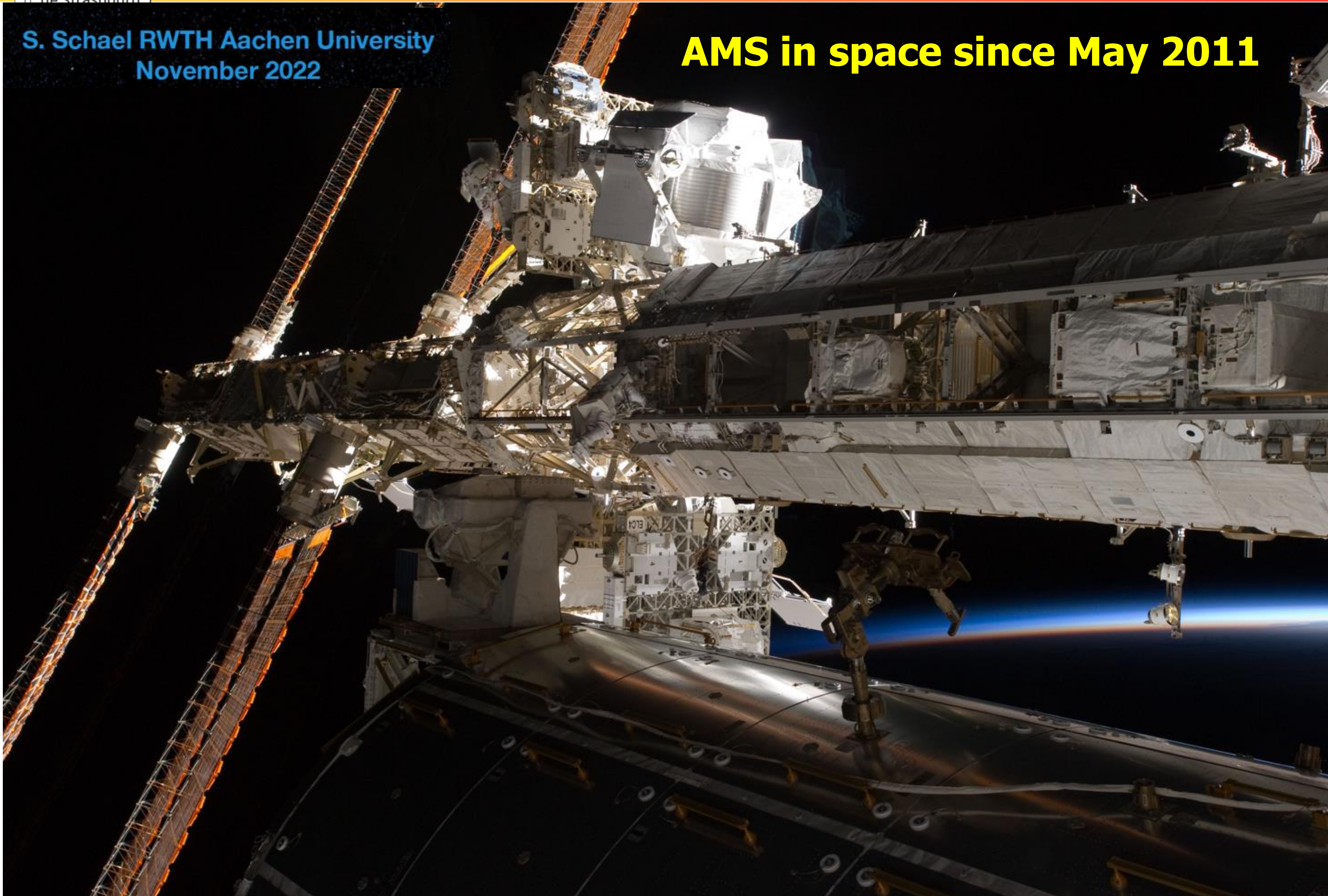

IPHC Institut Pluridisciplinaire Hubert CURIEN STRASBOURG

Université de Strasbourg

AMS → AMS100

S. Schael RWTH Aachen University
November 2022

It took 600 Physicists and Engineers from 16 Countries and 60 Institutes
17 years to construct the Alpha Magnetic Spectrometer.

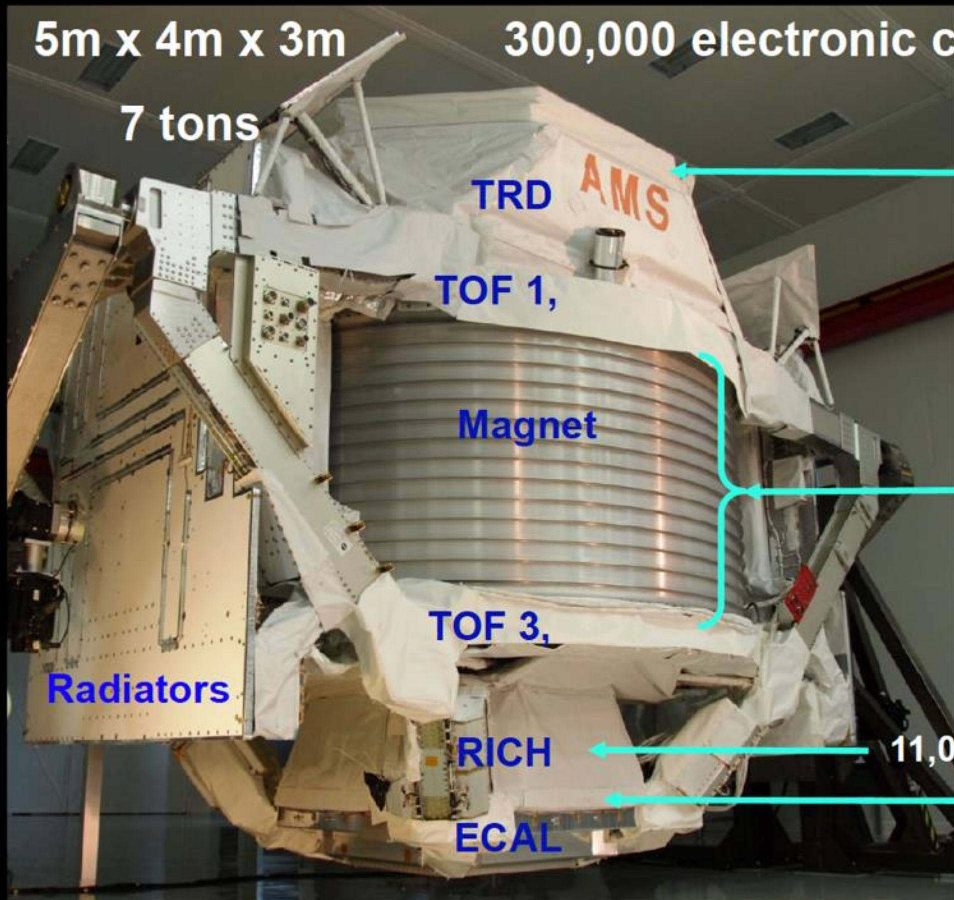

We have to start now to work on the next generation magnetic spectrometer in space !

12

Université de Strasbourg

S. Schael RWTH Aachen University
November 2022

AMS → AMS100

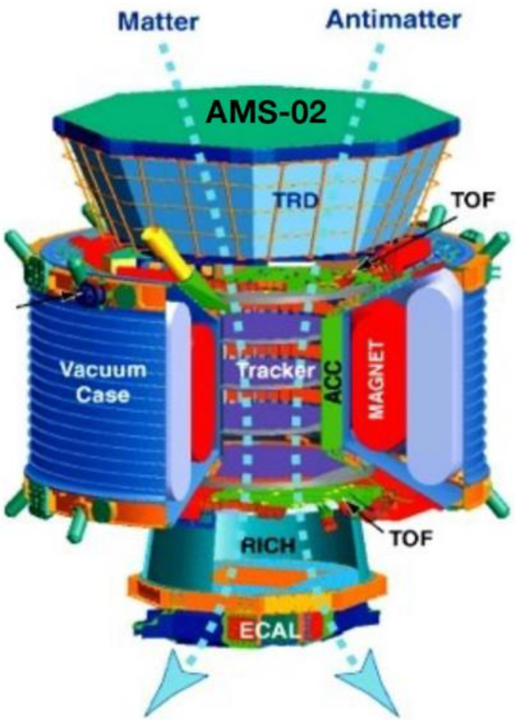

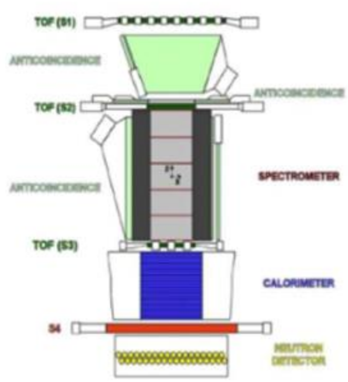

PAMELA

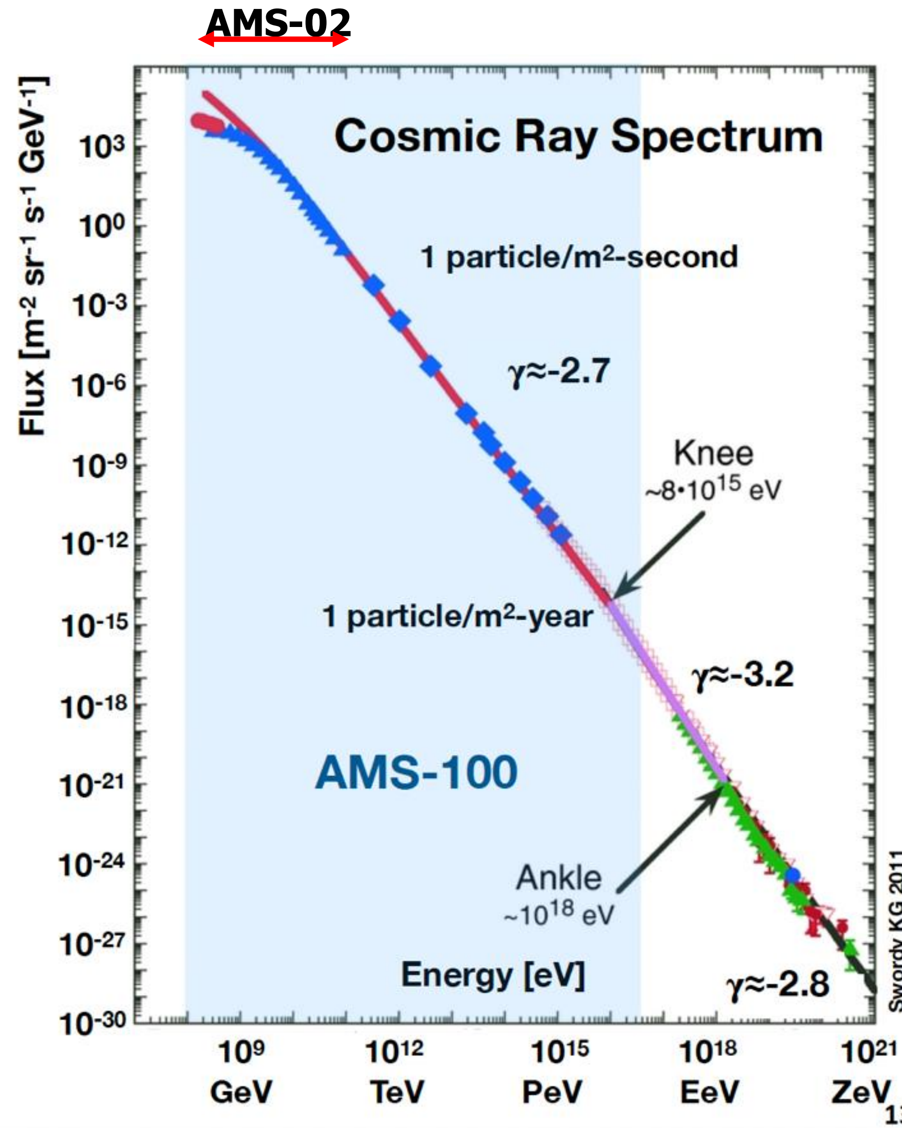

- The cosmic ray flux follows a power law $\Phi \approx C\,E^{-3}$
- An increase in energy by a factor 10 requires an increase in acceptance by 1000. AMS-02 weights 7 tons.
- Both PAMELA and AMS-02 have a telescope like geometry.
- Just scaling such a geometry does not allow to increase the energy reach by a factor 10 and simultaneously the acceptance by a factor 1000.

Université de Strasbourg

AMS 100

S. Schael RWTH Aachen University
November 2022

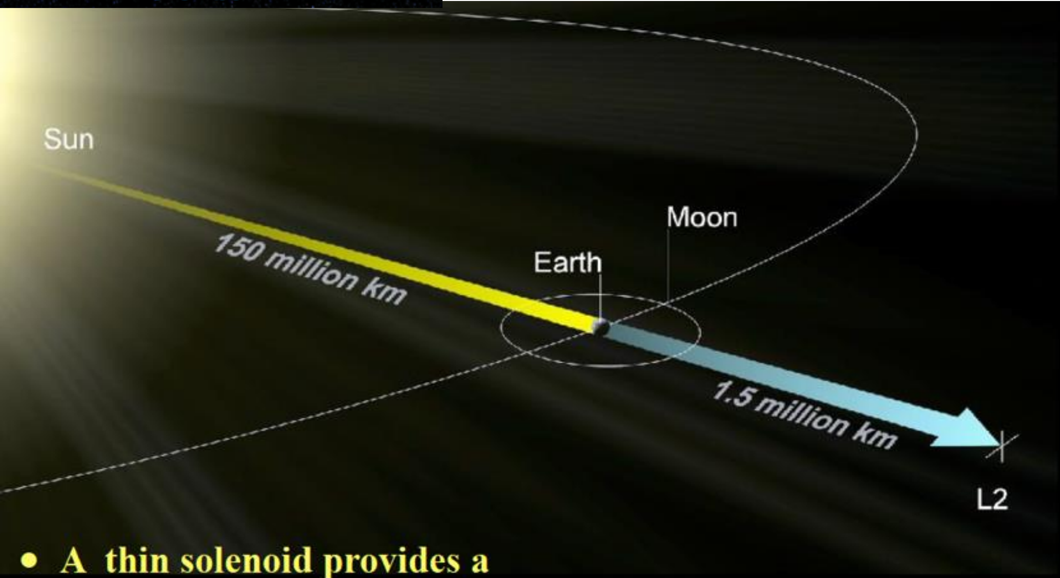

- A thin solenoid provides a magnetic field of 0.5 Tesla.
- The solenoid is operated at 60 K behind the sunshield in thermal equilibrium with the environment.
- A compensation coil balances the magnetic dipole moment of the solenoid.
- The solenoid is instrumented on the inside with a silicon tracker and a calorimeter system.

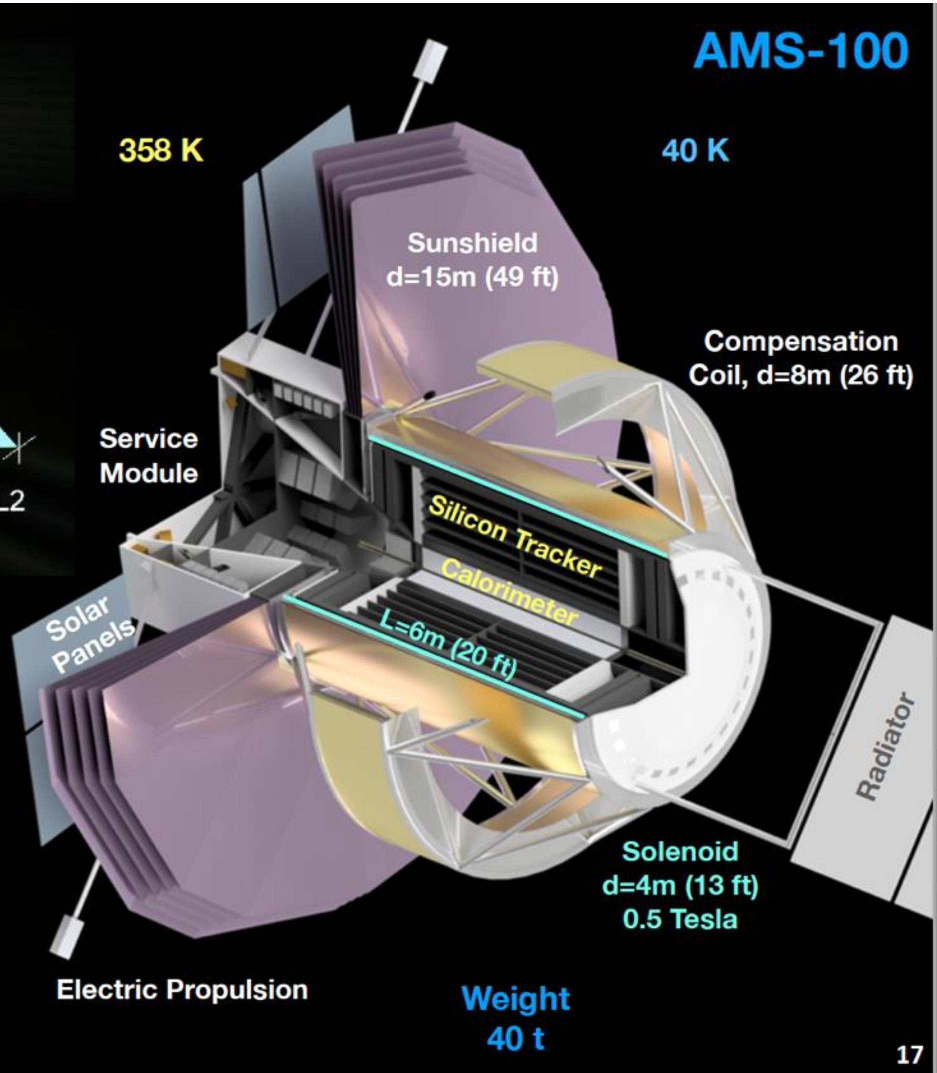

17

As a Magnetic Spectrometer AMS-100 can separate Anti-Matter from Matter.

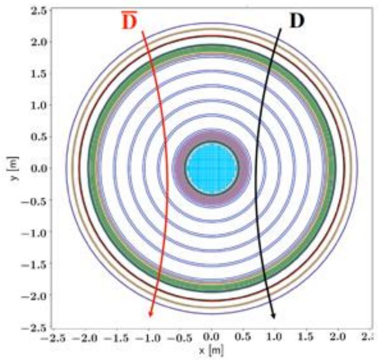

S. Schael RWTH Aachen University
November 2022

AMS-100

Weight: 40 t	Readout-Channels: $8\ 10^6$	Power: 15 kW	Measurement Time: 10 years
MDR: 70 TV	Acceptance: 100 m^2 sr	B-Field: 1 Tesla	Calorimeter: 70 X_0, 4λ

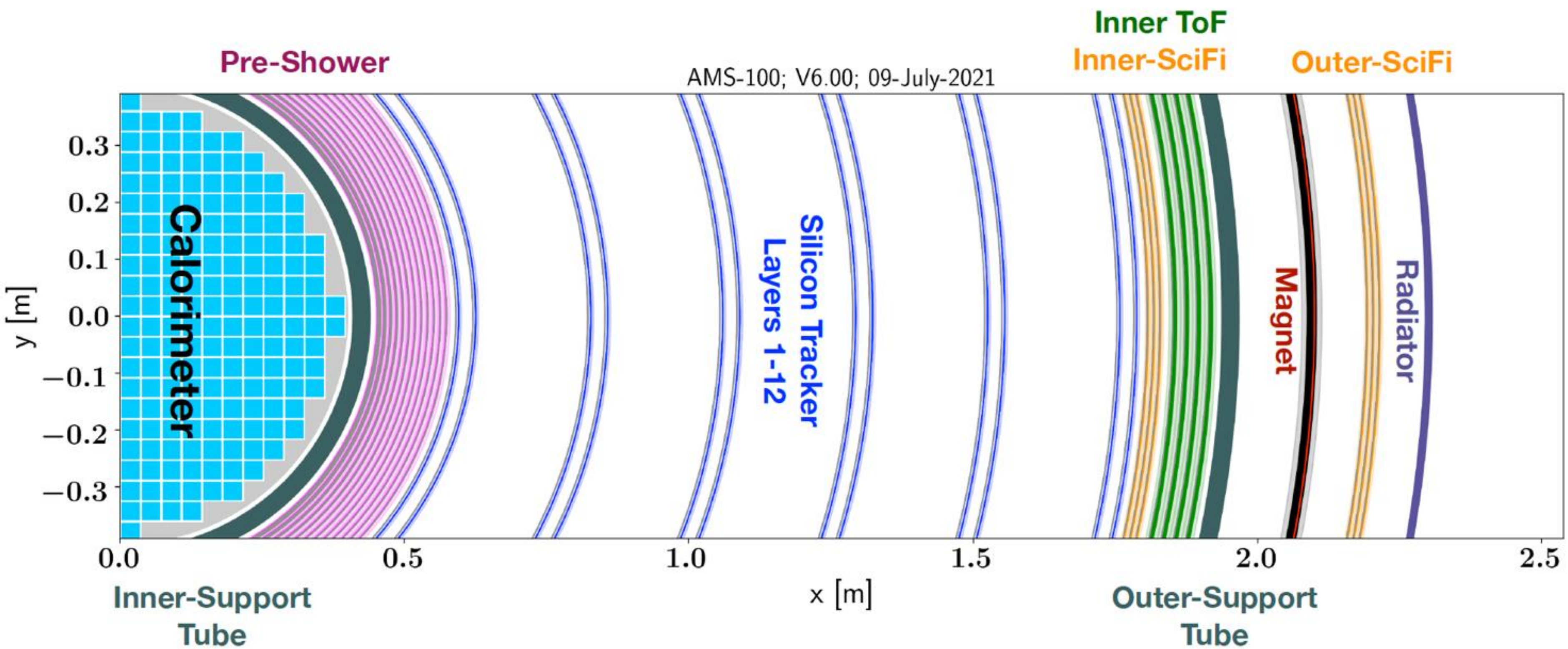

Th. Kirn, "The AMS-100 experiment: The next generation magnetic spectrometer in space", Nucl.Instrum.Meth.A 1040 (2022) 167215 • Proceedings of: VCI2022

Université de Strasbourg

AMS 100

S. Schael RWTH Aachen University
November 2022

AMS-100 Solenoid - a non-insulated coil

90 km
of High Temperature Superconducting Tape

Thickness: 18 x 0.04 mm = 0.72 mm !

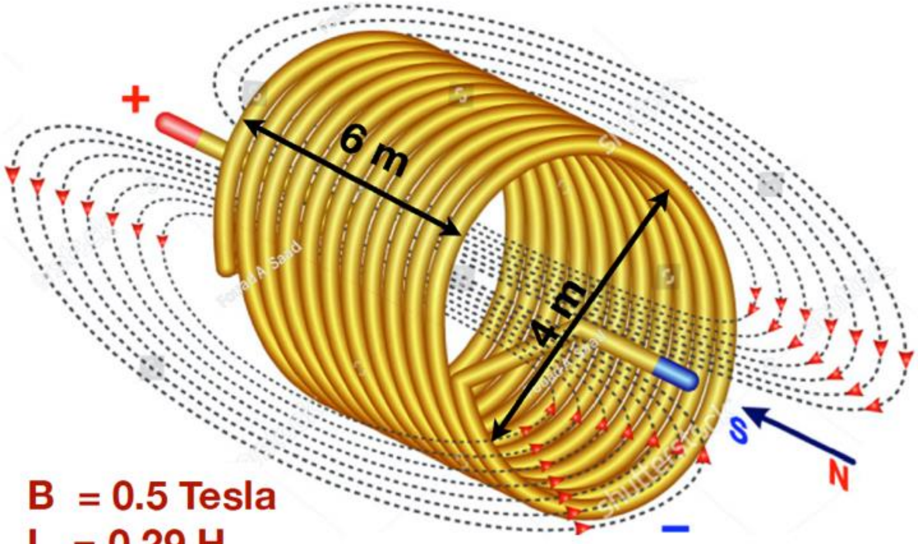

B = 0.5 Tesla
L = 0.29 H
E = 14 MJ

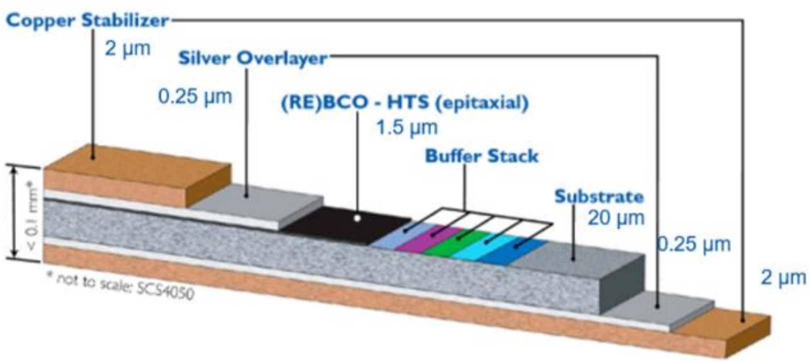

Stack of 18 Tapes
12 mm wide; Fujikura, 700 A @ 77K, SF

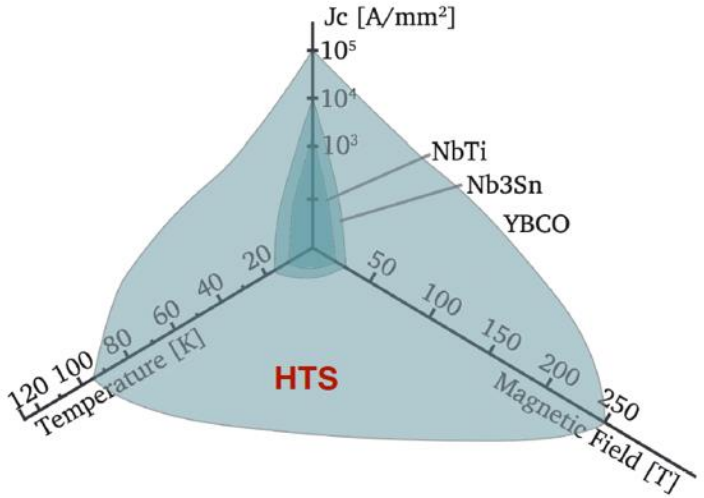

iPHC Institut Pluridisciplinaire Hubert CURIEN

S. Schael RWTH Aachen University
November 2022

AMS 100

AMS-100: A Magnetic Spectrometer

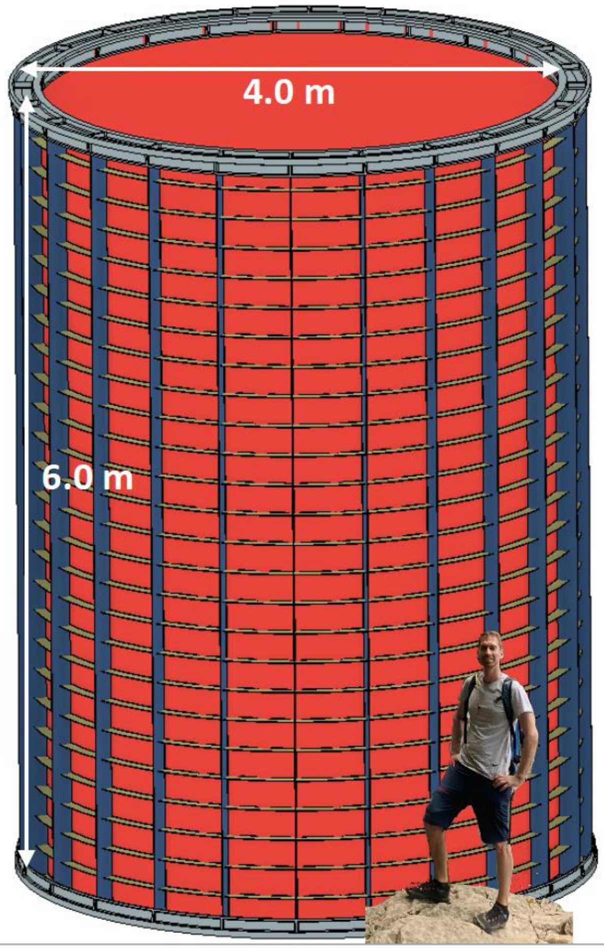

Table of properties for the AMS-100 main solenoid and compensation coil.

	Main	Compensation	Combined	Unit
Coil radius	2.0	4.0		m
Coil length	6.0	1.5		m
Tape width	12	12		mm
Stabilizer	Al-6063	Al-6063		
Cable thickness	2.85	2.85		mm
Cable width	16	16		mm
Layers	1	1		-
Turns	376	94		-
Inductance	286	114	287	mH
Number of tapes	18	18		-
Total tape length	85	43	128	km
Operating current	10.0	-10.0		kA
Cable mass	1090	545	1635	kg
Stored Energy	14.3	5.7	14.4	MJ
Energy Density*	14	11	9	kJ/kg

*Considering only the mass of the cable.

Université de Strasbourg

S. Schael RWTH Aachen University
November 2022

- In 2005 NASA canceled the AMS-02 Space Shuttle Flight.
- At RWTH Aachen a concept for a balloon experiment (PEBS) was developed to measure cosmic ray positrons.
- A new scintillating fiber tracker with SiPM readout was the key element for the tracking system.
- In 2008 the group of T. Nakada, EPFL joined the team.
- In 2010 a prototype (PERDAIX) was launched from Kiruna, Sweden. 300 000 protons and Helium nuclei were recorded at an altitude of 34 km.
- The paper describing this new SciFi detector was published in Nucl. Instrum. Meth.A 622 (2010) 542-554 (10.1016/j.nima.2010.07.059).
- In 2014 the LHCb Upgrade I TDR was published, describing a 360 m^2 version of this detector build from 11,000 km of fiber.

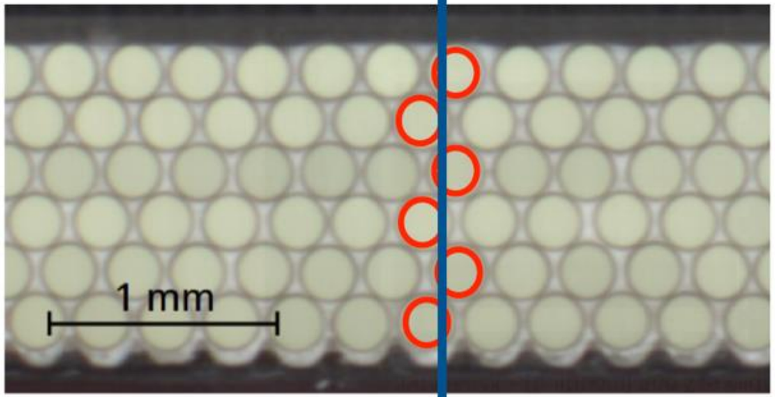

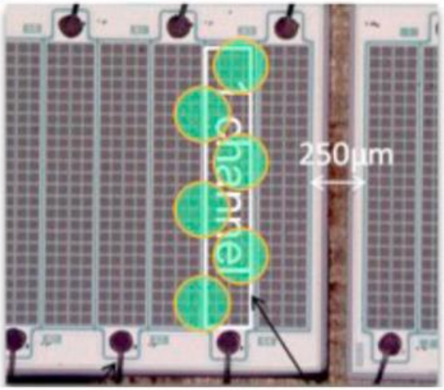

42

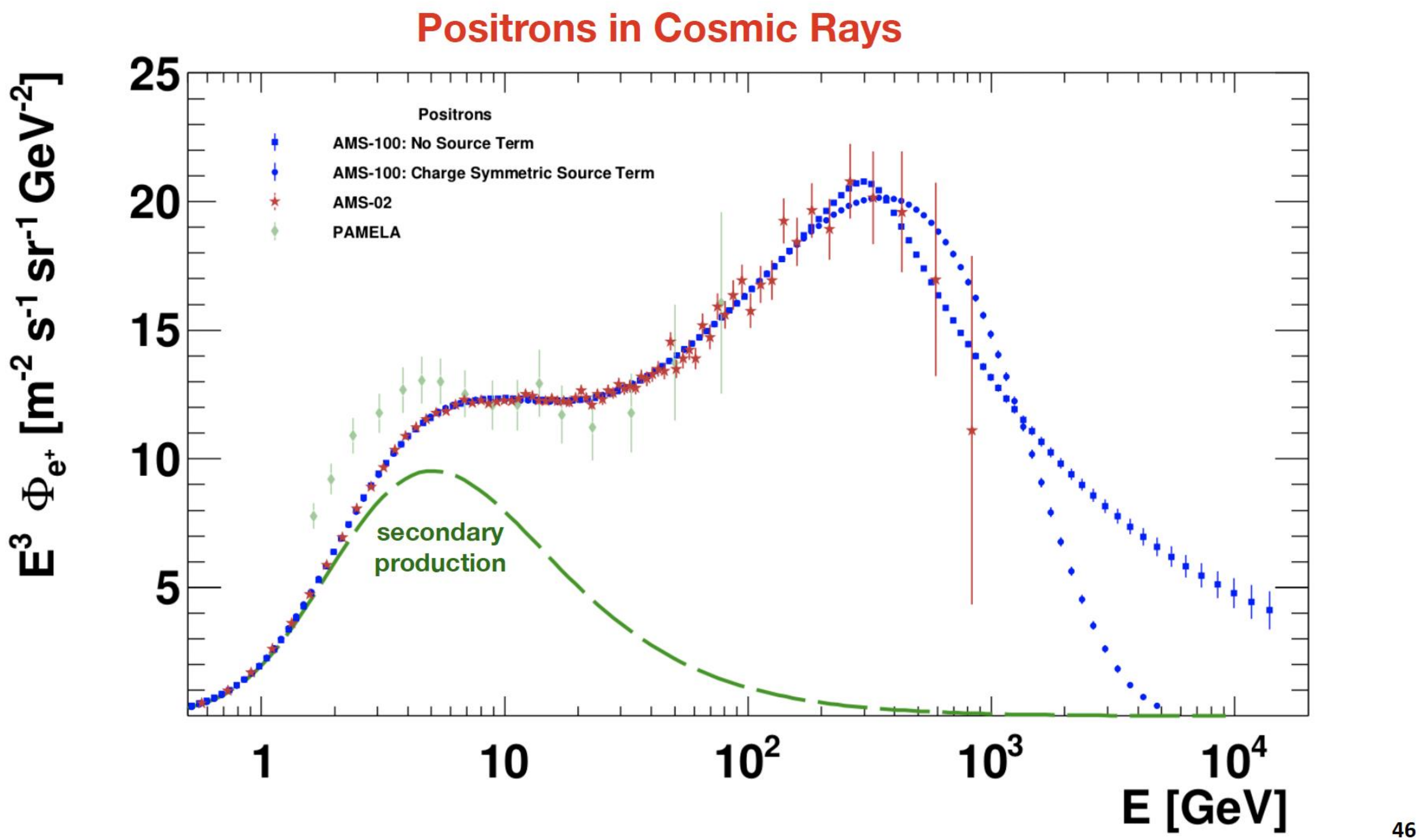

S. Schael RWTH Aachen University
November 2022

Résumé

- **This was a very short and limited snapshot of some of the many ideas and developments on detectors.**

Reserve

Resolution

Ulrich.Goerlach@iphc.cnrs.fr, ASP Particle detectors

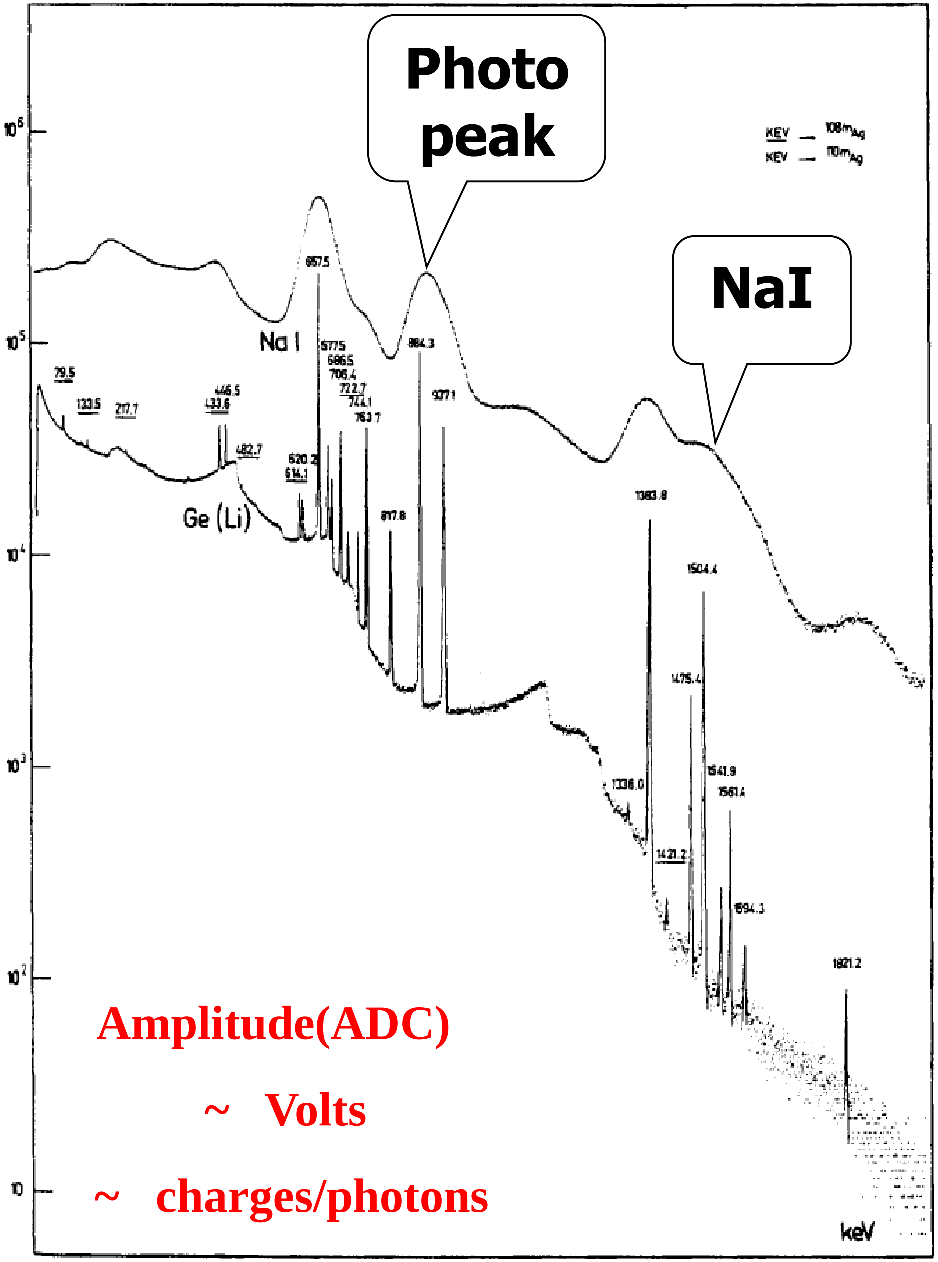

Amplitude(ADC)

~ Volts

~ charges/photons

~ energy of gamma

$$N_{h\nu} = \frac{E}{w};\ dN_{h\nu} = \sqrt{N_{h\nu}} = \sqrt{\frac{E}{w}}$$

Statistics strictly Poisson $\Rightarrow \sigma^2 = \mu$;

$$dE/E = dN_{h\nu}/N_{h\nu} \sim \frac{1}{\sqrt{N_{h\nu}}}$$

$NaI : w \approx 25\,eV / photon_{\text{scint}} \Rightarrow 40000\,h\nu / MeV$

Incomplete collection of scintillation photons and finite quantum efficiency will reduce the mean number of photo-electrons

$$N_{pe} = N_{h\nu} \times \varepsilon_{collection} \cdot \varepsilon_{quantic};$$

$$dN_{pe} = \sqrt{N_{pe}} = \sqrt{N_{h\nu} \times \varepsilon_{coll.} \cdot \varepsilon_{quant.}}$$

$$\varepsilon_{coll.} \approx 0.2 - 0.8;\ \varepsilon_{quant.} \approx 0.2(PM)$$

$$dE/E = dN_{pe}/N_{pe} \cong \frac{1}{\sqrt{N_{pe}}} = \frac{1}{\sqrt{N_{h\nu} \times \varepsilon_{coll.} \cdot \varepsilon_{quant.}}}$$

$$F \approx 1;\ \varepsilon_{coll.} \approx 0.4;\ \varepsilon_{quant.} \approx 0.2(PM)$$

$$\Rightarrow dE/E = \sigma_E / E \approx 1.5\% \text{ à } 1.333\ MeV$$

$$R = 2.35 \times 1.5\% = 3.6\% \xrightarrow{\text{experimental}} (5-8)\%$$

Université de Strasbourg

HP-Ge detector

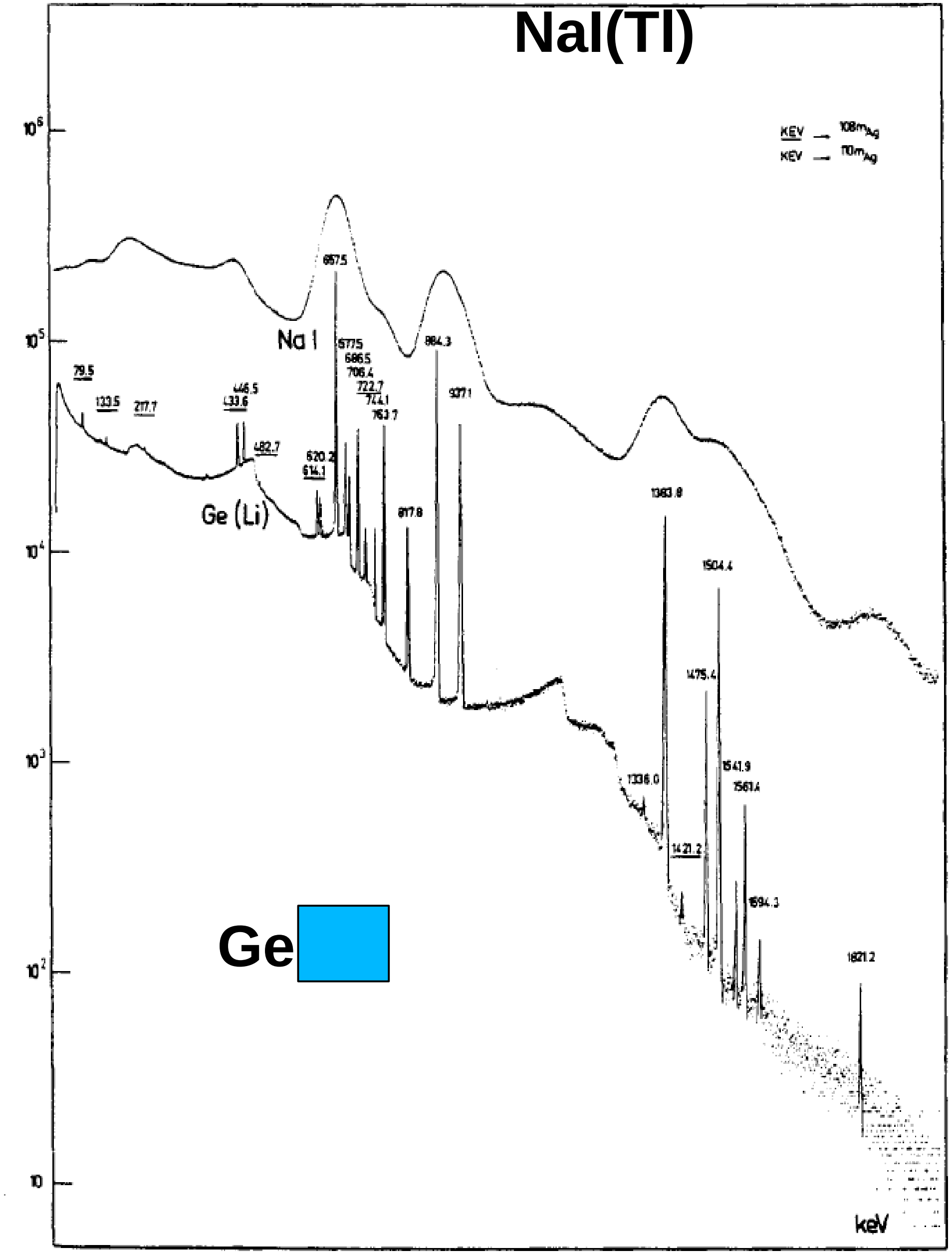

$$N_{eh} = \frac{E}{w}\varepsilon_{collection}$$

$$dN_{eh} = \sqrt{N_{eh}} = \sqrt{\frac{E}{w}\varepsilon_{collection}}$$

Statistics : Poisson

$$\Rightarrow \sigma^2 = \mu; \quad \mu = \text{mean}; \sigma^2 = \text{variance}$$

$$dE/E = dN_{eh}/N_{eh} \sim \frac{1}{\sqrt{N_{eh}}} = \frac{1}{\sqrt{\frac{E}{w}\varepsilon_{collection}}}$$

$$\varepsilon_{collection} \approx 100\%; \; w = 2.98\,eV \quad E = 1\,MeV$$

$$\Rightarrow dE/E \approx 0.0017; \; \text{Resolution} \; R = 2.35 \times dE/E = 0.4\%$$

Fano factor:

$$\sigma^2 = F_{ano}\mu;$$

$$F_{ano} \simeq 0.12\,(Ge, Si); \quad \sqrt{0.12} = 1/2.9$$

$$dE/E = dN_{eh}/N_{eh} \sim \frac{\sqrt{F}}{\sqrt{N_{eh}}} = \frac{1}{\sqrt{\frac{E}{wF}\varepsilon_{collection}}}$$

$$dE/E = 0.0006; \; \text{Resolution} \; R = 2.35 \times dE/E = 0.14\%$$

Comparison with NaI:

$$w = 25\,eV / photon_{scint} \; \text{Light collection: } 0.5 \;\; \text{PM}: Q.E. \approx 0.20$$

$$dE/E \approx 1.6\% \;\; \text{Resolution} \; R = 2.35 \times dE/E = 3{,}7\% \text{ à } 1\,MeV$$

The EUROBALL Cluster Detector 10kg HPGe

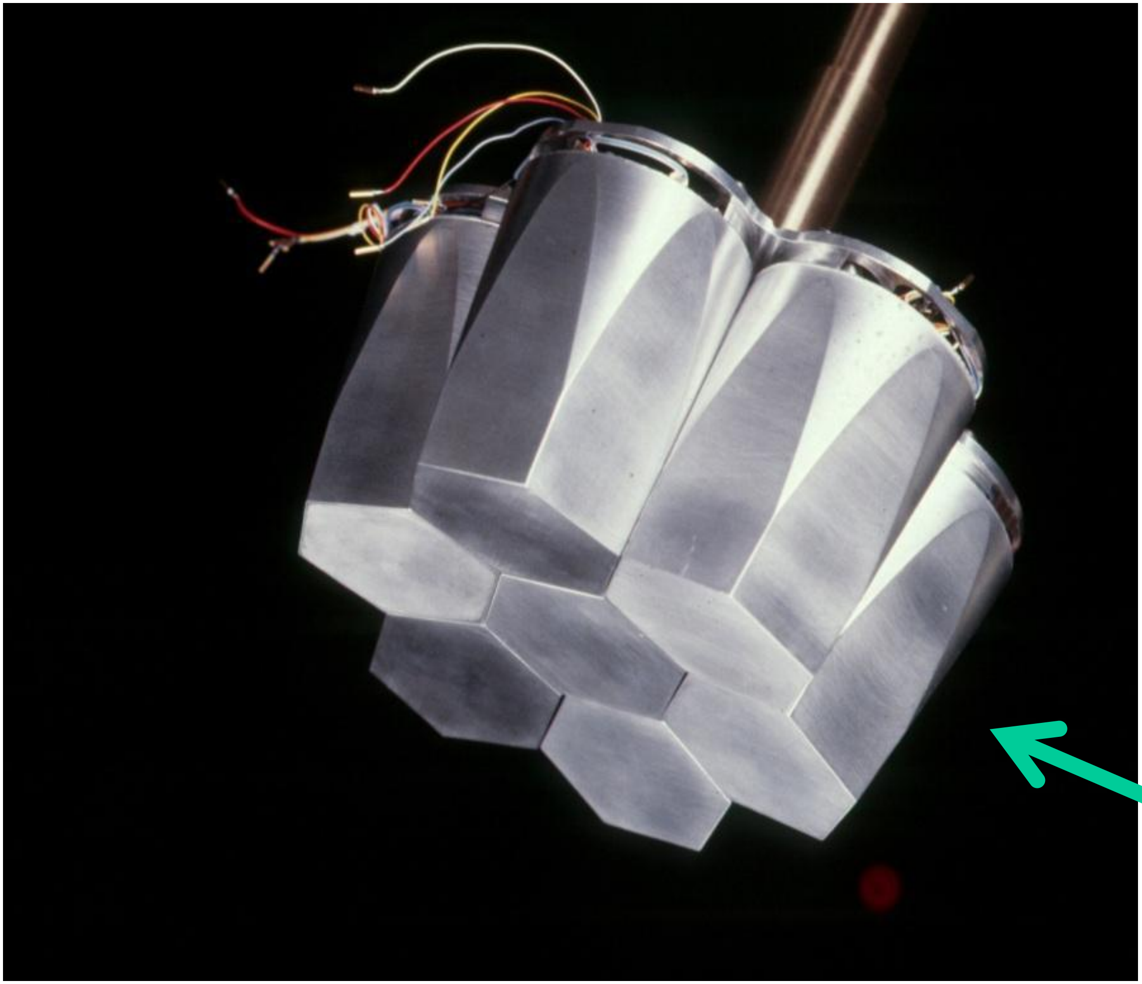

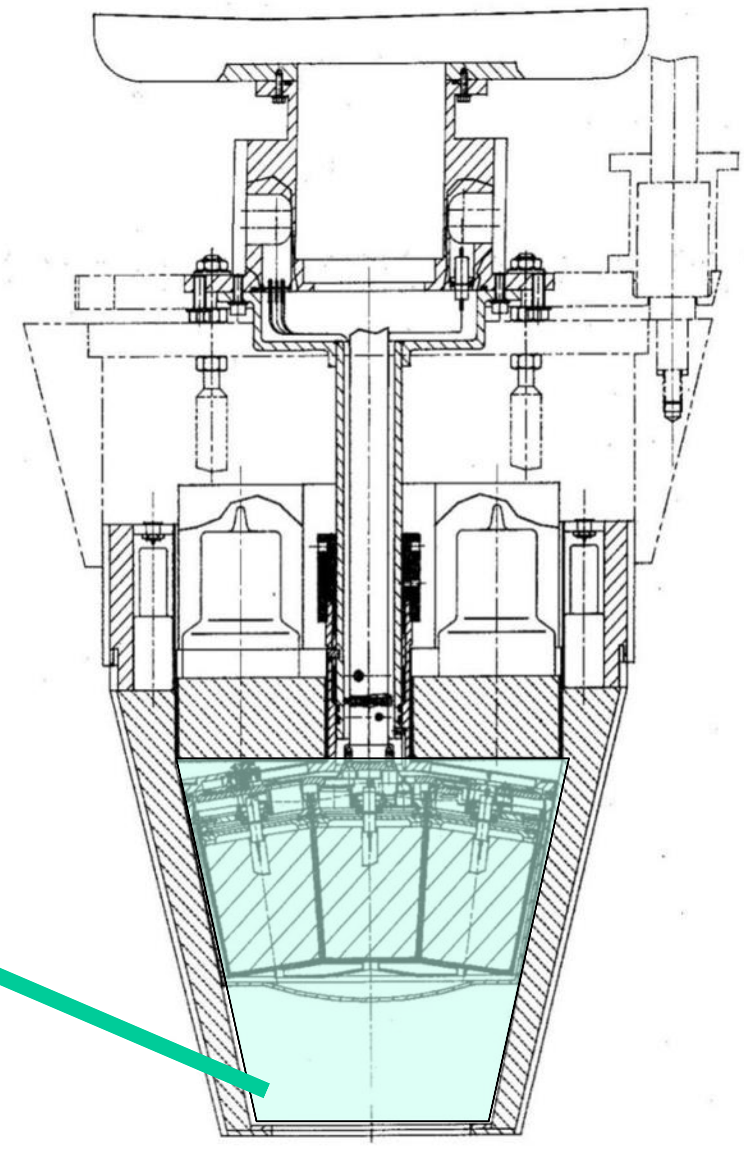

Université de Strasbo

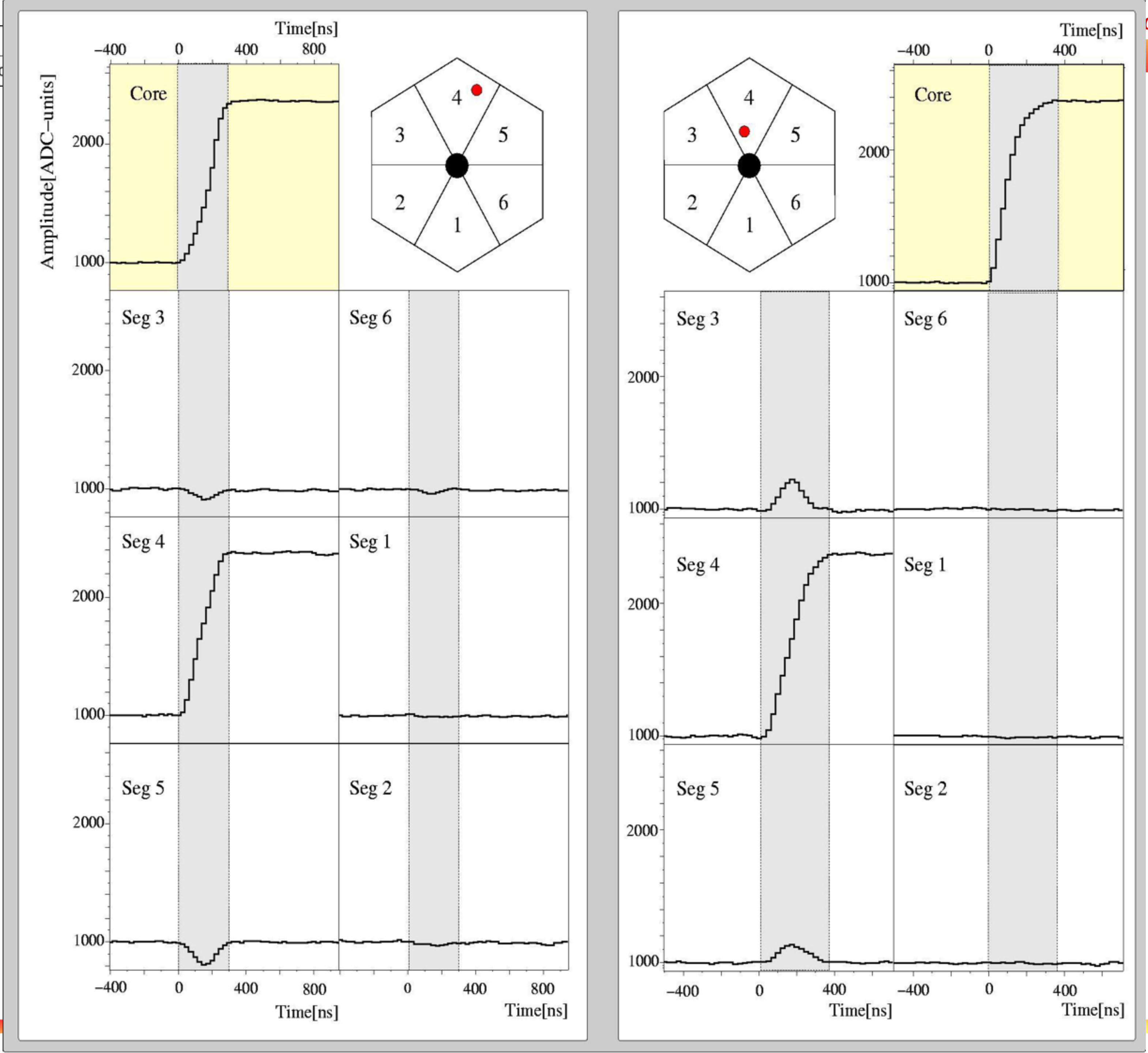

3D Silicon

The CMS Inner Tracker upgrade for the High Luminosity-LHC

HL-LHC operation conditions	Sensor design constraints
Luminosity 7.5x10^{34}/(cm^2•s) ➜ up to **200 events/25 ns** bunch crossing	Maintain occupancy at ‰ level and increase spatial resolution ➜ pixel size x6 smaller then present pixels ➜ 25x100 μm^2 (current detector in CMS 100x150 μm^2)
CMS baseline choice: replace pixel layer closer to beamline at integrated fluence **~1.9x10^{16} n$_{eq}$/cm^2** (end of *"Run5"*, i.e. after ~6 years of operation) ➜ electron **mean free path** greatly **reduced** (also damaged readout ASIC at ~1 Grad)	Reduce electrodes distance (L) to increase electric field and thus the signal ➜ thin planar or 3D columnar technologies

3D silicon sensors made by

- Fondazione Bruno Kessler-***FBK*** (Trento, Italy), **n-in-p** sensors on **150 mm FZ wafers** in collaboration with ***INFN***
- Centro Nacional Microtecnologia-***CNM*** (Barcelona, Spain), **n-in-p** sensors on **100 mm FZ wafers**

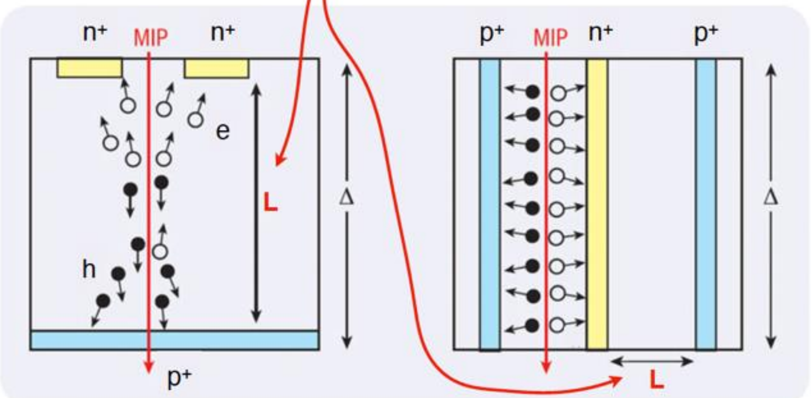

C. Da Vià et al., NIMA (2012)

Université de Strasbourg

Inspiration for ITS3

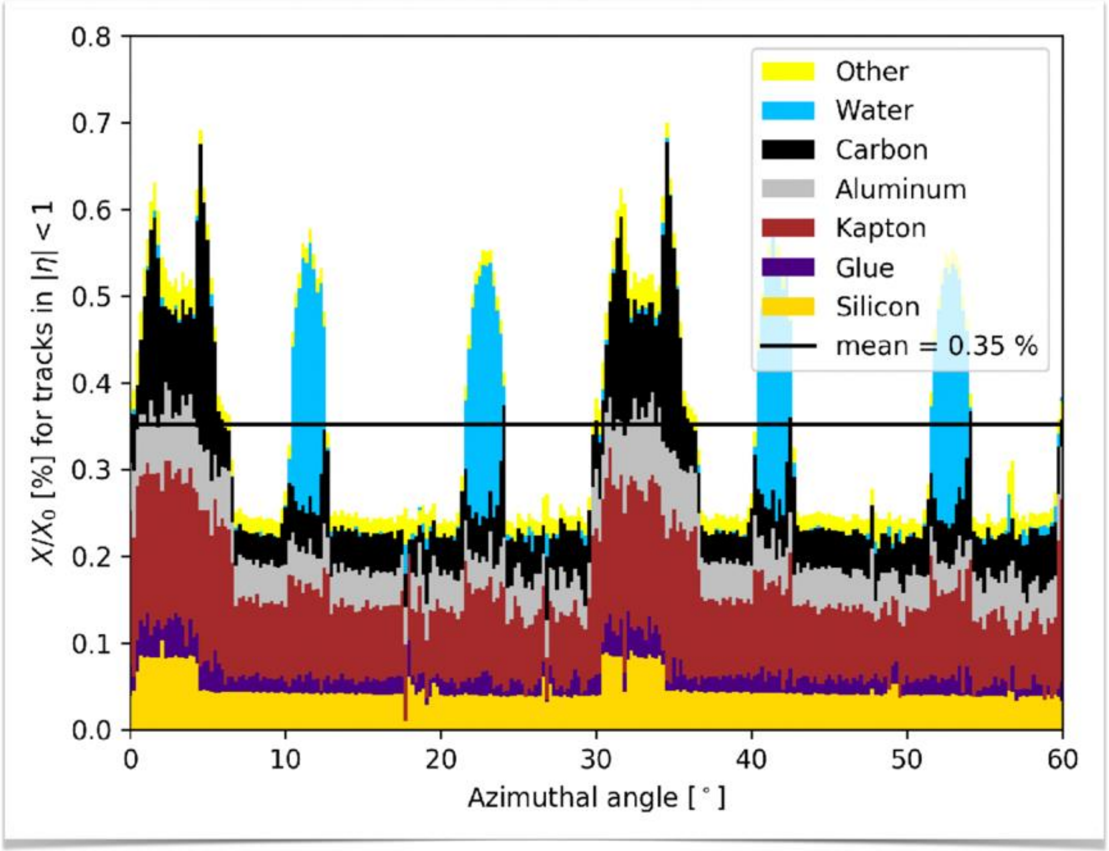

- Observations:
  - Si makes only **1/7th** of total material
  - **irregularities** due to support/ cooling

Magnus Mager (CERN) | ALICE ITS3 | CERN detector seminar | 24.09.2021 | 8

Inspiration for ITS3

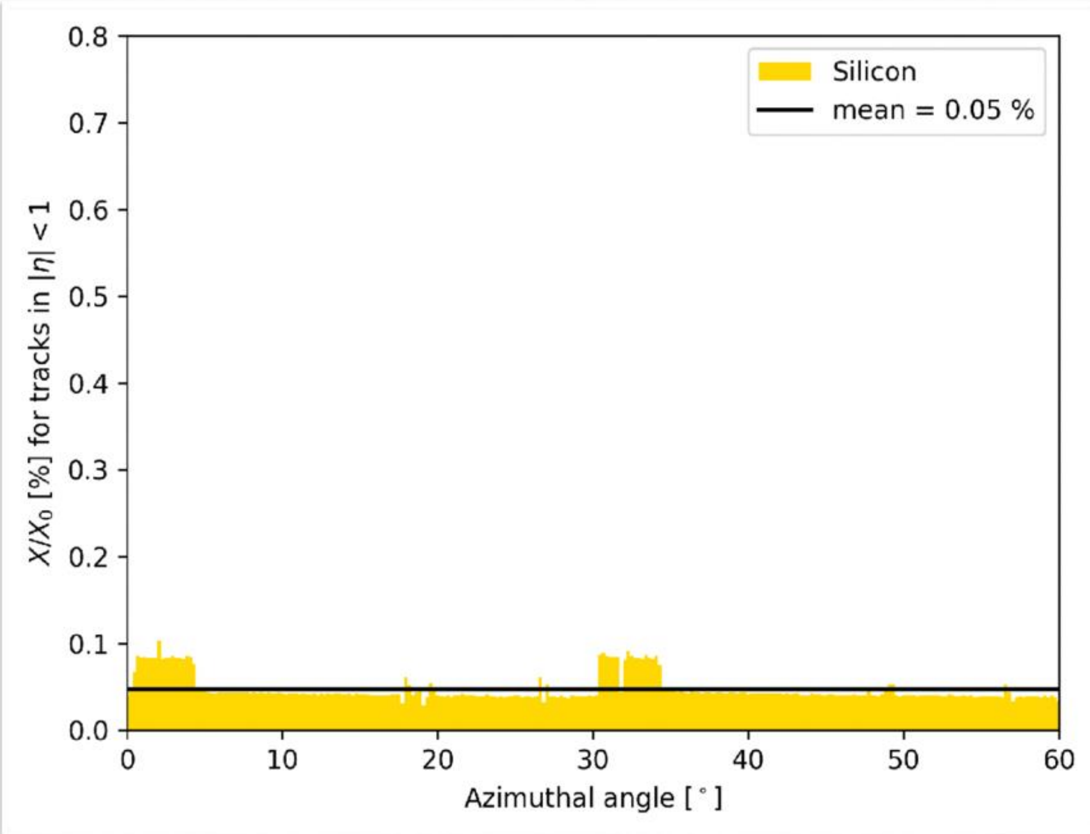

- Observations:
  - Si makes only **1/7th** of total material
  - **irregularities** due to support/ cooling
- Removal of water cooling
  - **possible** if power consumption stays below 20 mW/cm^2
- Removal of the circuit board (power+data)
  - **possible** if integrated on chip
- Removal of mechanical support
  - **benefit** from increased stiffness by rolling Si wafers

Magnus Mager (CERN) | ALICE ITS3 | CERN detector seminar | 24.09.2021 | 8

ITS3

the idea (2): build wafer-scale sensors

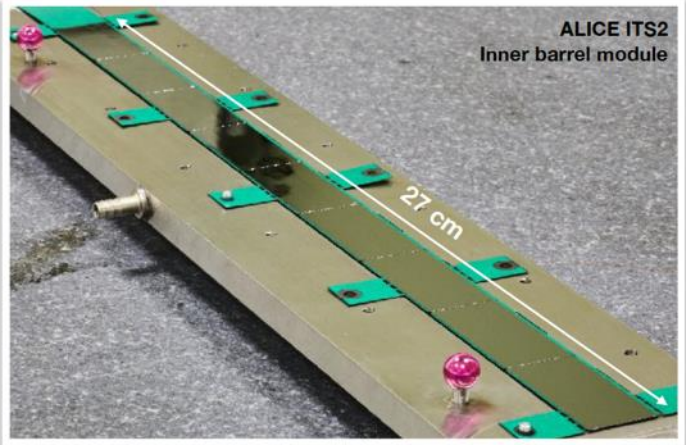

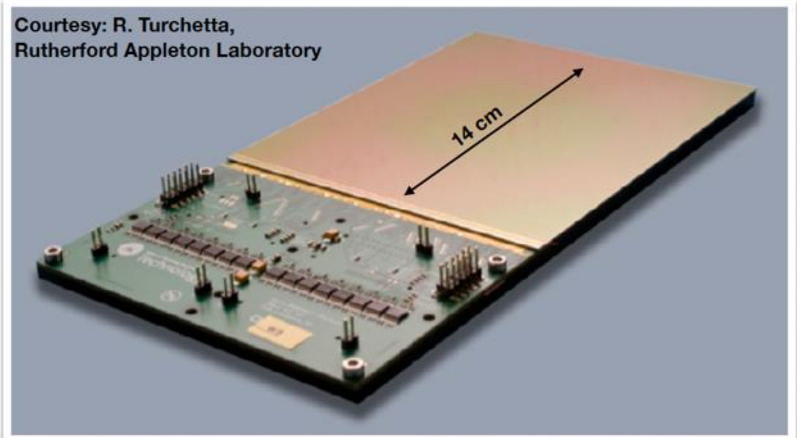

- Chip size is traditionally limited by CMOS manufacturing ("reticle size")
  - typical sizes of few cm^2
  - modules are tiled with chips connected to a flexible printed circuit board
- New option: stitching, i.e. aligned exposures of a reticle to produce larger circuits
  - actively used in industry
  - a 300 mm wafer can house a sensor to equip a full half-layer
  - ***requires dedicated sensor design***

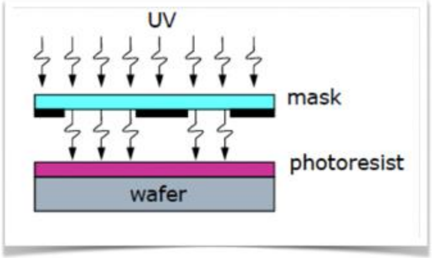

Magnus Mager (CERN) | ALICE ITS3 | CERN detector seminar | 24.09.2021 | 10

High Granularity for Particle Flow

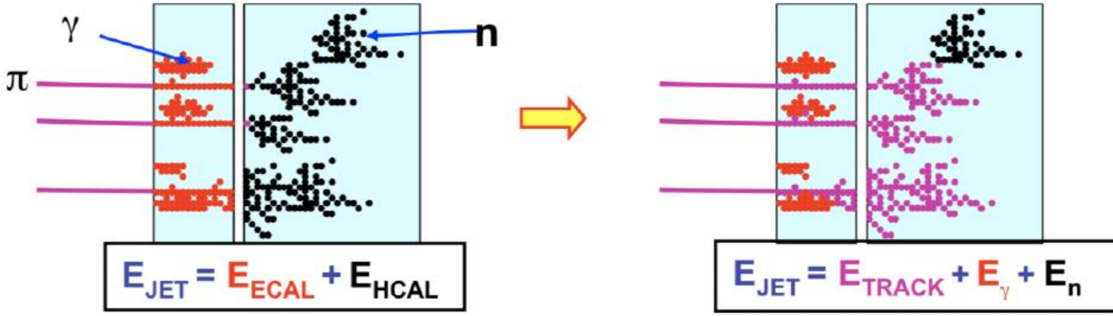

- **CMS uses particle flow algorithms to improve on jet energy resolution**
  - reconstruct every particle in a jet
  - For each particle use the detector with best energy/ momentum measurement
  - High granularity is key for correct assignment of energy deposits to tracks

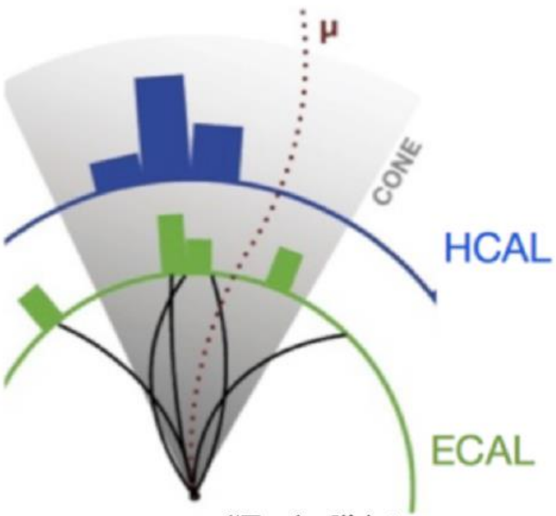

"Typical" jet:

~62% charged particles (mainly hadrons)
~27% photons
~10% neutral hadrons
~1% neutrinos

Compact Muon Solenoid

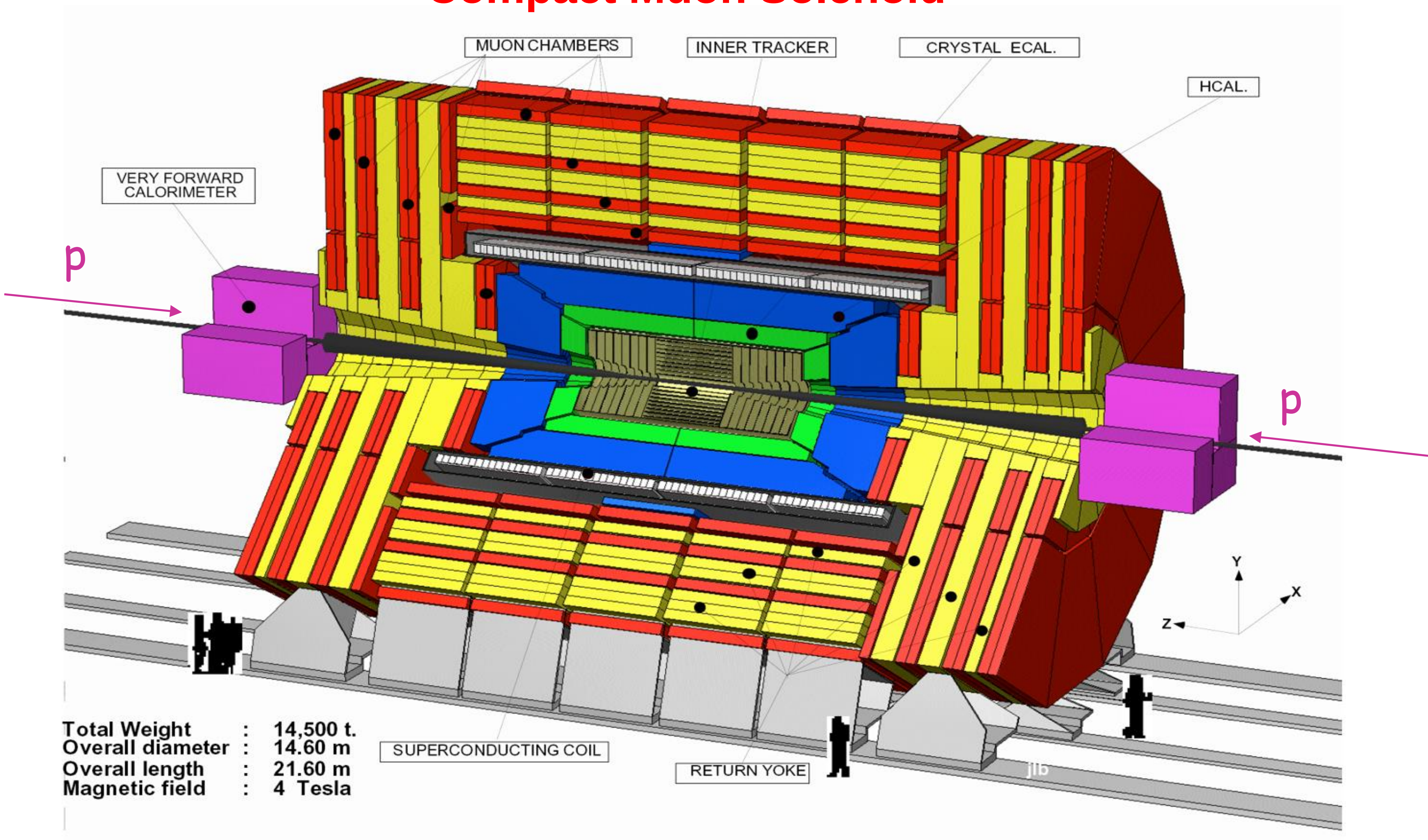

S. Schael RWTH Aachen University
November 2022

Conductor Testing: Single- and Multi-Tape Samples

- Single tapes have been extensively characterized .
- Many short samples of Al-alloy stabilized multi-tape HTS conductors are in preparation.
- Few-tape samples in good agreement with expectations.
- Next: more tapes, bending, micro-meteorite impact testing, etc.

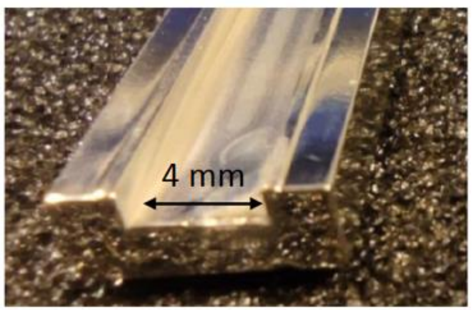

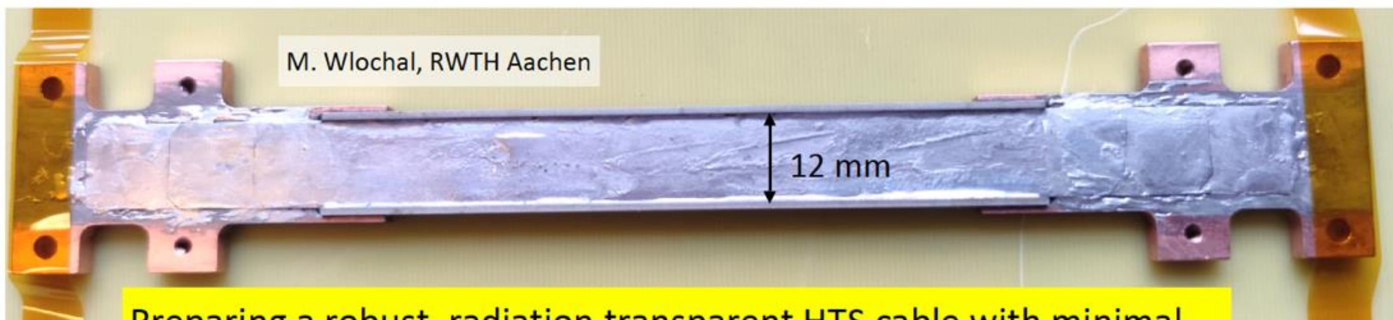

Preparing a robust, radiation transparent HTS cable with minimal amount of solder and proper bonding is still a **major challenge**!

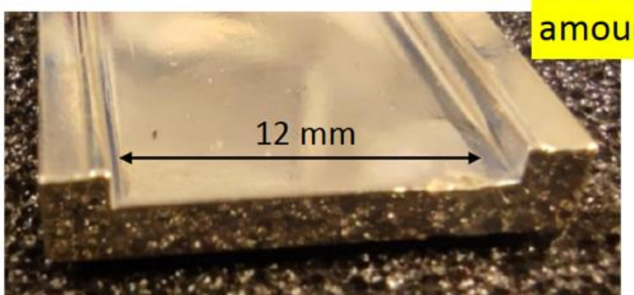

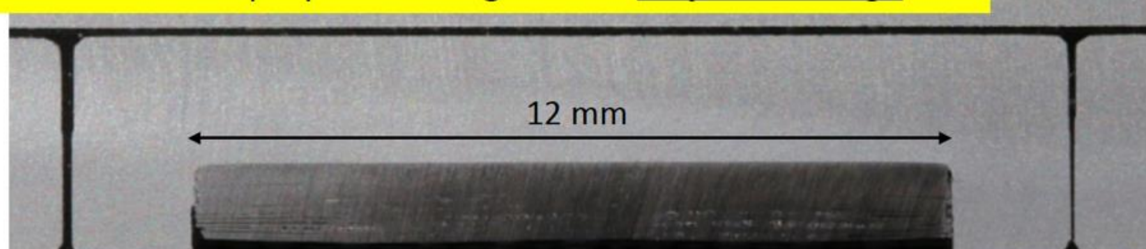

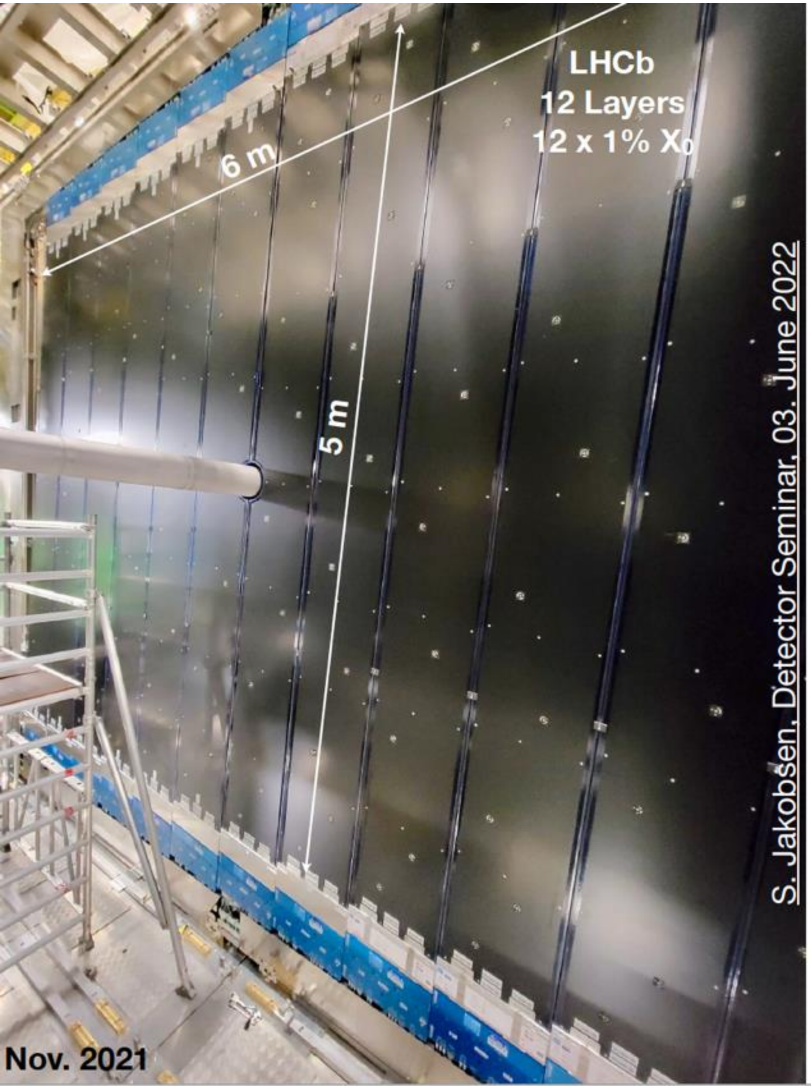

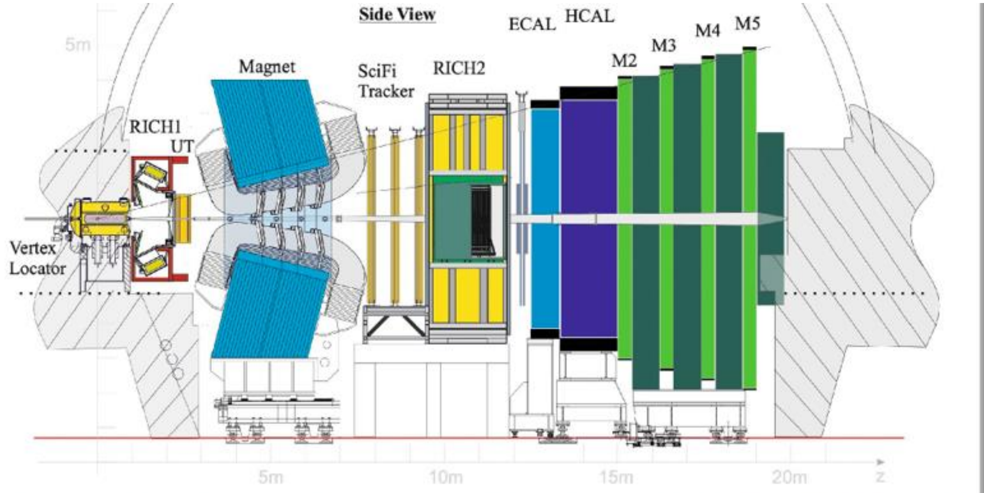

A large international team from several institutes, including EPFL and RWTH Aachen, constructed the LHCb SciFi Tracker in the past years.